LATITUDE DEPENDENCE OF IONOSPHERIC ELECTRON CONTENT

by
A. P. WEISE and K. C. YEH

April 1967

Sponsored by
National Aeronautics and Space Administration
NsG 24

ELECTRICAL ENGINEERING RESEARCH LABORATORY
ENGINEERING EXPERIMENT STATION
UNIVERSITY OF ILLINOIS
URBANA, ILLINOIS

LATITUDE DEPENDENCE OF IONOSPHERIC ELECTRON CONTENT

by

A. P. Weise and K. C. Yeh

April 1967

Sponsored by

National Aeronautics and Space Administration
NsG 24

Electrical Engineering Research Laboratory
Engineering Experiment Station
University of Illinois
Urbana, Illinois

ACKNOWLEDGEMENT

The suggestions and comments of several members of the Ionosphere Radio Laboratory were very much appreciated during the course of this work. Support was provided by a National Aeronautics and Space Administration Grant NSG-24.

TABLE OF CONTENTS

LIST OF TABLES

LIST OF FIGURES

ABSTRACT

This paper describes a method for obtaining total columnar electron content of the ionosphere from Faraday rotation data on closely spaced frequencies. The method is applied to Faraday fading signals received at the University of Illinois tracking station in Urbana, Illinois from the polar orbiting satellite, Explorer 22. Approximately five months of these data (October 1964 to March 1965) have been analyzed. The content results are presented in the form of diurnal variation and constant electron content contours as a function of latitude and time. Also investigated are variations of electron content with respect to sunrise effects and planetary magnetic index.

1. INTRODUCTION

The ionosphere has been the subject of much study since 1902 when Oliver Heaviside postulated that ions in the upper atmosphere were responsible for Marconi's successful transatlantic radio transmission [Ratcliffe, 1959]. The ionosphere is thought to be made up of layers as is the atmosphere. The layers or regions as they are called shall not be distinguished in this paper since the total columnar electron content measured sums all the electrons in a square meter column extending from the ground to a satellite orbiting above the peak of electron density in the upper layer of the ionosphere. The F-region contains the peak electron density and is the major contributor to the total electron content. Although electron content does not directly give information about the distribution of the ionized layers along the ray path, it can be used as an aid in understanding the factors which effect the ionosphere and in turn radio wave propagation which is ionosphere dependent. Electron content is known to vary diurnally, seasonally and with the solar cycle. The period of time included in this study runs from October 1964 to March 1965 when the sunspot number is just beginning to increase from minimum.

The ionosphere is a birefringent medium. At the satellite signal frequencies concerned, the phase velocities are different for the ordinary and extraordinary waves of a signal in the ionosphere. This difference in phase velocity rotates the plane of polarization of a plane polarized wave as it passes through the ionosphere. Michael Faraday discovered this phenomenon in a laboratory experiment with polarized light more than a hundred years ago; it is now called the Faraday effect.

The ionospheric Faraday rotation is dependent on the earth's magnetic field, signal frequency and the number of free electrons encountered along the path of the signal. The satellite signals monitored for Faraday rotation are received on linearly polarized dipole antennas thus a null is detected every time the plane of polarization rotates 180^{o}, one half-rotation. Two frequencies are used to determine the actual number of rotations which have occurred along the path from the satellite to the receiving station.

The Faraday fading detected in the receiver automatic gain control circuit is recorded on a strip chart recorder in order to determine null occurrence as a function of time.

The satellite used for this experiment was Explorer 22 also known as S-66 or BE-B. The more important information of this satellite is given in the following:

Launch date	October 10, 1964
Period	104.75 minutes
Inclination	79.69 degrees
Apogee	1080 Km
Perigee	886 Km
Signals received	20.0, 40.0, 41.0, and 360.0 MHz

There are several characteristics of the satellite and its orbit worth noting here. The inclination is nearly 80^{o} and thus the satellite travels approximately in a north-south direction at mid-latitudes. The highly polar orbit yields a good latitude cross section while on the other hand minimizes longitudinal effects at times other than sunrise and sunset. The rapid change in latitude for a satellite pass gives rise to large changes in $\overline{M}$.

The change in $\bar{M}$ generally makes the total Faraday rotation a decreasing function of time for a north bound pass and an increasing function of time for a south bound pass.

Generally, one north bound and one south bound satellite pass was observed each day for the above mentioned period. The average time for the occurrence of a satellite pass decreased each day thus the diurnal variation could be observed for both north and south bound passes.

Finally, the transmitted frequencies at 40 and 41 MHz were chosen for this experiment so that one could assume equal path and also Faraday rotation ambiguity can be nearly always eliminated at sunspot minimum. The ambiguity in rotation has been a troublesome problem in many experiments and we shall discuss this problem later.

2. THEORY OF MEASUREMENTS

The theory applied is based on the quasi-longitudinal approximation of the Appleton-Hartree Equation for the refractive index of the ionosphere. The equation for the Faraday rotation of the plane of polarization in the ionosphere is:

$$\Omega = \frac{K}{f^2} \int NMdh \quad \text{radians} \tag{1}$$

where

$K = 2.97 \times 10^{-2}$ in rationalized MKS units.

f = frequency of signal in Hz.

N = electron density.

$M = H \sec i \cos \Theta$.

H = intensity of the geomagnetic field.

i = angle between ray path and vertical.

Θ = angle between ray path and geomagnetic field.

dh = differential height element.

Since M is a slowly varying function, it is taken outside of the integral and evaluated at a mean ionospheric height. Equation (1) now becomes

$$\Omega = \frac{K}{f^2} \bar{M} \int Ndh \tag{2}$$

where

$\int Ndh$ = the integrated electron content.

$\bar{M}$ = M evaluated at mean height.

The mean height used to evaluate M was chosen on the basis of an ionosphere model study by Yeh and Gonzalez [1960]. Restricting the zenith angle to less than 40^{o}, the optimum value for the mean height is 350 Km. Certain passes were rejected when the zenith angle limitation was severely violated. The first order equation shall be applied to two frequencies to find the actual number of rotations for one frequency. Writing Equation (2) for two frequencies at the same time in units of half-rotations where $R = \Omega/\pi$ gives

$$R_1 = \frac{K\bar{M}}{\pi f_1^2} \int Ndh \ , \qquad R_2 = \frac{K\bar{M}}{\pi f_2^2} \int Ndh \ .$$

The differential Faraday rotation can be found by subtraction

$$R_1 - R_2 = \Delta R = \frac{K\bar{M}}{\pi} \int Ndh \left[\frac{1}{f_1^2} - \frac{1}{f_2^2}\right] . \tag{3}$$

Now divide R_1 by ΔR keeping in mind that $\bar{M}$ and $\int Ndh$ are at the same time and will cancel leaving the constant ratio of single frequency Faraday rotation to differential rotation

$$\frac{R_1}{\Delta R} = \frac{f_2^2}{f_2^2 - f_1^2} \ . \tag{4}$$

The right side of Equation (4) is approximately 20.75 when $f_1 = 40$ and $f_2 = 41$.

Below is a list of assumptions made in the theory:

1. Plane earth.
2. Plane ionosphere represented by a horizontally stratified layer at some mean ionospheric height above the earth but below the satellite.

3. High frequency, i.e. refraction neglected.
4. Satellite height change has negligible effect.
5. Satellite antenna orientation does not change with respect to receiving antenna during a pass, e.g. neglect satellite spin.
6. Polarization of transmitted signals at different frequencies are the same at the satellite antenna.

Limitation of these assumptions have been discussed in the literature and hence shall not be repeated here [Arendt, Papayoanou and Soicher, 1965; Garriott and de Mendonca, 1963; Yeh and Swenson, 1961].

3. ELECTRON CONTENT CALCULATION

The calculation of satellite ephemeris and $\overline{M}$, the earth's magnetic field contribution, have been programmed and are used as subroutines in a computer program to calculate electron content as described in this section. The computer used is the IBM 7094-1401 at the University of Illinois. The satellite tracking station is also located near the University and has geographic coordinates of 40.1^{o} north and 88.2^{o} west.

The Faraday rotation null times are recorded and punched on data cards for each pass. The data cards are read into the computer and stored in arrays. Null times can be recorded in hours, minutes and seconds (HH MM SS.S) or in chart divisions using a reference time on the record and a division scale. The null times for each frequency are now consecutively numbered and put into two tables so that differential rotation can be calculated using an interpolation routine available in the computer subroutine library.

To calculate differential rotation at 40 MHz nulls, some type of interpolation is required for the 41 MHz rotation between nulls. Linear interpolation is not enough for most of the passes, therefore, a higher order interpolation is used. The interpolation routine passes a curve through 41 MHz null numbers versus time of null occurrence. Assuming that Faraday rotation decreases to the north and increases to the south, the differential rotation is calculated for each 40 MHz null time. The ambiguity of the integral number of half-rotations between 40 and 41 MHz nulls can usually be eliminated during quiet sun conditions to obtain the correct differential rotation.

Now that the differential rotation is calculated for all the 40 MHz nulls, the actual value of rotation can be found for each of these nulls using the

constant ratio of differential rotation to actual rotation, given by Equation (4). Notice that there should be one half-rotation difference going from one null to the next, assuming there are no reversals of Faraday rotation.

Since the electron content profile is of major interest, the Faraday rotation values for each 40 MHz null in a pass must be consistent in that pass, i.e. there must be one half-rotation between adjacent nulls in order for a consistent electron content profile, again assuming no Faraday rotation reversals.

If the number of rotations from satellite to ground is known for one null in a pass, then the proper number of rotations can be added or subtracted to determine the number of rotations for all other nulls in a pass. The following technique is used to find the number of rotations which should be assigned to one 40 MHz null in the pass.

Consider a pass which should have decreasing rotations to the north. Thus the southern most null has the highest number of half-rotations. The next null going north should have one half-rotation less than the first and so on to the north end of the pass, each null having one half less rotations than the previous null. Let R_i be the number of half-rotations calculated using differential Faraday for the i th null in the pass counting from south to north, i.e. R_1 is the southern most null in the pass. To compare the number of half-rotations of the first null with any other null add i - 1 half-rotations to R_i. The simple average value of the R_i + i - 1 terms yields a value for the southern most null of the pass which can be used to determine the number of rotations for all other 40 MHz nulls in the pass.

The new values for R_i are now calculated and set up in an interpolation table so that the number of 40 MHz half-rotations can be found for any time

during the pass.

The electron content can be calculated for any time in the pass using R(t), interpolated half-rotations, since $\Omega(t) = \pi R(t)$ and $\int Ndh = \frac{f^2}{K\bar{M}} \Omega(t)$.

The number of half-rotations calculated for the 40 MHz null times before averaging were compared with the value calculated at the point of closest approach. First, the number of half-rotations were calculated at each 40 MHz null, and the value for the null occurring nearest to the point of closest approach was used to renumber the half rotations at the other null times. The percent of difference between the original number and the referred number of half-rotations was computed at each null. Figure 1 shows some typical examples of percent of difference plotted versus zenith angle of the satellite. The above procedure is not an attempt to justify the averaging technique but only to show the order of deviations which occur when calculating differential Faraday rotation at several null times in a pass. A certain amount of the deviation can be attributed to scaling and interpolation errors; however, some discrepancy still remains after these errors have been accounted for, thus the averaging was used as a compromise of the existing situation. Resolution of the discrepancy could possibly come about through careful ray tracing techniques since the problem may be due to unequal signal path for the two frequencies used to calculate differential Faraday rotation. Other possible causes for such errors might be transmitting antenna orientation changes due to satellite spin and also path splitting between ordinary and extraordinary rays.

Below is a typical example of how the computer program determines the actual number of half-rotations from satellite to ground. The pass used in

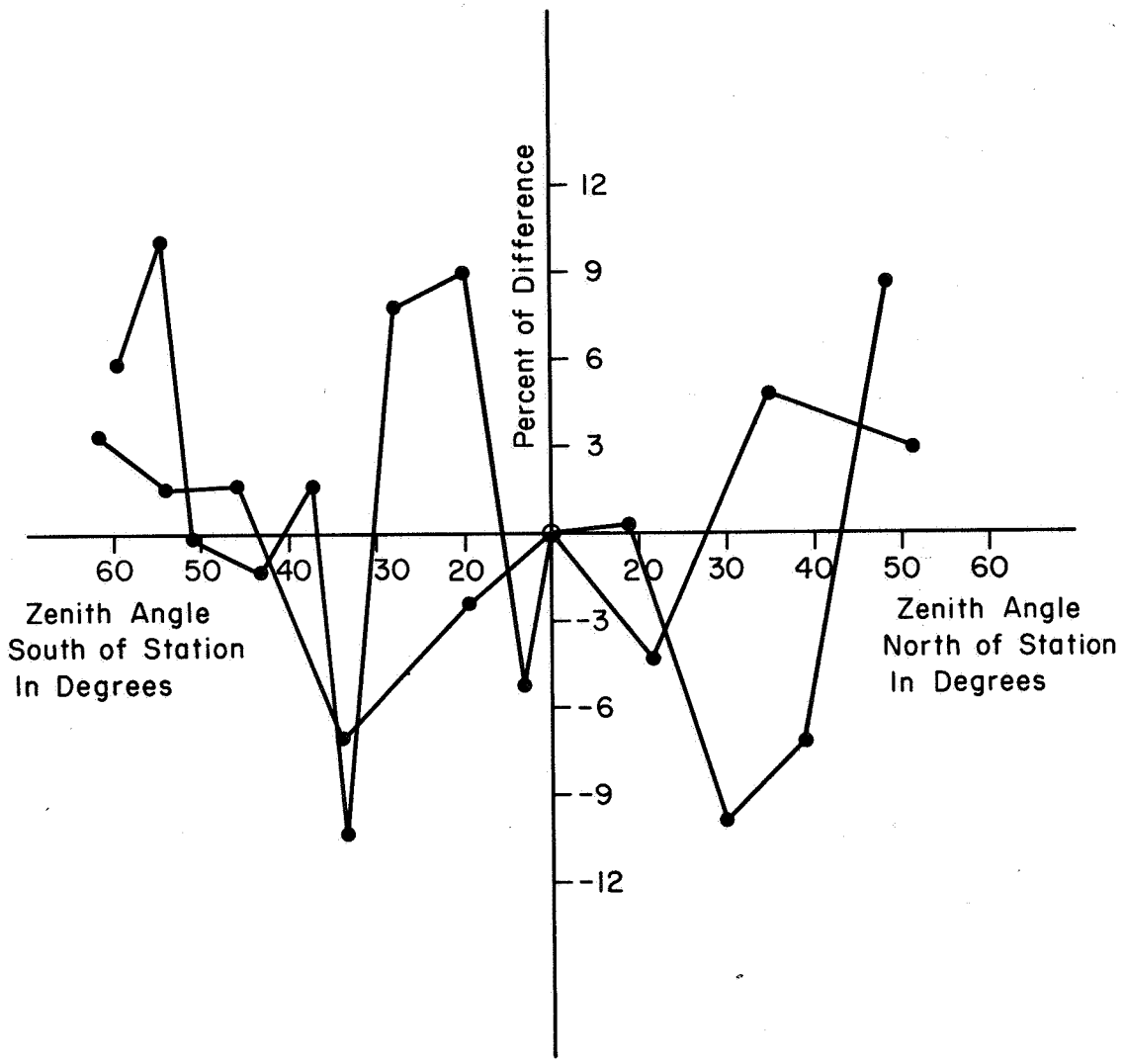

Figure 1. Comparison of actual number of half-rotations calculated at several nulls in a pass with values calculated for null of closest approach. Result for two passes shown.

this example was recorded at Urbana, Illinois on December 21, 1964. The null times are shown in Table 1 along with their respective numbers P_{40} and P_{41}. The initial null numbers, P_{40} and P_{41} simply start with the first null of the pass and are numbered consecutively to the end. Determining differential rotation from the initial null numbering must take into account the direction of the pass since we have assumed rotation decreases to the north. The pass for this example is south bound, thus differential rotation at 40 MHz null times can be calculated by subtracting the interpolated value of 41 MHz numbers from the 40 MHz number; however, one half-rotation must be added in this case since 40 MHz rotations are always greater than 41 MHz rotations, i.e. differential rotation must be positive. Differential rotations for 40 MHz null times are listed in Column 5 of the table.

Column 6 of the table lists the first approximation of the number of half-rotations in the pass. For a north bound pass the first null has the highest number of half-rotations. In this example, the last null has the largest number, therefore the proper number of half-rotations are added to each rotational value resulting in the list in Column 7. By taking the common average of Column 7, one obtains a weighted value of half-rotations for the southern most null in the pass. The weighted value of half-rotations is now used to renumber the 40 MHz nulls and these values shown in Column 8 are used to calculate the electron content profile. Figure 2 is a representation of Faraday fading as recorded on 40 and 41 MHz. The initial numbering is shown for both frequencies and calculated values for 40 MHz null times are shown taken from the table.

As mentioned previously, the number of half-rotations at the 40 MHz null times are used to find the Faraday rotation as a function of time for the pass.

Table 1. Example Pass December 21, 1964

NULL TIMES							
41 MHz HHMMSS.S	P_{41}	40 MHz HHMMSS.S	P_{40}	Differential Rotation calculated at 40 MHz null times (ΔR)	First approx. of number of 40 MHz half-rotations ($20.75 \times \Delta R$)	Column at left refered to highest number of half-rotations by adding $14 - P_{40}$	Renumbered 40 MHz null times
085522.7	1	085534.9	1	0.538	11.159	24.159	10.333
085550.6	2	085608.0	2	0.500	10.379	22.379	11.333
085627.0	3	085645.3	3	0.530	10.991	21.991	12.333
085705.5	4	085718.9	4	0.638	13.240	23.240	13.333
085741.5	5	085752.0	5	0.684	14.186	23.186	14.333
085815.3	6	085826.7	6	0.691	14.345	22.345	15.333
085851.3	7	085856.4	7	0.856	17.764	24.764	16.333
085916.1	8	085917.8	8	0.892	18.514	24.514	17.333
085931.4	9	085935.1	9	0.786	16.299	21.299	18.333
085951.2	10	085952.5	10	0.940	19.507	23.507	19.333
090015.3	11	090016.6	11	0.959	19.901	22.901	20.333
090051.0	12	090050.4	12	1.020	21.165	23.165	21.333
090113.5	13	090111.0	13	1.137	23.584	24.584	22.333
090129.9	14	090127.1	14	1.187	24.629	24.629	23.333
					Total	326.663	
					Average	23.333	

By calculating $\overline{M}$ at the mean ionospheric height, one can find electron content from Equation (2). The computer output lists date, electron content, subionospheric latitude and longitude, satellite zenith angle, the number of half-rotations and the time of calculation for the desired number of points in the pass. The subionospheric latitude and longitude are the coordinates of the ionospheric point which is the intersection point of a line from the satellite to the receiving station and a shell 350 Km above the earth. Unless stated otherwise, any further mention of latitude and longitude implies the above mentioned subionospheric coordinates.

Electron content versus latitude are plotted on a CALCOMP plotting machine and also punched on cards so that further plotting can be done by machine. Figures 3, 4 and 5 are examples of passes which have been grouped and plotted by machine. The annotation on each curve is placed at the end of the pass, thus pass directions can be determined by the placement of the annotation. A north bound pass is annotated at the northern end of the pass. The annotation gives date and Central Standard Time. The six digit number is the year, month and day. The number below is the time of the beginning of the pass. The time is left justified below the date with no preceeding zeros, e.g. 130 means one hour, thirty minutes. The label below the graph also shows time with no preceeding zeros.

When the zenith angle of the satellite becomes greater than 40^{o}, the electron content is drawn as a dotted line with the best portion of the pass drawn as a solid line.

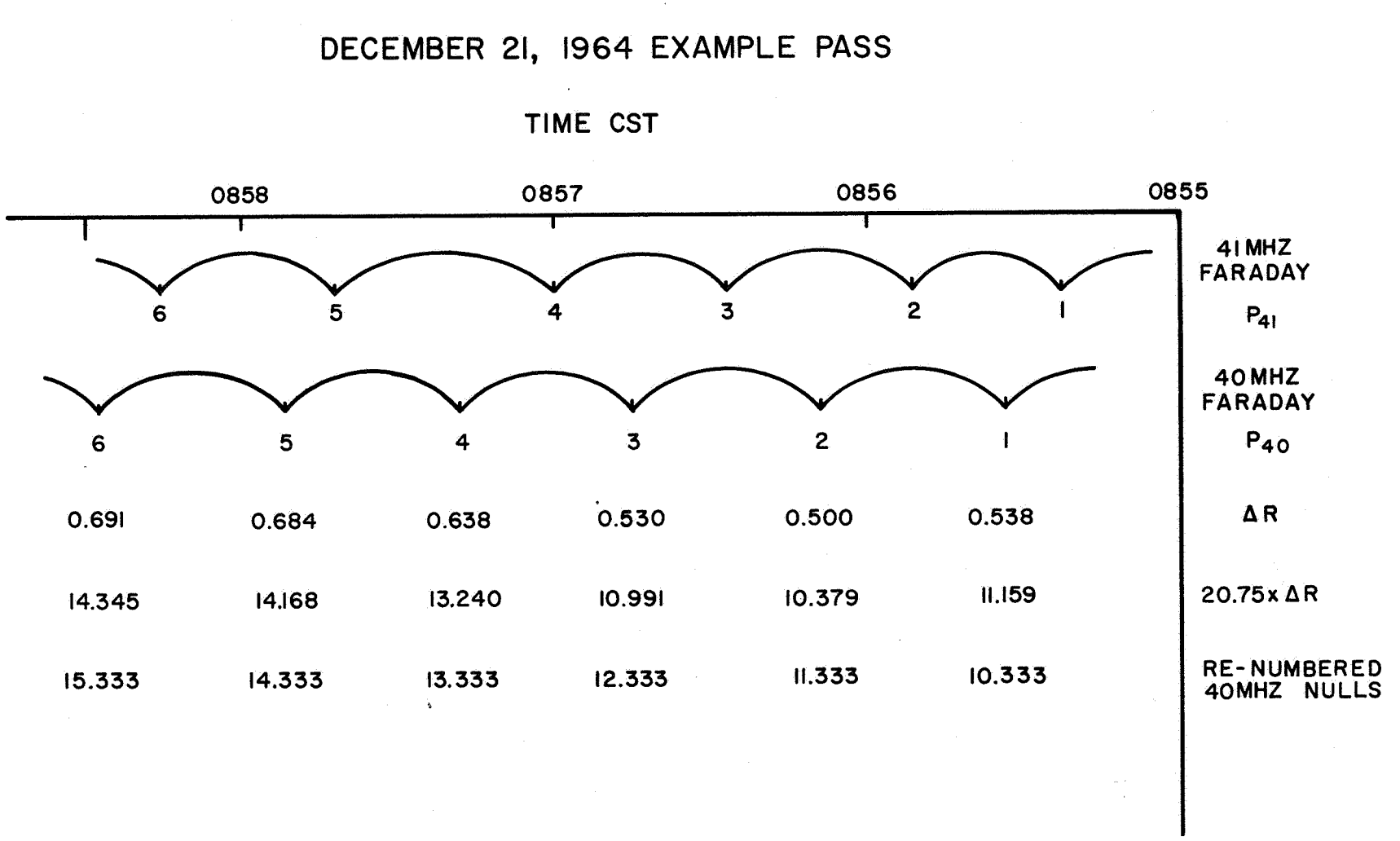

Figure 2. Partial representation of strip chart recording of Faraday fading on 40 and 41 MHz with initial numbering for both frequencies and calculated numbering of 40 MHz null times taken from Table 1 described in text.

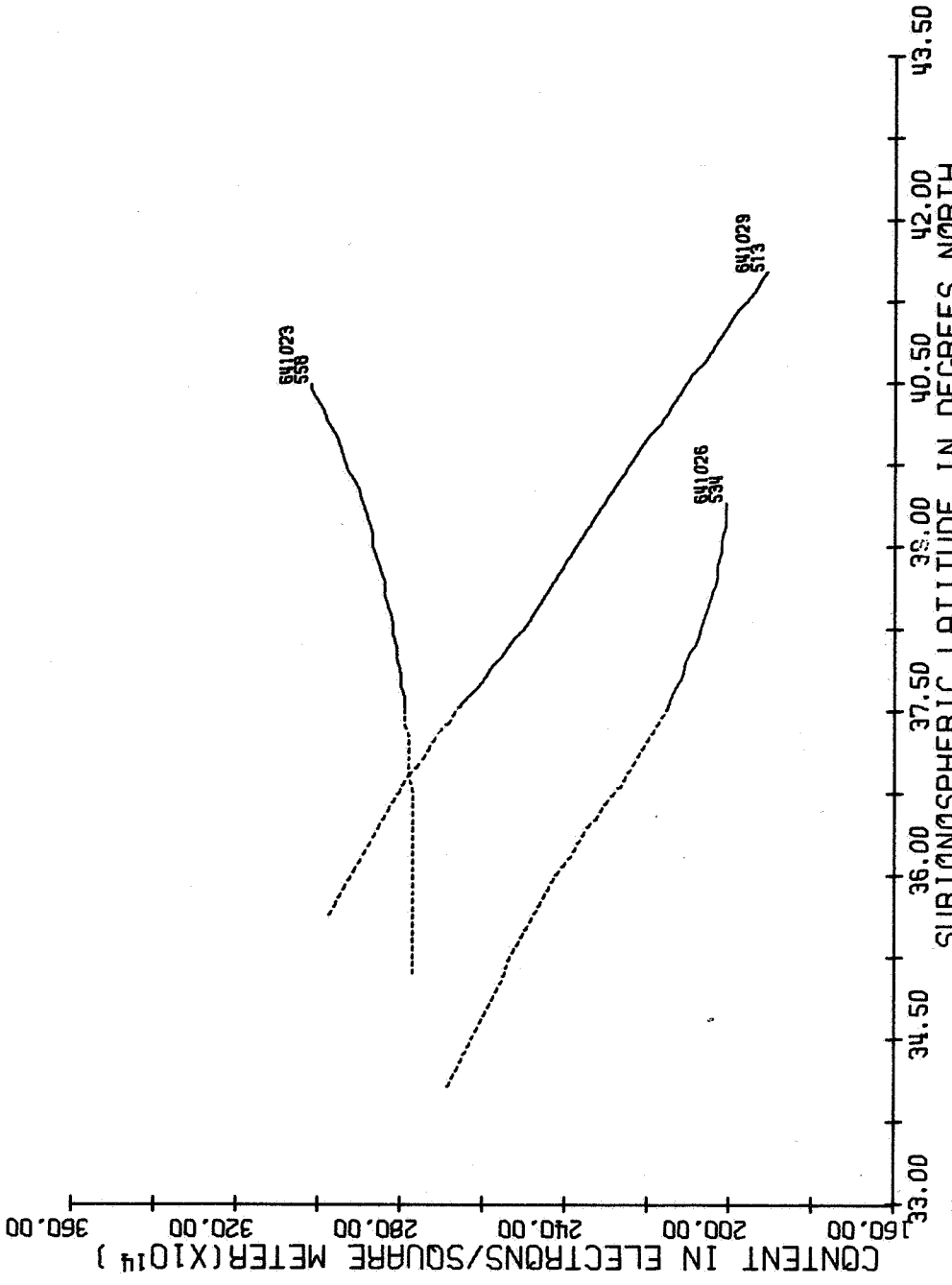

Figure 3. North bound passes during sunrise 0500 to 0600 CST (CALCOMP output).

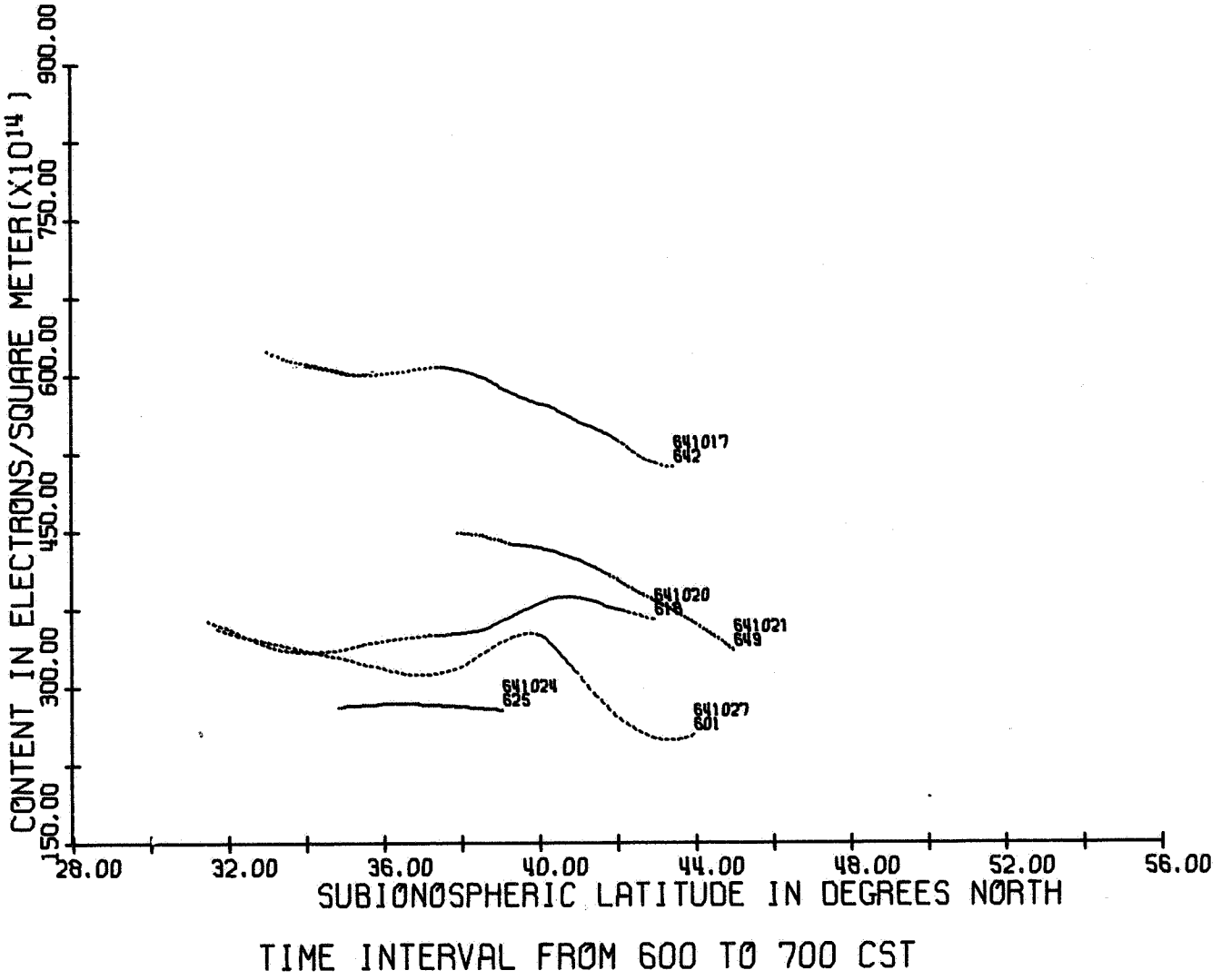

Figure 4. North bound passes during sunrise 0600 to 0700 CST (CALCOMP output).

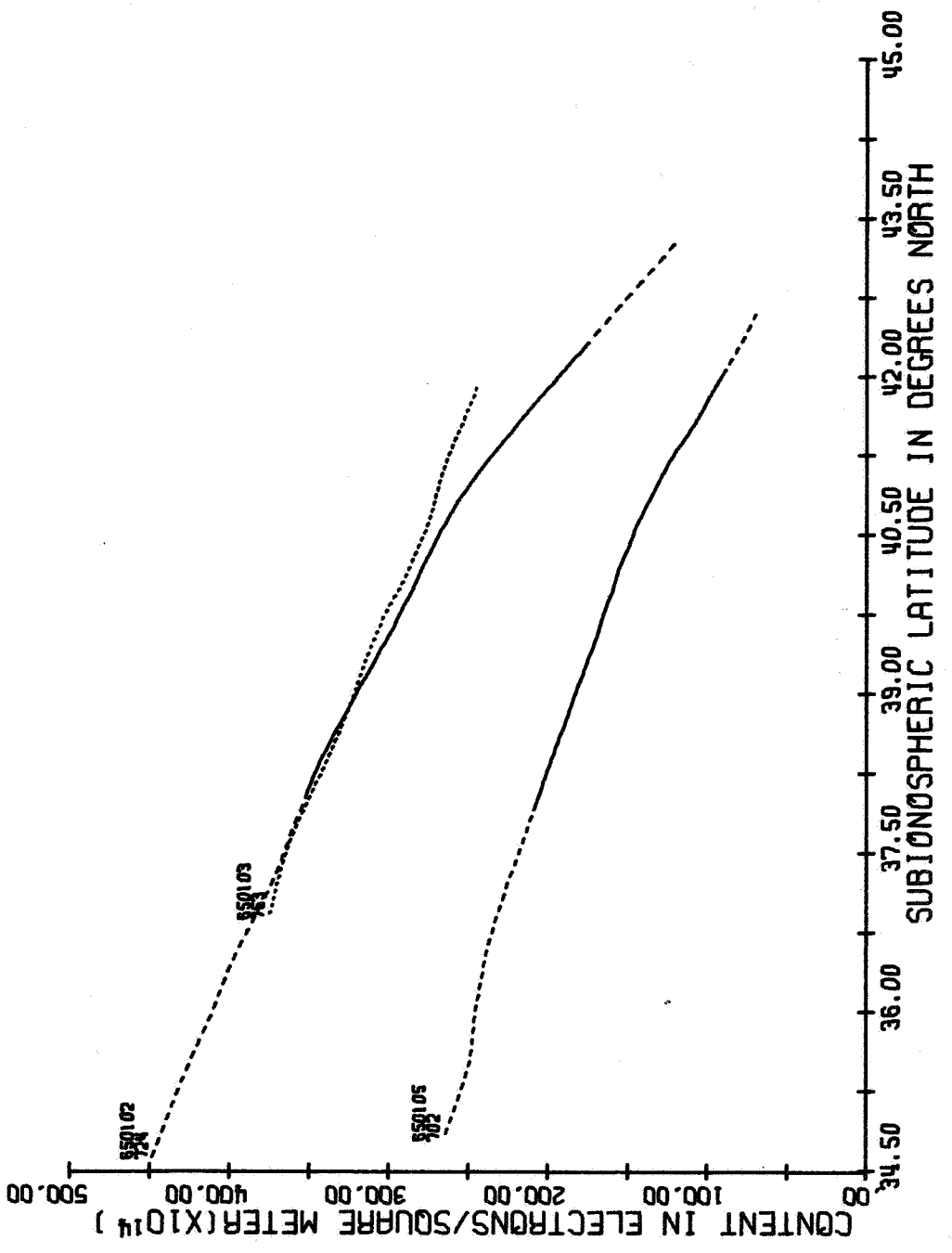

Figure 5. South bound passes during sunrise 0700 to 0800 CST (CALCOMP output).

4. RESULTS

Aspects investigated include diurnal variation of columnar electron content, constant content contours, morning content gradients and electron content correlation with magnetic indices.

4.1 Diurnal Variation

To obtain diurnal variation, electron content at 40^{o} north subionospheric latitude has been plotted versus time. Two diurnal variations are presented in Figures 6 and 7 representing south bound and north bound satellite passes respectively. The months from which the data were taken are also shown so that seasonal effects may be considered along with diurnal variations.

The sunrise and sunset effects appear much as was expected with sunrise occuring at the point of increasing electron content and sunset taking place about where content is midway between maximum and minimum for the day. Portions of the diurnal variations corresponding to sunrise and sunset are similar in both cases; however, two noticeable differences occur during midday hours. The midday values for north bound passes are higher and more dispersed than the south bound values. The south bound midday passes were recorded in November while the north bound passes were recorded in February and March, thus the midday content difference could be partly due to seasonal anomaly and to the lower sunspot number in November. This observation was also made by Solomon [1965] in a similar study concerning the same period of time.

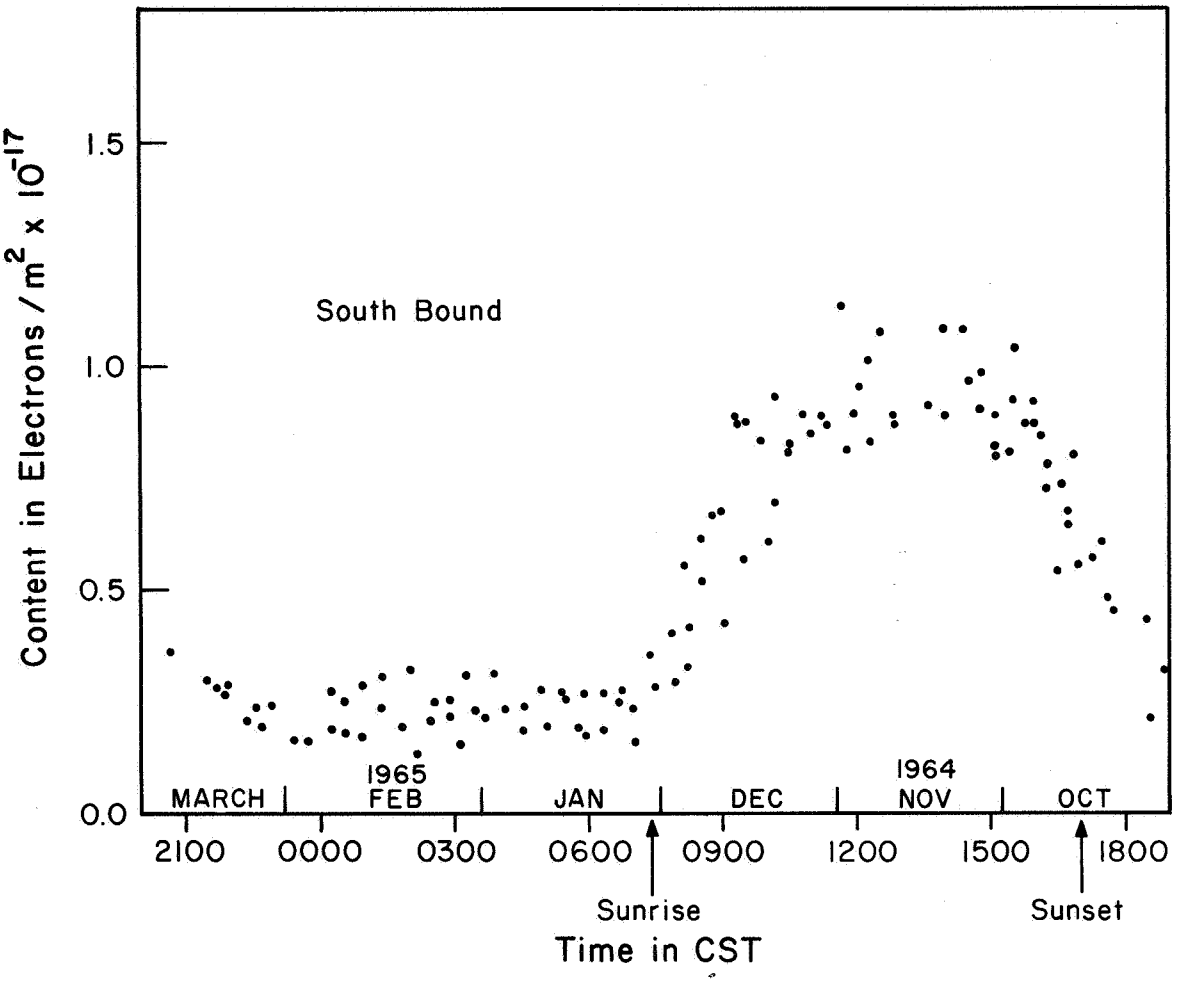

Figure 6. Diurnal variation obtained from south bound passes.

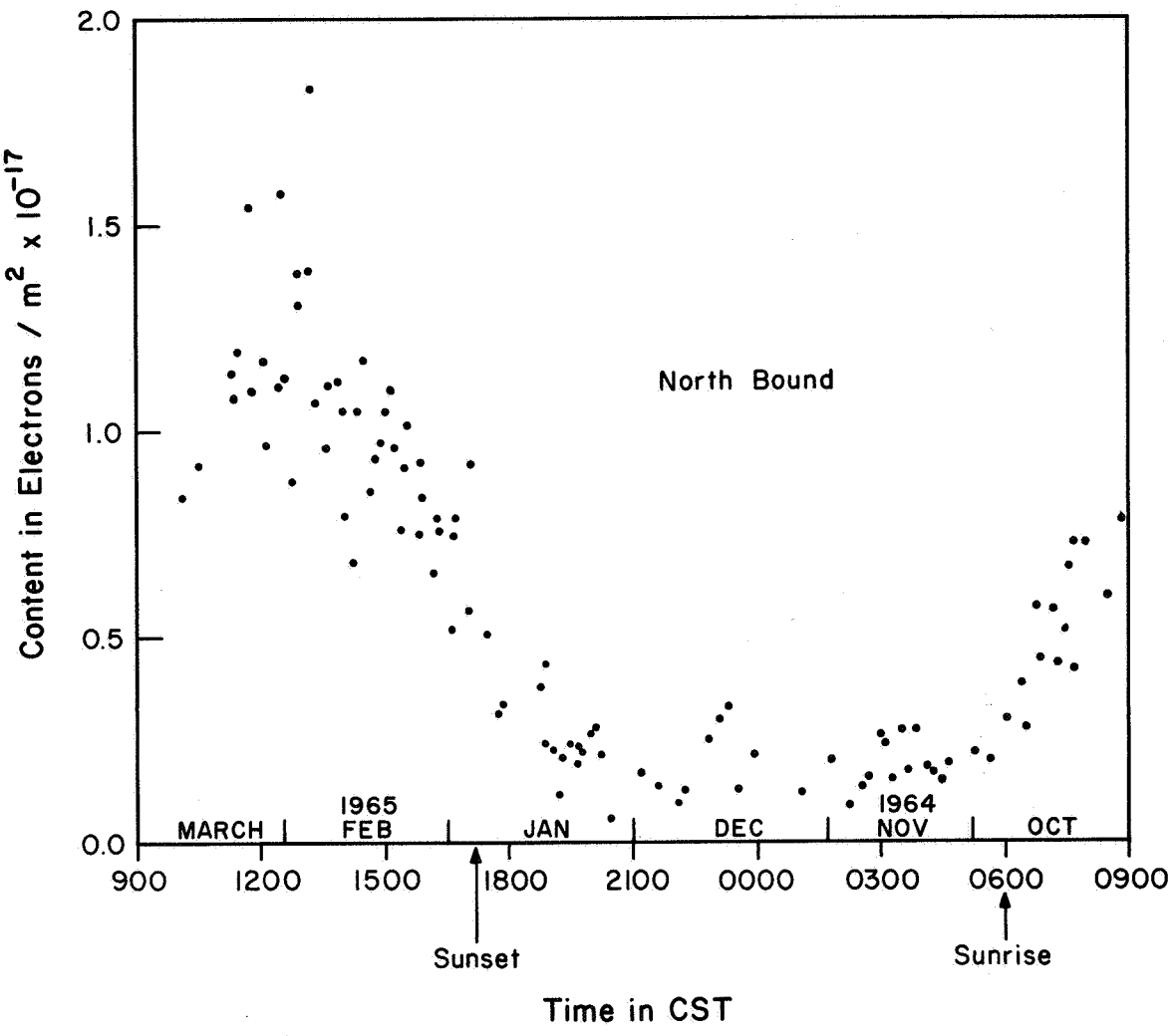

Figure 7. Diurnal variation obtained from north bound passes.

4.2 Constant Electron Content Contours

The constant electron content contours shown in Figures 8 and 9 are a result of grouping and averaging electron content versus latitude curves. The procedure for drawing the constant content contours is given below. First the six months data were divided into two main groups: group one included data from October through December; group two included data from January through March. Each seasonal group was processed separately resulting in the two Figures 8 and 9.

Considering data from group one, notice that we will have electron content versus latitude curves calculated for satellite passes which have occurred at many different times of the day during the three month period. The passes of group one are now sorted and electron content versus latitude plotted according to which hour of the day the satellite pass was recorded. In three months time, several content versus latitude curves usually occur during the same hour of the day. A smooth average curve is drawn to represent all the electron content curves as a function of latitude for a particular hour of the day. With an average electron content curve for each hour interval of the day, one can proceed to draw contours of constant content as a function of latitude and hour of the day.

A simple procedure for drawing contours is to choose a value of content which lies in the range of several neighboring hour average curves and plot points corresponding to content, latitude, and hour on coordinates of latitude and hours. Constant content lines are drawn off scale when the average content for the next hour interval appears to be converging to some latitude off scale. The actual shape of content contour is not as important as the

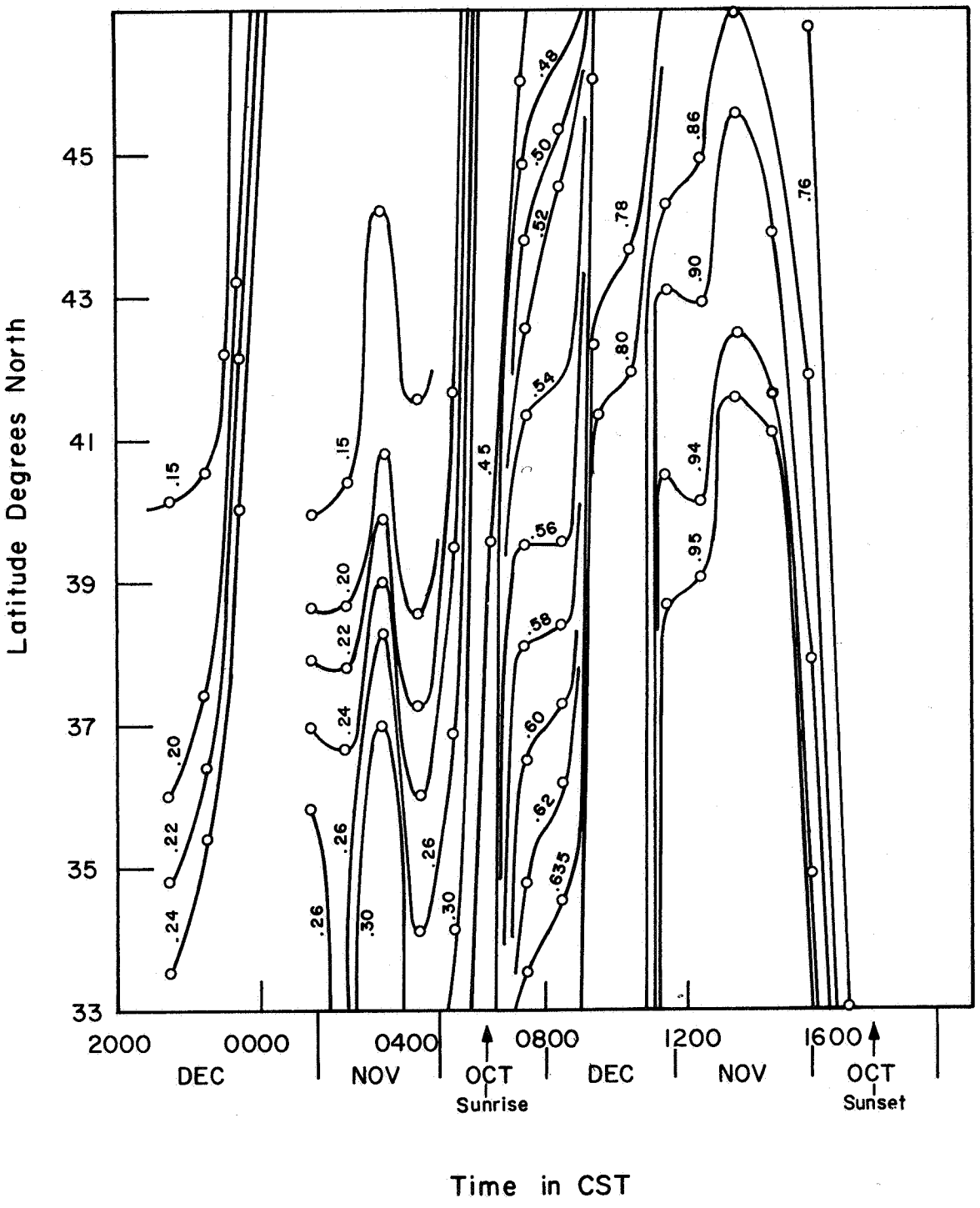

Figure 8. Constant electron content contours obtained from both north and south bound passes (contour units are 10^{17} elec/m^2).

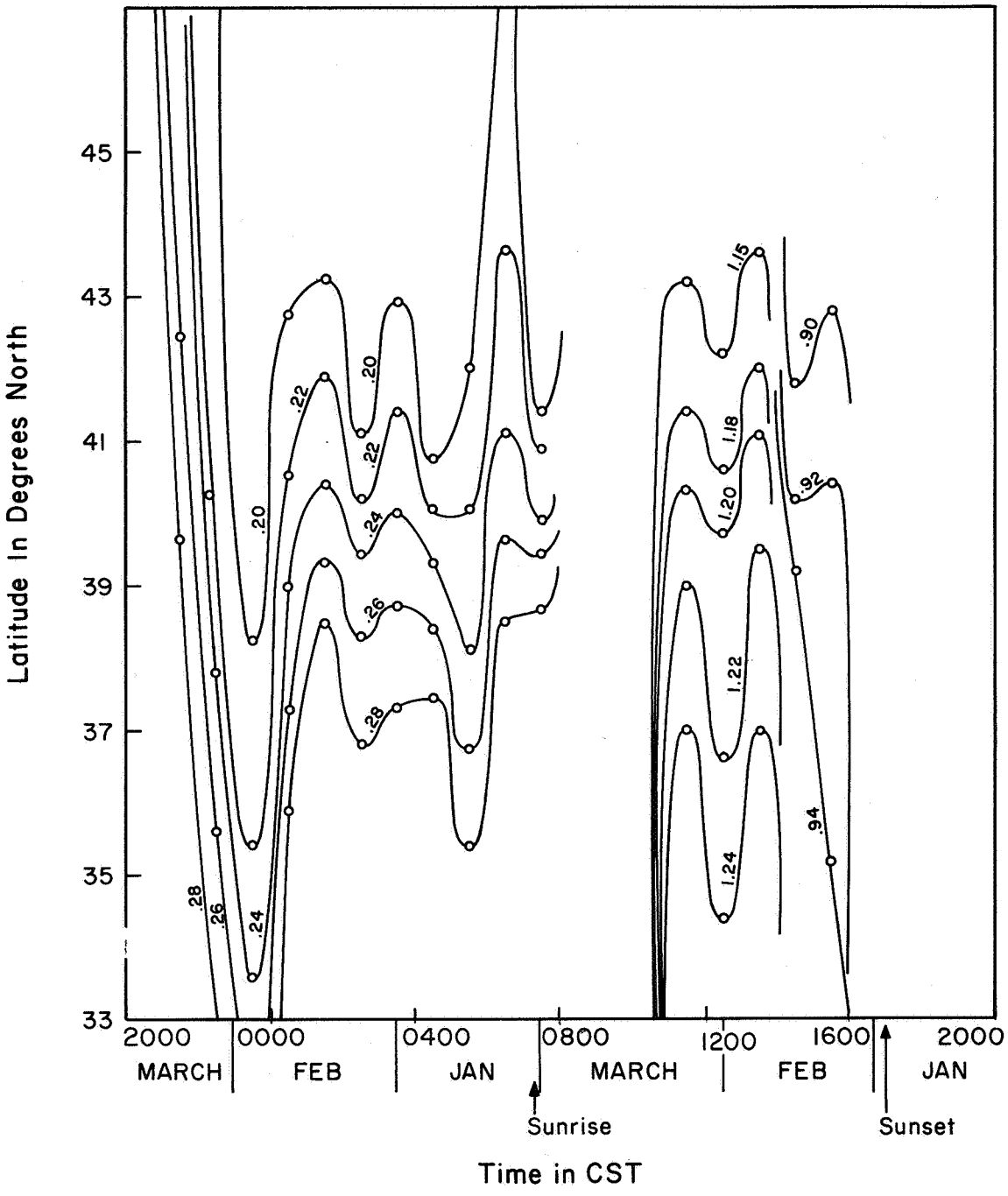

Figure 9. Constant electron content contours obtained from both north and south bound passes (contour units are 10^{17} elec/m^2).

plotted points. These lines connecting the points serve to indicate the point value more conveniently.

The contours may be confusing at first since content variations appear distorted unless one notices the contour values objectively. The mere ability to draw contours without running off the scale indicates that the average electron content is fairly constant for the period of time involved. The period of time from 0000 to 0700 of Figure 9 illustrates the relatively constant content of the ionosphere at that time. Content during the same period shown on the diurnal curve of Figure 6 also appears constant.

Comparing both Figures 8 and 9, one finds the expected midday peak leveling after the sunrise increase. The afternoon recession of electron content begins slightly after local noon. Some intervals of the day have been omitted due to insufficient data; however, in spite of the omissions an anomaly appears around midnight on both contour plots. Since a small number of passes were analyzed for these periods, one can not make a definite statement about causes or existance of such an anomaly. It should be noted that night anomalies have been observed by others during winter months [Arendt and Soicher, 1964; Evans, 1965; Rastogi, 1960] and also that the increase after midnight in Figure 9 occurs at the approximate sunrise time for the magnetic conjugate point of the receiving station.

By observing the number of degrees latitude between constant content points for a particular hour, one can acquire a feeling for the gradient of the average electron content versus latitude curve of that hour. Comparing gradients of the different hour intervals of Figure 9, the 0700 to 0800 interval has a very high content versus latitude gradient indicated by closer

spacing of content points along a line of constant time. This period is an average of content plots during sunrise which shall be discussed in detail later.

4.3 Morning Gradients

The morning passes observed all occurred when the sun rose earlier at the southern end of the pass. The constant content contours in Figure 9 are very closely spaced during sunrise, however Figure 8 does not agree in that the contours are widely spaced at sunrise; thus, Figure 9 indicates steep content versus latitude slopes while Figure 8 displays almost no slope.

The morning passes averaged to obtain Figures 8 and 9 differ by two important factors which are pass direction and the seasonal difference. North bound passes during sunrise period occurred in October. For a typical north bound pass, it takes 3 1/2 minutes for 5^{o} change in subionospheric latitude and 1^{o} change in subionospheric longitude in the eastward direction, thus one has a change in local time of 7 1/2 minutes for 5^{o} in subionospheric latitude. The difference in sunrise time from 35 to 40^{o} north latitude is approximately 7 minutes in October which explains the relatively constant electron content curves of Figure 4. Thus, if morning gradients are entirely due to sunrise effects, one might expect all north bound morning passes to have content profiles with small gradients and some passes to have increasing content to the north for the season involved in this case. The reason to expect increasing content to the north is that the local time change can be greater than the difference in sunrise time for the duration of the pass. Such a case occurred on October 23, 1964 shown in Figure 3 when the local

time change was greater than sunrise time difference (also this was an extremely quiet day magnetically, e.g. 24 hour K_p sum was equal to 1_o). Some of the passes in Figure 4 also show increasing content to the north while others do not. To get a better picture of these passes with respect to sunrise, Figure 10 was drawn. Figure 10 shows the subionospheric latitude versus local time for the passes of Figures 3 and 4, also the ground sunrise line has been drawn. The area to the right of the sunrise line has been illuminated while that to the left is still in darkness at the ground level. The sunrise line was calculated for October 23 and moves to the right about one minute per day, thus the change is not critical for the purpose intended here. The passes drawn as solid lines in Figure 10 seem to have been effected most by the sunrise effect with the exception of the 641027 pass which shows an abrupt change at 40^{o}N where considerable scintillation appeared on the record possibly indicating the presence of an irregularity in the ionosphere.

In contrast to the north bound sunrise passes, Figure 5 shows south bound passes which occurred during the January sunrise period. The slopes are much greater than those which were found for the north bound passes. Figure 11 was drawn for the January sunrise in the same manner as Figure 10. Notice how the path of the satellite cuts across the ground sunrise line for two of the cases shown giving more reason for the steep gradients. Sunrise lines were drawn using sunrise times computed by Colin and Myers [1966].

4.4 Magnetic Index Correlation

The months of January and February yielded many well behaved content values during the night passes. This period of time was examined carefully

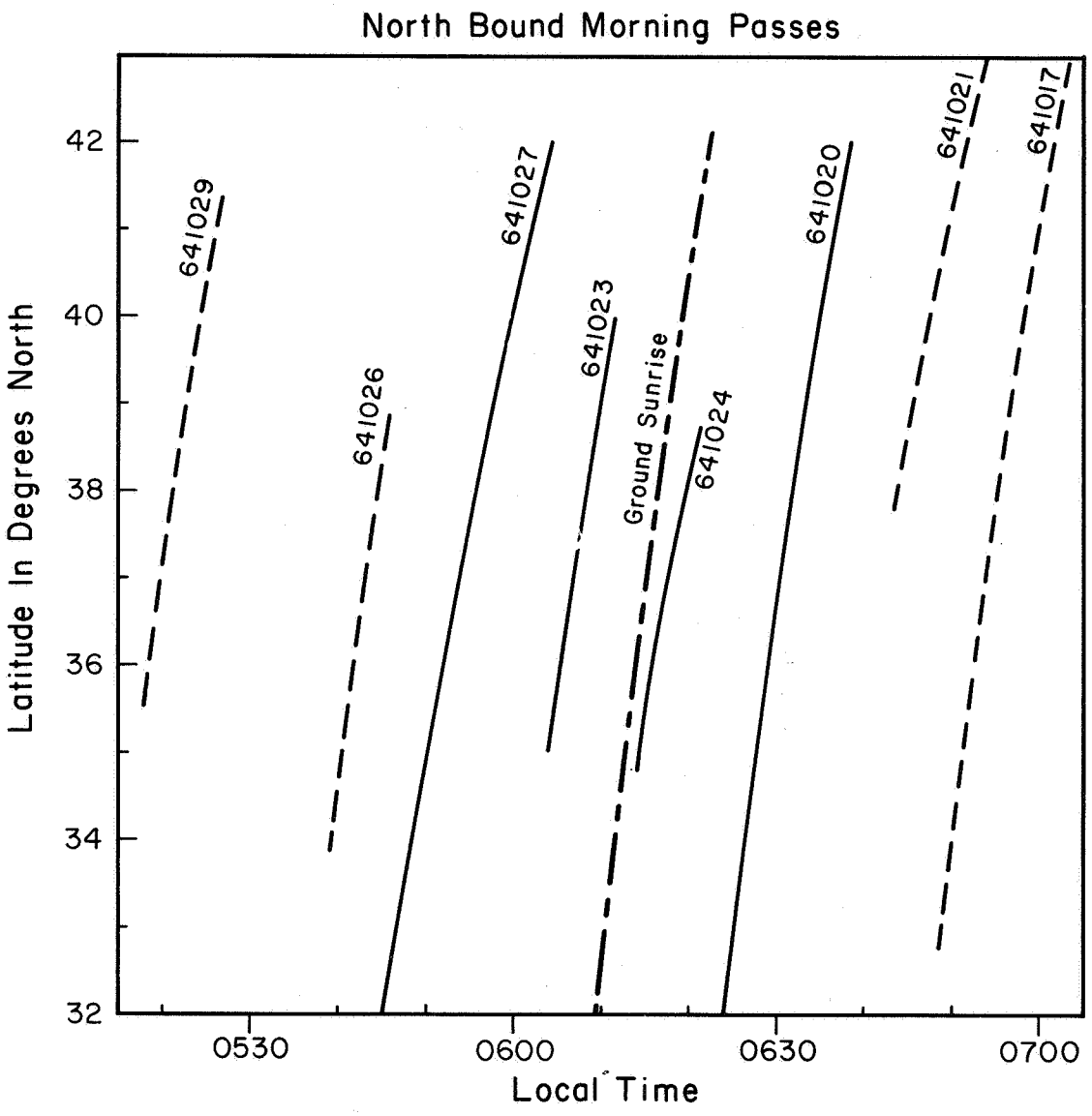

Figure 10. Subionospheric path for each north bound pass in Figures 3 and 4 plotted with ground sunrise line.

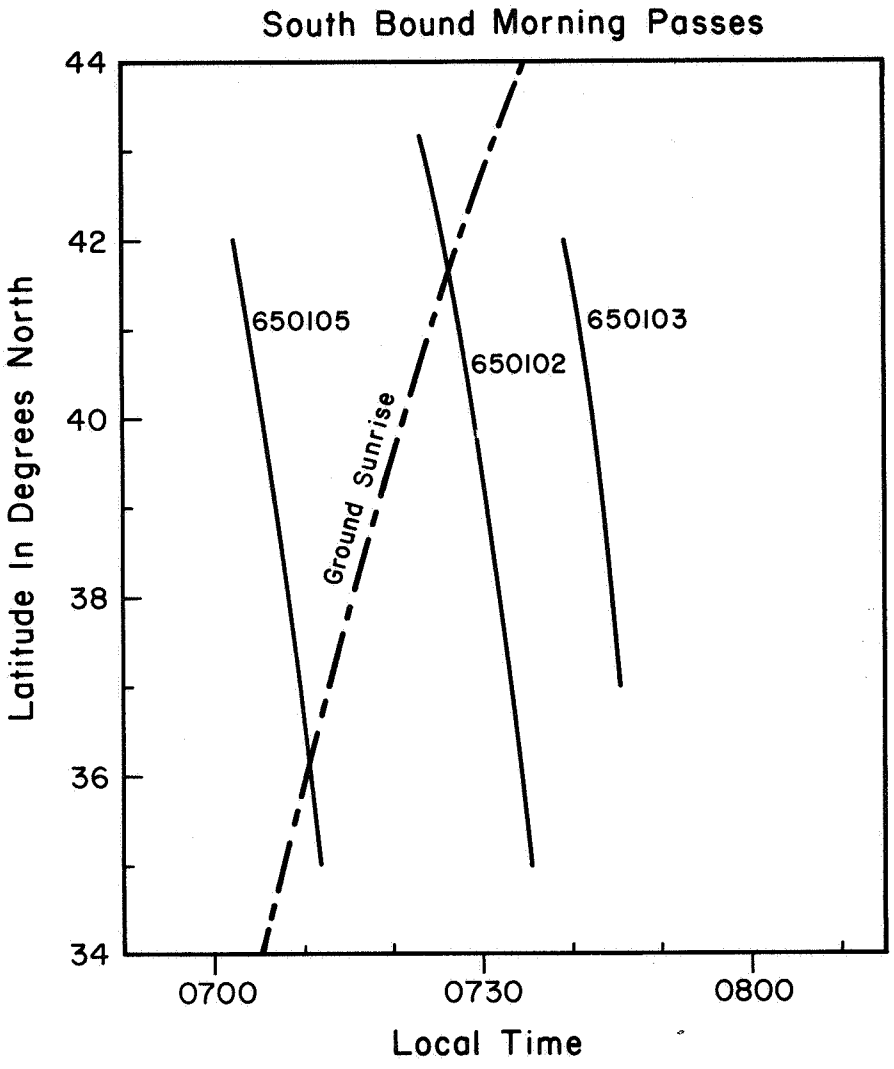

Figure 11. Subionospheric path for each south bound pass in Figure 5 plotted with ground sunrise line.

for any correlation of electron content with several magnetic indices. Electron content was plotted versus date; the magnetic index was plotted below the content curve so comparisons could be made. Also magnetic indices were plotted on one sheet and an electron content curve laid over the magnetic index curve for closer comparisons. The three hour range indices of K_p were plotted taking into consideration intervals during and before the time of content calculation. Frederickburg's three hour range K values were also considered in a similar manner. Twenty four hour K_p sums were also tried. None of the above procedures produced a satisfactory correlation; however, observing the ten quiet days (Q or q) and the five disturbed days (D) selected by the Committee on Characterization of Magnetic Disturbances, it was found that quiet days usually had lower contents and disturbed days usually had higher contents.

5. CONCLUSIONS

The following are summaries of the results with some suggestions for improvements.

The diurnal variations appeared much as expected in the light of similar studies [Solomon, 1965; Yeh and Flaherty, 1966]. The variation was effected by both seasonal change and solar activity owing to the fact that nearly six months data were required to obtain a complete diurnal cycle.

Both figures of electron content contours indicate some evidence of an anomaly around midnight. Because of the lack of data, nothing definite can be said about such an observation in relation to the winter night increases found by other investigators [Arendt and Soicher, 1964; Evans, 1965; Rastogi, 1960]. The methods of obtaining the contours could be modified in several ways. The smoothing technique used in averaging the content versus latitude curves of a particular interval of the day could be changed possibly to a least square fit.

The observation of morning passes around sunrise indicated that north bound passes had very little slope while south bound passes show steep slopes increasing to the south. When gradient is mostly due to the ionizing effect of the sun, the difference in slope appears to be caused by the pass geometry with respect to the sunrise line. The ground sunrise line is not the actual production line but does indicate the trend of increased production. A detailed examination of many satellite passes during sunrise may lead to a more thorough understanding of electron production due to solar ionization.

The attempt to correlate magnetic index with electron content was done for a period of time when magnetic activity was relatively low, e.g. K_p

reached a high of 6- on only two separate occasions. The general trend, although not conclusive, appeared to be that lower content was more likely to be observed for lower K_p while higher content was associated with high K_p.

REFERENCES

Arendt, P. R., A. Papayoanou and H. Soicher, "Determination of the Ionospheric Electron Content Utilizing Satellite Signals," Proc. IEEE, 53, 268-277, 1965.

Arendt, P. R. and H. H. Soicher, "Downward Electron Flux at 1000 Km Altitude from Electron Content Measurement at Mid-Latitudes," Nature, 204, 983-984, 1964.

Colin, L. and M. A. Myers, "Computed Times of Sunset and Sunrise in the Ionosphere," NASA Technical Memorandum, X-1233, 1966.

Evans, J. V., "Cause of the Midlatitude Winter Night Increase in f_0F2," J. Geophys. Res., 70, 4331-4345, 1965.

Evans, J. V. and G. N. Taylor, "The Electron Content of the Ionosphere in Winter," Proc. Roy. Soc. London, A, 263, 189-211, 1961.

Garriott, O. K. and F. de Mendonca, "A Comparison of Methods Used for Obtaining Electron Content from Satellite Observations," J. Geophys. Res., 68, 4917-4927, 1963.

Rastogi, R. G., "Asymmetry between the F2 Region of the Ionosphere in Northern and Southern Hemispheres," J. Geophys. Res., 65, 857-868, 1960.

Ratcliffe, J. A., The Magneto-Ionic Theory and Its Application to the Ionosphere, Cambridge: Cambridge University Press, 1959.

Solomon, S. L., "Variations in the Total Electron Content of the Ionosphere at Mid-Latitudes during Quiet Sun Conditions," Scientific Rept. 256, Ionosphere Res. Lab., Pennsylvania State University, November 30, 1965.

Yeh, K. C. and B. J. Flaherty, "Ionospheric Electron Content at Temperate Latitudes during the Declining Phase of the Sunspot Cycle," J. Geophys. Res., 71, 4557-4570, 1966.

Yeh, K. C. and V. H. Gonzalez, "Note on the Geometry of the Earth Magnetic Field Useful to Faraday Effect Experiment," J. Geophys. Res., 65, 3209-3214, 1960.

Yeh, K. C. and G. W. Swenson, Jr., "Ionospheric Electron Content and Its Variations Deduced from Satellite Observations," J. Geophys. Res., 66, 1061-1067, 1961.

APPENDIX A

Electron Content Calculation Using Two Frequencies with Non-Linear Faraday Rotation Interpolation.

The fortran program listed is the main deck for electron content calculation using two frequency Faraday rotation from a polar orbiting satellite such as S-66.

Several functions and subroutines are incorporated in the program which are not standardized. Below is a list of the functions and subroutines with a general description:

CENSEC	changes hours minutes seconds (HHMMSS.S) to hundreds of seconds.
HMS	changes hundreds of seconds to hour minutes seconds (HHMMSS.S).
FAROT*	sets up arrays of null number and null time (hundreds of seconds) from arrays of input data.
TELSAP	calculates satellite position for a particular date and time from space elements of the satellite.
MAGFLD	calculates effective earth's magetic field ($\bar{M}$) at mean ionospheric height (VLTH) from satellite position coordinates.
D(S,M)	determines rotation difference at time S for south bound (M = 1) or north bound (M = 2) pass.
RENUM*	calculates number of half-rotations to be used in FAROT for proper renumbering of nulls, employs averaging technique. (- if north bound or + if south bound).

*Contains common statement--COMMON X1, Y1, X2, Y2, N1, N2 where Y1 and Y2 are null numbers, X1 and X2 are null times in hundreds of seconds and N1 and N2 are the number of nulls for the respective frequencies.

SUBSAT calculates coordinates of ionosphere point at height VLTH.

ROTN(T,N)* interpolates the rotation number table at time T. N = 1, 2 indicates table to be interpolated Y1 or Y2.

DRAW plots output on CALCOMP plotter.

The following is a description of the variables read in by the RIT 7 statements in the order of their appearance in the main program. The first input statement reads identification of the run and is not used for any calculation. The remaining input variables are:

MB the number of sets of orbital elements to be processed.

SAT satellite name, e.g. S-66.

STAT station name, e.g. Urbana.

TIM standard time specification, e.g. CST.

A(1) to A(23) elements required to calculate satellite orbit.

VLTH mean ionospheric height in Km.

FREQ1 lower frequency of Faraday rotation data.

FREQ2 higher frequency of Faraday rotation data.

N11 number of passes to be processed for a particular set of orbital elements.

TINC time increment for calculation of output in seconds, if zero output is calculated at FREQ1 null times.

FROT number of half-rotations added to differential rotation

*Contains common statement--COMMON X1, Y1, X2, Y2, N1, N2 where Y1 and Y2 are null numbers, X1 and X2 are null times in hundreds of seconds and N1 and N2 are the number of nulls for the respective frequencies.

(initially set to zero; program adjusts for positive differential rotation).

REF — some time during the pass.

REFS — division number corresponding to time above (REF).

SCALE — number of divisions per minute of time (if zero program assumes null times are not given in divisions but in hours minutes and seconds, HHMMSS.S).

J — number of cards for pass to be read next.

K — order of least square polynomial fit for output (if zero least square fit is not done).

ROT — number of half-rotations added to FROT (not controlled by program).

DA(L) — year, month and day (YYMMDD.) for Faraday data of pass (Lth card in pass).

T1(L) — null time of division number corresponding to FREQ1 (Lth card in pass). Value ignored if negative.

R1(L) — number of half-rotations going from T1(L - 1) to T1(L) (zero for L = 1).

T2(L) — same as T1(L) except corresponding to FREQ2.

R2(L) — same as R1(L) except corresponding to T2(L).

The column headings shown on the printed output are self-explanatory; however, some clarification is necessary. The time given is Central Standard Time. Asterisks printed on either side of the electron content indicate that zenith angle is greater than 40^{o}. The half-rotations printed out under 40 MHz are the final values used for the calculation of electron content. The 40 MHz

half-rotations are negative for north bound passes and positive for south bound passes; however, the sign is ignored for content calculation. The 41 MHz half-rotations printed out are interpolated values from the initial null numbering. The AVERAGE ELECTRON CONTENT and PERCENT RMS are calculated for points with zenith angle less than 40^{o}. The NUMBER OF HALF-ROTATIONS ADDED is the integral number added to the differential rotation to eliminate the rotation ambiguity between the initial numbering of 40 and 41 MHz nulls.

Figure 12 is the CALCOMP output for the above pass. The data points are indicated by crosses for zenith angle less than 40^{o} and by squares when the zenith angle is equal to or greater than 40^{o}.

UNIVERSITY OF ILLINOIS, FASTRAN COMPILER (16 JUN 1966 VERSION)

```
      CALL CP81
      CALL CCP1PL(0.0,6.0,3)
      CALL CCP1PL(0.0,4.0,2)
      DIMENSION A(23),B(11),C(19),CNT(200),T1(50),T2(50),R1(50),R2(50),D
     1A(50),X1(200),X2(200),Y1(200),Y2(200),CT(200),SLT(200),NV(3),CLD(2
     200)
      COMMON X1,Y1,X2,Y2,N1,N2
      RADDEG=0.0174532925
      RIT 7,2
      RIT 7,4,MB
      DO 66 I3=1,MB
      RIT 7,32,SAT,STAT,TIM
      RIT 7,5,A(1),A(2),A(3),A(4),A(5),A(6),A(7),A(8),A(9),A(10),A(11),
     1A(12),A(13),A(14),A(19),A(20),A(21),A(22),A(23),VLTH,FREQ1,FREQ2
      RIT 7,4,N11
      WOT 6,2
      WOT 6,7,A(1),A(2),A(3),A(4),A(5),A(6),A(7),A(8),A(9),A(10),A(11),
     1A(12),A(13),A(14),A(19),A(20),A(21),A(22),A(23),FREQ1,FREQ2
      CONST=FREQ1*FREQ1*3.14592654E12/0.0297
      DO 65 NM=1,N11
      RIT 7,31,TINC,FROT,REF,REFS,SCALE
      RIT 7,20,J,K,ROT
      LOOK AT 22,DATE
      RIT 7,19,(DA(L),T1(L),R1(L),T2(L),R2(L),L=1,J)
30    WOT 6,6
      WOT 6,8,(VLTH)
      WOT 6,6
      WOT 6,9
      WOT 6,10,FREQ1,FREQ2
      WOT 6,6
      IF(SCALE-1.0) 38,38,33
33    REF=CENSEC(REF)
      DO 37 I=1,J
      IF(T1(I)) 35,34,34
34    T1(I)=HMS(REF+(T1(I)-REFS)/SCALE*6000.0)
35    IF(T2(I)) 37,36,36
36    T2(I)=HMS(REF+(T2(I)-REFS)/SCALE*6000.0)
37    CONTINUE
38    CALL FAROT(T1,T2,R1,R2,J)
      IF(N1-1)65,65,39
39    IF(X1(1)-X2(1))40,41,41
40    S=X2(1)
```

```
      GO TO 42
   41 S=X1(1)
   42 IF(X1(N1)-X2(N2))43,44,44
   43 F=X1(N1)
      GO TO 45
   44 F=X2(N2)
   45 A(15)=DA(1)
      STAR=S
      A(16)=S
      A(17)=DA(1)
      A(18)=S
      CALL TELSAP(A,B,C,1)
      CALL MAGFLD(A(21),A(22),C(1),C(2),VLTH,HR,HTHETA,HPHI,FLDMA)
      A(16)=A(16)+6000.0
      A(18)=A(18)+6000.0
      CALL TELSAP(A,B,C,1)
      CALL MAGFLD(A(21),A(22),C(1),C(2),VLTH,HR,HTHETA,HPHI,FLDMB)
      IF(FLDMB-FLDMA)46,47,47
   46 M=2
      GO TO 48
   47 M=1
   48 IF(D(S,M)+FROT)49,49,50
   49 FROT=FROT+1.0
      GO TO 48
   50 IF(D(F,M)+FROT)49,49,51
   51 CALL RENUM(FREQ1,FREQ2,ROT,FROT,M)
      RONE=R1(1)
      R1(1)=Y2(1)
      CALL FAROT(T1,T2,R1,R2,J)
      R1(1)=RONE
      IF(TINC)251,251,151
  151 THMS=HMS(X1(1))
      THM=INTF(THMS/100.0)*100.0
      S=THM+(INTF((THMS-THM)/TINC)+1.0)*TINC
      T=CENSEC(S)
      TDIST=T+TINC*100.0
      GO TO 351
  251 TDIST=X1(2)
  351 CLD(1)=0.0
      NUL=1
      NP=0
      NV(1)=0
      NV(2)=0
      NV(3)=0
      IN=0
      A(15)=DA(1)
      A(17)=DA(1)
      IF(TINC)152,152,52
  152 T=X1(1)
   52 A(16)=T
      A(18)=T
      CALL TELSAP(A,B,C,1)
      CALL MAGFLD(A(21),A(22),C(1),C(2),VLTH,HR,HTHETA,HPHI,FLDM)
      CALL SUBSAT(A(21),A(22),C(1),C(2),VLTH,TH,RLAT,RLNG)
      EL=C(4)
      THET1=RLAT*RADDEG
      CCSTH1=COS(THET1)
```

UNIVERSITY OF ILLINOIS, FASTRAN COMPILER (16 JUN 1966 VERSION)

```
      SINTH1=SIN(THET1)
      CONTNT=ABSF(ROTN(T,1))/FLDM*CONST/1.0E17
      TIME1=HMS(T)
      A(16)=TDIST
      A(18)=A(16)
      CALL TELSAP(A,B,C,1)
      CALL SUBSAT(A(21),A(22),C(1),C(2),VLTH,TH,RLAT1,RLNG1)
      RN1=ROTN(T,1)
      RN2=ROTN(T,2)
      NP=NP+1
      CT(NP)=CONTNT*1.0E17
      SLT(NP)=RLAT
      THET2=RLAT1*RADDEG
      COSTH2=COS(THET2)
      SINTH2=SIN(THET2)
      DELPHI=(RLNG-RLNG1)*RADDEG
      CLD(NP+1)=ARCOS(COSTH1*COSTH2*COS(DELPHI)+SINTH1*SINTH2)*(VLTH+637
     18.388)+CLD(NP)
      ZE1=90.0-EL
      IF(EL-50.0)54,53,53
   53 IN=IN+1
      CNT(IN)=CONTNT
      WOT 6,12,A(17),TIME1,CONTNT,RLAT,RLNG,ZE1,RN1,RN2
      NV(2)=NV(2)+1
      GO TO 55
   54 WOT 6,13,A(17),TIME1,CONTNT,RLAT,RLNG,ZE1,RN1,RN2
      IF(NV(2)) 155,155,255
  155 NV(1)=NV(1)+1
      GO TO 55
  255 NV(3)=NV(3)+1
   55 T=T+TINC*100.0
      IF(TINC)157,157,257
  157 NUL=NUL+1
      T=X1(NUL)
      TDIST=X1(NUL+1)
      IF(NUL-N1)52,357,57
  357 TDIST=X1(N1)
      GO TO 52
  257 IF(X1(N1)-T)57,52,52
   57 AIN=IN
      SMCN=0.0
      SMDIF=0.0
      IF(AIN-1.0)62,61,58
   58 DO 59 LN=1,IN
   59 SMCN=CNT(LN)+SMCN
      AVE=SMCN/AIN
      DO 60 LM=1,IN
      DIFF=CNT(LM)-AVE
   60 SMDIF=SMDIF+DIFF*DIFF
      RMS=SQRT(SMDIF/AIN)
      PCRMS=RMS/AVE*100.0
      WOT 6,14,AVE
      WOT 6,15,PCRMS,IN,FROT
      GO TO 63
   61 WOT 6,16,FROT
      GO TO 63
   62 WOT 6,17,FROT
```

```
UNIVERSITY OF ILLINOIS, FASTRAN COMPILER (16 JUN 1966 VERSION)

   63  TI=HMS(X1(1))/100.0
       NTOT=NV(1)+NV(2)+NV(3)
       DO 100 N=1,NTOT
  100  CNT(N)=CT(N)/1.0E17
       WOT 5,23,DA(1),S,TINC,NV(1),NV(2),NV(3),(CNT(N),SLT(N),N=1,4)
       WOT 5,24,(CNT(N),SLT(N),N=5,NTOT)
       IF(SLT(NP)-SLT(1))265,265,465
   265 DO 365 I=1,NP
   365 CLD(I)=CLD(NP)-CLD(I)
   465 CALL DRAW(SLT,CT,NV(1),NV(2),NV(3),K ,FREQ1,FREQ2,SAT,STAT,DATE ,T
      1I,TIM,CLD)
       WOT 6,21
       IF(ROTN(F,1)-ROTN(STAR,1)+ROTN(STAR,2)-ROTN(F,2))67,65,65
   67  SCALE=0.0
       DO 68 N=1,J
       CT(N)=T1(N)
   68  SLT(N)=R1(N)
       DO 69 N=1,J
       T1(N)=T2(N)
       R1(N)=R2(N)
       T2(N)=CT(N)
   69  R2(N)=SLT(N)
       WOT 6,25
       FROT=0.0
       GO TO 30
   65  CONTINUE
   66  CONTINUE
     2 FORMAT(8CH
      1                          )
     3 FORMAT(8F10.8)
     4 FORMAT(I2)
     5 FORMAT(F20.8)
     6 FORMAT(1HO)
     7 FORMAT(10X,5F20.6)
     8 FORMAT(35X,49HTHE LATITUDES AND LONGITUDES ARE FOR A HEIGHT OF F6.
      12,2HKM)
     9  FORMAT(6X,4HDATE,7X,4HTIME,7X,16HELECTRON CONTENT,8X,8HLATITUDE,8X
      1,9HLONGITUDE,8X,12HZENITH ANGLE,8X,24HNUMBER OF HALF-ROTATIONS)
    10  FORMAT(5X,6HYYMMDD,5X,6HHHMMSS,7X,13HELEC/M*M E 17,10X,7HDEGREES,1
      10X,7HDEGREES,11X,7HDEGREES,11X,F5.1,4H MHZ,7X,F5.1,4H MHZ)
    12  FORMAT(5X,F6.0,5X,F6.0,11X,F6.3,11X,F9.3,10X,F7.3,11X,F7.3,11X,F8.
      13,8X,F8.3)
    13  FORMAT(5X,F6.0,5X,F6.0,8X,3H***,F6.3,3H***,8X,F9.3,10X,F7.3,11X,F7
      1.3,11X,F8.3,8X,F8.3)
    14 FORMAT(25HOAVERAGE ELECTRON CONTENT,F10.3,13H E17 ELEC/M*M)
    15 FORMAT(13H PER CENT RMS,12X,F10.1,5X,13HPER CENT FOR ,I2,7H POINTS
      1/31H NUMBER OF HALF-ROTATIONS ADDED,F5.0)
    16 FORMAT(76HOONLY ONE POINT WAS USABLE, HENCE THE AVERAGE EQUALS THE
      1VALUE AT THE POINT./31H NUMBER OF HALF-ROTATIONS ADDED,F5.0)
    17 FORMAT(54HONO POINTS WERE USABLE, HENCE NO AVERAGE WAS COMPUTED./3
      11H NUMBER OF HALF-ROTATIONS ADDED,F5.0)
    19 FORMAT(5F10.8)
    20  FORMAT(2I2,F6.3)
    21  FORMAT(1H1)
    22  FORMAT(A6)
    23  FORMAT(2F7.0,F3.0,3I3,4(F6.3,F7.3))
    24  FORMAT(6(F6.3,F7.3))
```

UNIVERSITY OF ILLINOIS, FASTRAN COMPILER (16 JUN 1966 VERSION)

```
  25   FORMAT(34H POSSIBLE DATA ERROR SEE NEXT PASS)
  31   FORMAT(2F6.2,F8.2,2F6.2)
  32   FORMAT(2A6,A4)
       END
```

THE LATITUDES AND LONGITUDES ARE FOR A HEIGHT OF 350.00KM

DATE YYMMDD	TIME HHMMSS	ELECTRON CONTENT ELEC/M*M E 17	LATITUDE DEGREES	LONGITUDE DEGREES	ZENITH ANGLE DEGREES	NUMBER OF HALF-ROTATIONS 40.0 MHZ	41.0 MHZ
650226	125050	1.323	38.590	89.185	29.236	-32.924	.477
650226	125100	1.333	38.803	89.134	26.043	-32.508	.963
650226	125110	1.339	39.015	89.083	22.757	-31.990	1.527
650226	125120	1.340	39.225	89.032	19.425	-31.384	2.162
650226	125130	1.334	39.435	88.980	16.124	-30.606	2.884
650226	125140	1.324	39.644	88.929	13.003	-29.742	3.669
650226	125150	1.315	39.853	88.877	10.361	-28.937	4.406
650226	125200	1.313	40.061	88.825	8.763	-28.304	5.090
650226	125210	1.305	40.270	88.772	8.858	-27.532	5.804
650226	125220	1.291	40.480	88.719	10.604	-26.684	6.590
650226	125230	1.283	40.690	88.666	13.337	-25.958	7.317
650226	125240	1.278	40.900	88.612	16.517	-25.298	7.923
650226	125250	1.269	41.113	88.557	19.868	-24.576	8.545
650226	125300	1.257	41.326	88.501	23.247	-23.827	9.281
650226	125310	1.250	41.541	88.444	26.578	-23.173	10.056
650226	125320	1.246	41.759	88.386	29.817	-22.593	10.556
650226	125330	1.243	41.978	88.327	32.938	-22.038	10.977
650226	125340	1.237	42.200	88.267	35.924	-21.453	11.581
650226	125350	1.228	42.425	88.206	38.774	-20.809	12.257
650226	125400	*** 1.214***	42.653	88.143	41.482	-20.125	12.909
650226	125410	*** 1.203***	42.884	88.079	44.050	-19.493	13.448
650226	125420	*** 1.195***	43.119	88.013	46.482	-18.922	13.927
650226	125430	*** 1.188***	43.358	87.945	48.782	-18.386	14.456
650226	125440	*** 1.179***	43.602	87.875	50.958	-17.842	15.029
650226	125450	*** 1.168***	43.850	87.803	53.017	-17.272	15.621
650226	125500	*** 1.156***	44.103	87.729	54.966	-16.715	16.212
650226	125510	*** 1.144***	44.361	87.652	56.811	-16.185	16.771
650226	125520	*** 1.133***	44.624	87.573	58.561	-15.675	17.234
650226	125530	*** 1.120***	44.894	87.492	60.219	-15.177	17.597
650226	125540	*** 1.107***	45.169	87.407	61.797	-14.689	17.931
650226	125550	*** 1.093***	45.452	87.319	63.297	-14.212	18.301

AVERAGE ELECTRON CONTENT 1.290 E17 ELEC/M*M
PER CENT RMS 2.9 PER CENT FOR 19 POINTS
NUMBER OF HALF-ROTATIONS ADDED 2

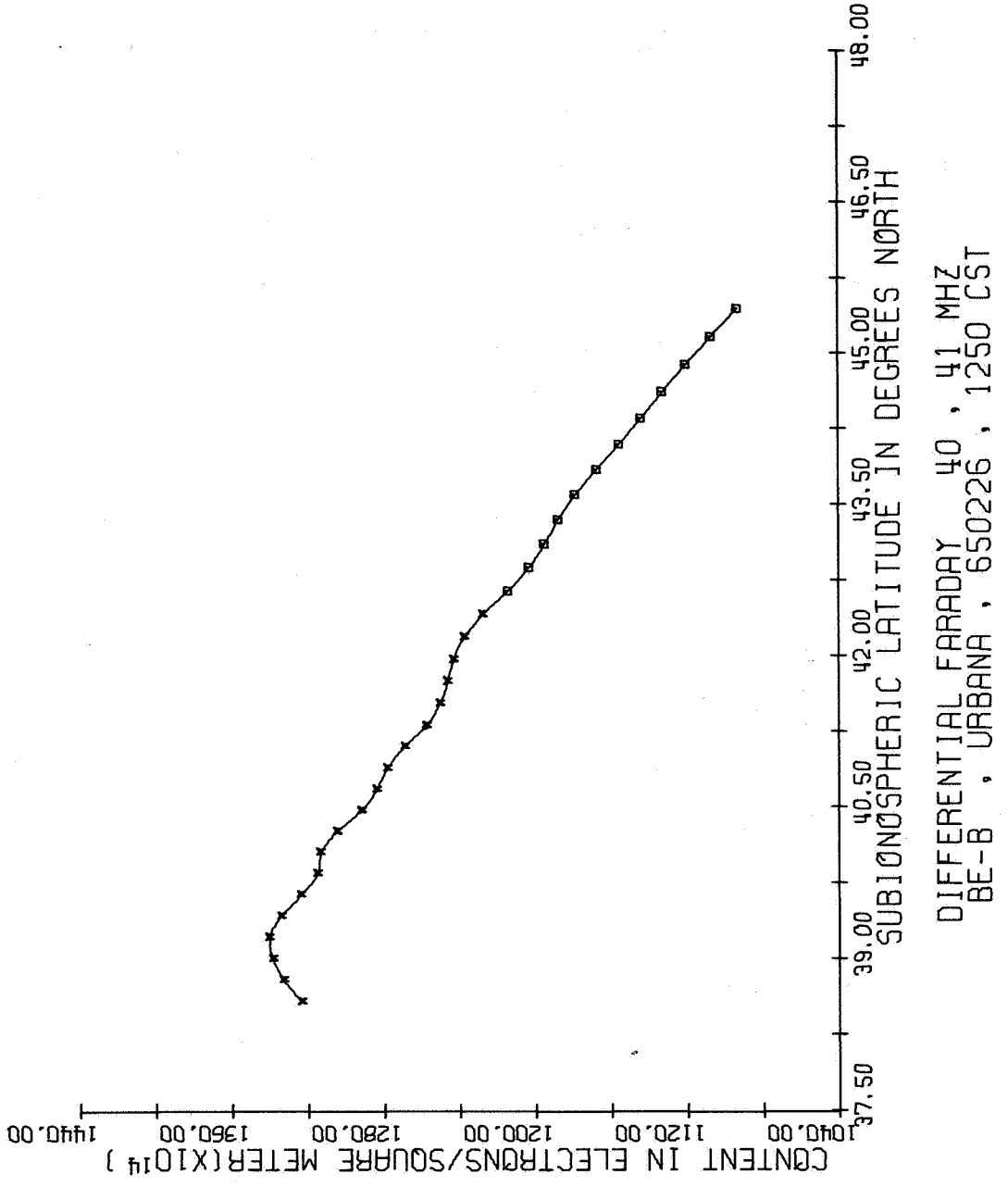

Figure 12. Example of CALCOMP output.

APPENDIX B

Figures 13 through 56 are plots of electron content versus subionospheric latitude. The data has been divided into two periods of three months each. Figures 13 through 34 show electron content plots for October, November and December, while Figures 35 through 56 show plots for January, February and March. The electron content curves for each three month period are grouped and plotted for one hour intervals of the day. The end of each pass is identified with a six digit number giving year, month and day. Immediately below this six digit number the time for the beginning of the pass is shown with no preceeding zeros. Pass direction is apparent since the annotation is at the end of the pass, e.g. annotation at the north end of the electron content curve indicates a north bound pass. Zenith angles greater than 40^{o} are indicated by the dotted curve.

All calculations and plotting were done by machine; thus, some figures may be difficult to understand when many passes occurred during the same hour interval of the day.

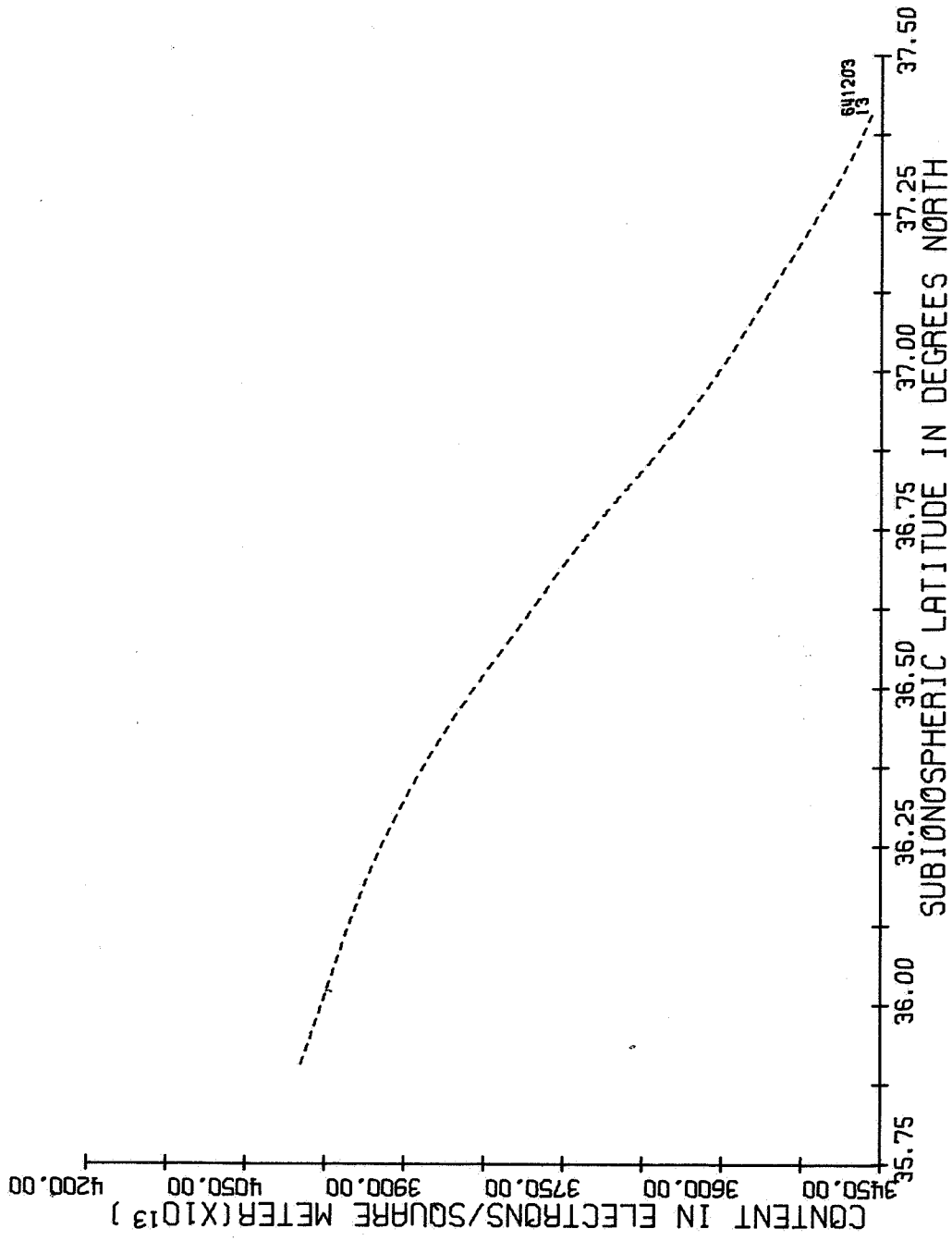
TIME INTERVAL FROM 0 TO 100 CST
SUBIONOSPHERIC LATITUDE IN DEGREES NORTH
35.75
36.00
36.25
36.50
36.75
37.00
37.25
37.50
CONTENT IN ELECTRONS/SQUARE METER(X10^13)
3450.00
3600.00
3750.00
3900.00
4050.00
4200.00
6U1203
13

Figure 13.

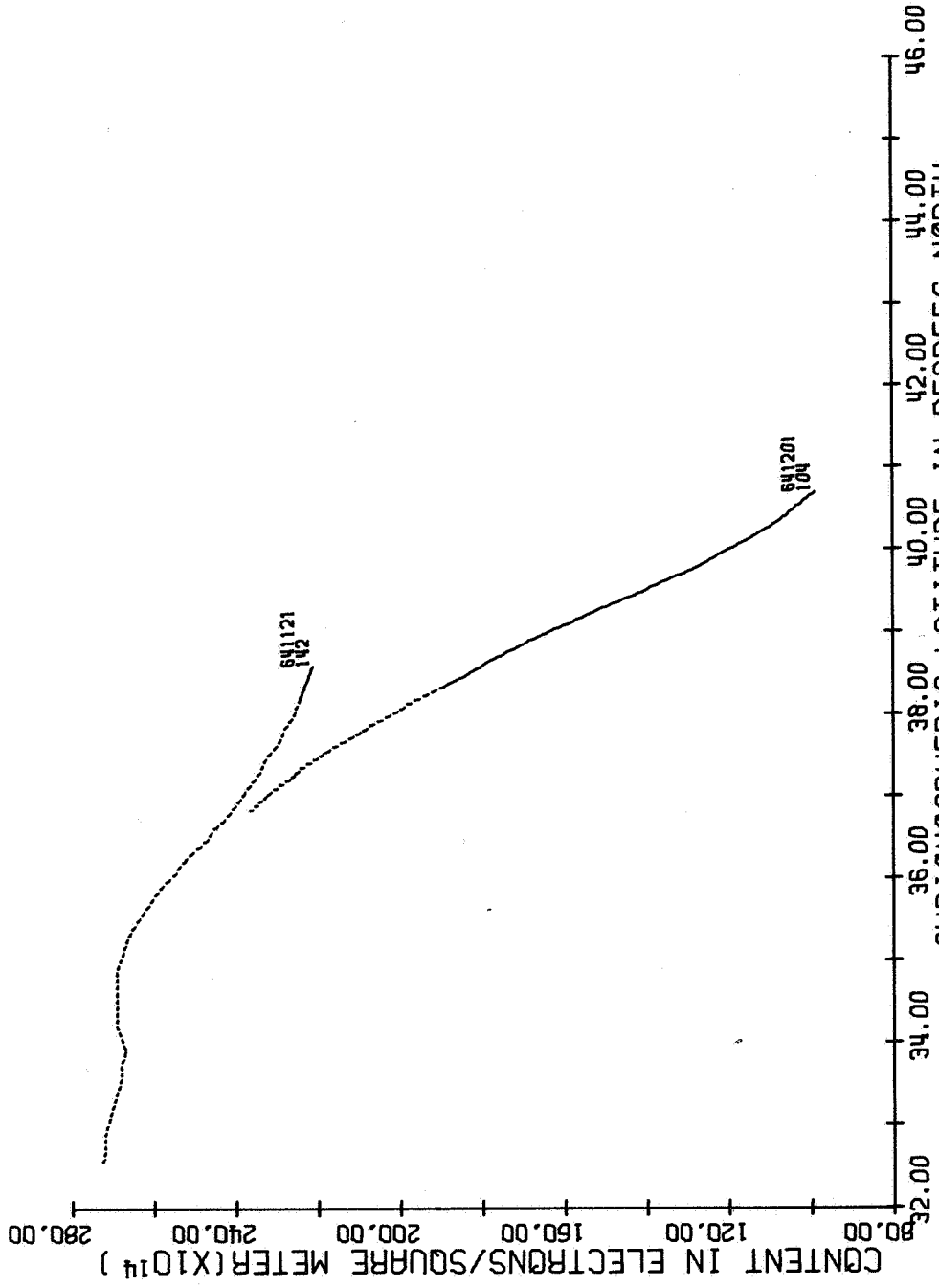
CONTENT IN ELECTRONS/SQUARE METER(X10¹⁴)
80.00
120.00
160.00
200.00
240.00
280.00
32.00
34.00
36.00
38.00
40.00
42.00
44.00
46.00
SUBIONOSPHERIC LATITUDE IN DEGREES NORTH
TIME INTERVAL FROM 100 TO 200 CST
6N1121
6N1201

Figure 14.

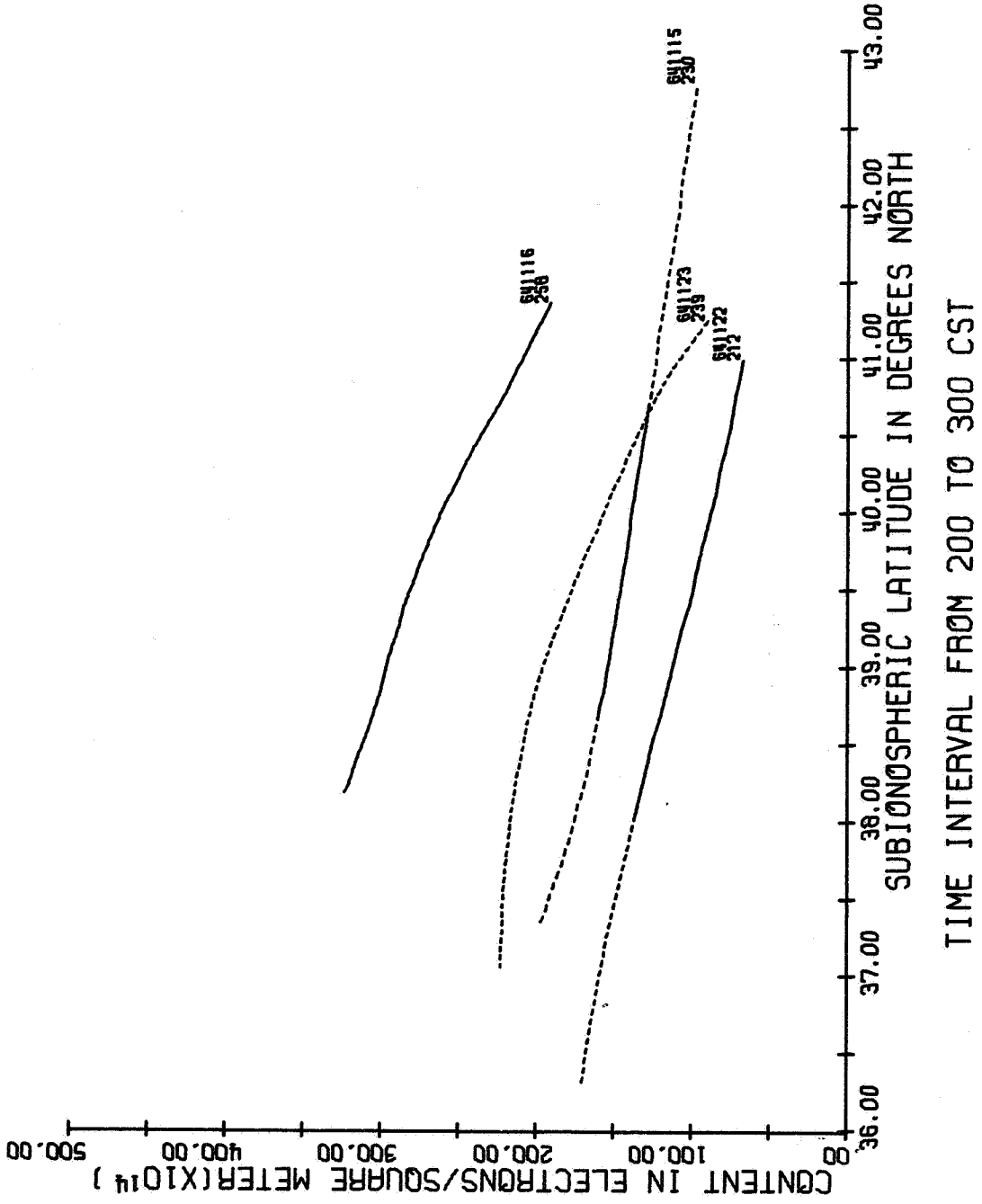
TIME INTERVAL FROM 200 TO 300 CST
SUBIONOSPHERIC LATITUDE IN DEGREES NORTH
36.00
37.00
38.00
39.00
40.00
41.00
42.00
43.00
CONTENT IN ELECTRONS/SQUARE METER(X10¹⁴)
00
100.00
200.00
300.00
400.00
500.00
6W1115
230
6W1116
238
6W1123
239
6W122
212

Figure 15.

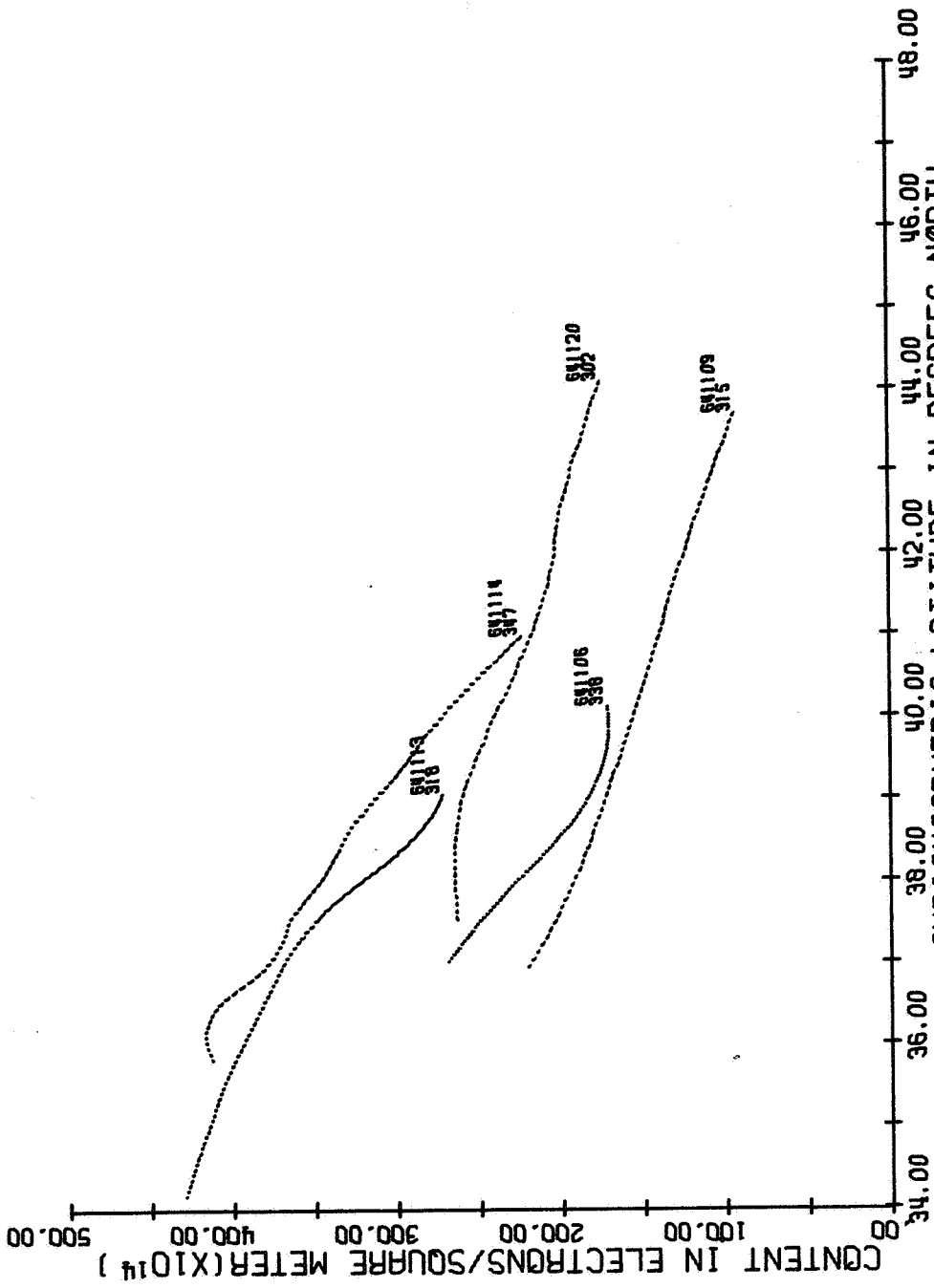
TIME INTERVAL FROM 300 TO 400 CST
SUBIONOSPHERIC LATITUDE IN DEGREES NORTH
34.00
36.00
38.00
40.00
42.00
44.00
46.00
48.00
CONTENT IN ELECTRONS/SQUARE METER(X10^14)
0
100.00
200.00
300.00
400.00
500.00
641120
641109
641114
641106
641113

Figure 16.

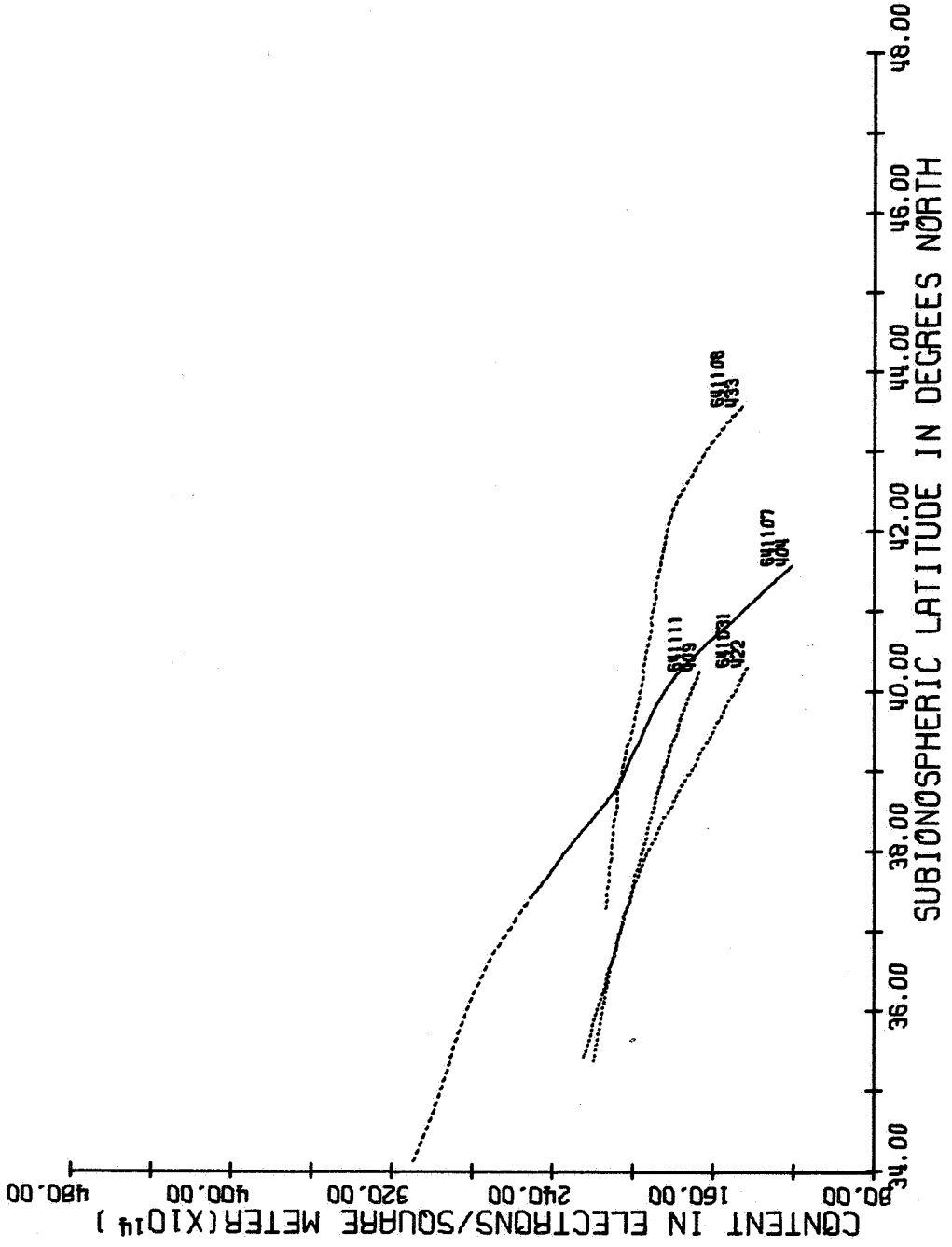
TIME INTERVAL FROM 400 TO 500 CST
SUBIONOSPHERIC LATITUDE IN DEGREES NORTH
34.00
36.00
38.00
40.00
42.00
44.00
46.00
48.00
CONTENT IN ELECTRONS/SQUARE METER(X10^14)
80.00
160.00
240.00
320.00
400.00
480.00

Figure 17.

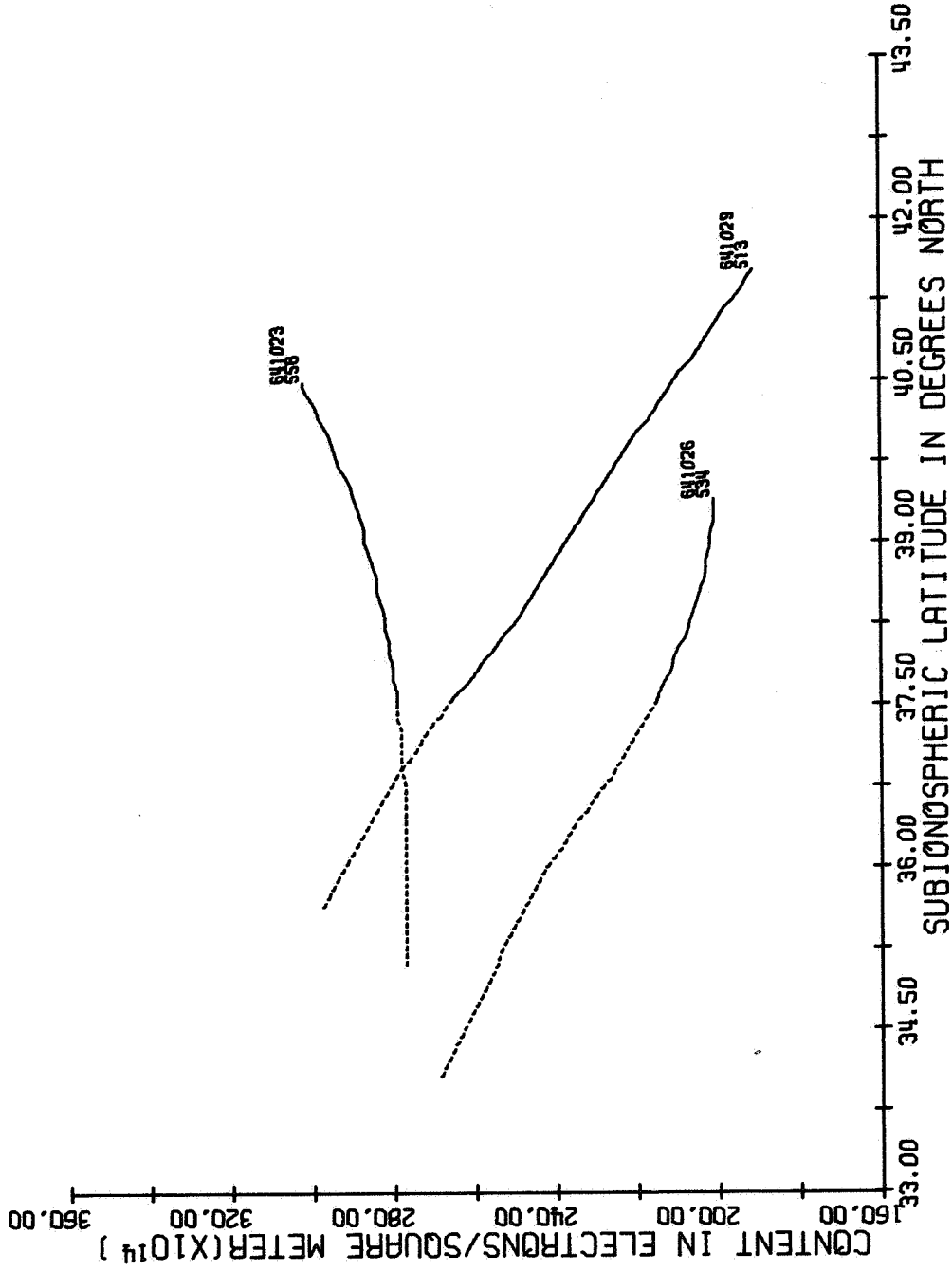
TIME INTERVAL FROM 500 TO 600 CST
SUBIONOSPHERIC LATITUDE IN DEGREES NORTH
33.00
34.50
36.00
37.50
39.00
40.50
42.00
43.50
CONTENT IN ELECTRONS/SQUARE METER(X10^14)
160.00
200.00
240.00
280.00
320.00
360.00
6W1023
556
6W1026
534
6W1029
513

Figure 18.

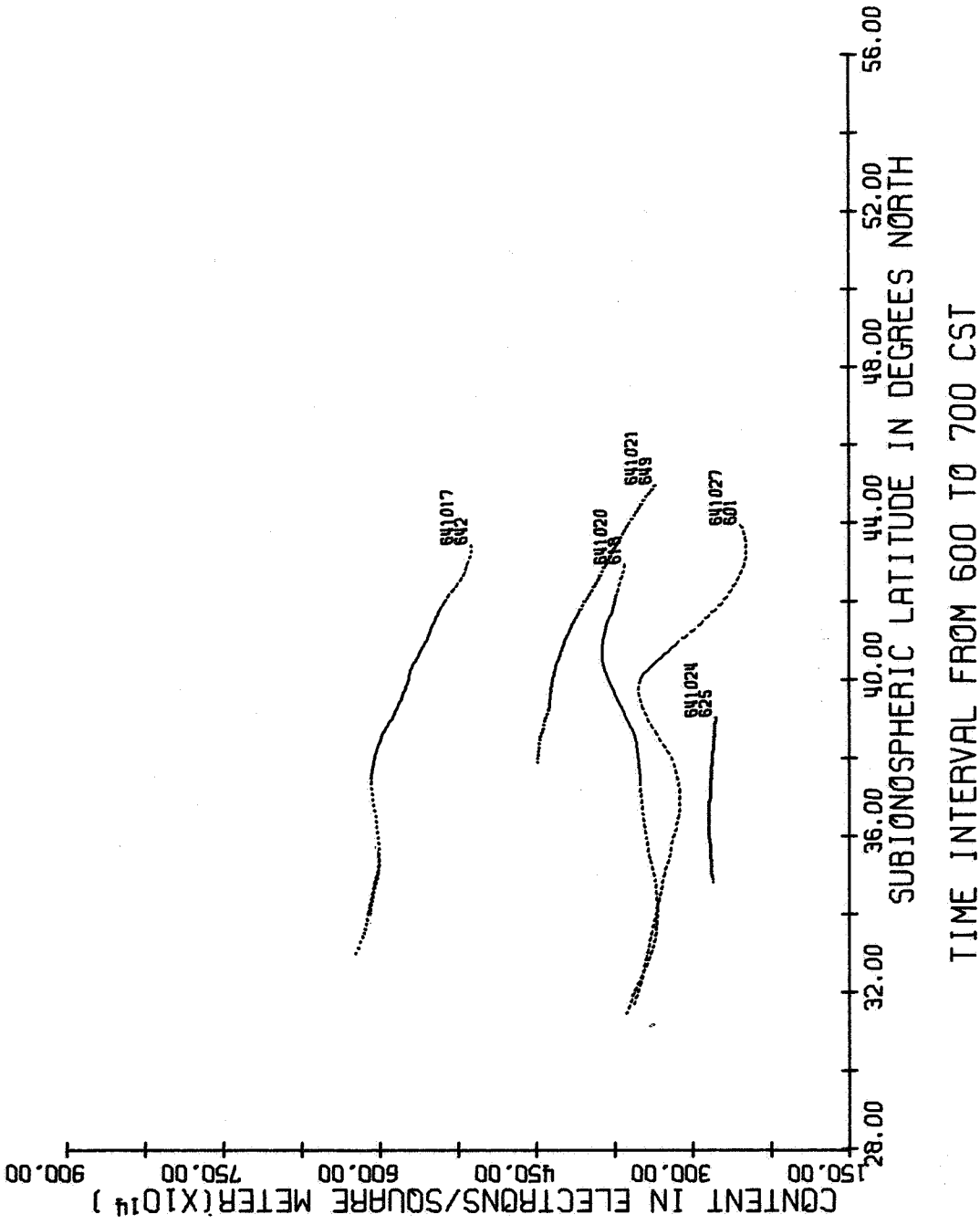
CONTENT IN ELECTRONS/SQUARE METER(X10¹⁴)
150.00
300.00
450.00
600.00
750.00
900.00
28.00
32.00
36.00
40.00
44.00
48.00
52.00
56.00
SUBIONOSPHERIC LATITUDE IN DEGREES NORTH
TIME INTERVAL FROM 600 TO 700 CST
6W1017
602
6W1020
618
6W1021
619
6W1027
601
6W1024
625

Figure 19.

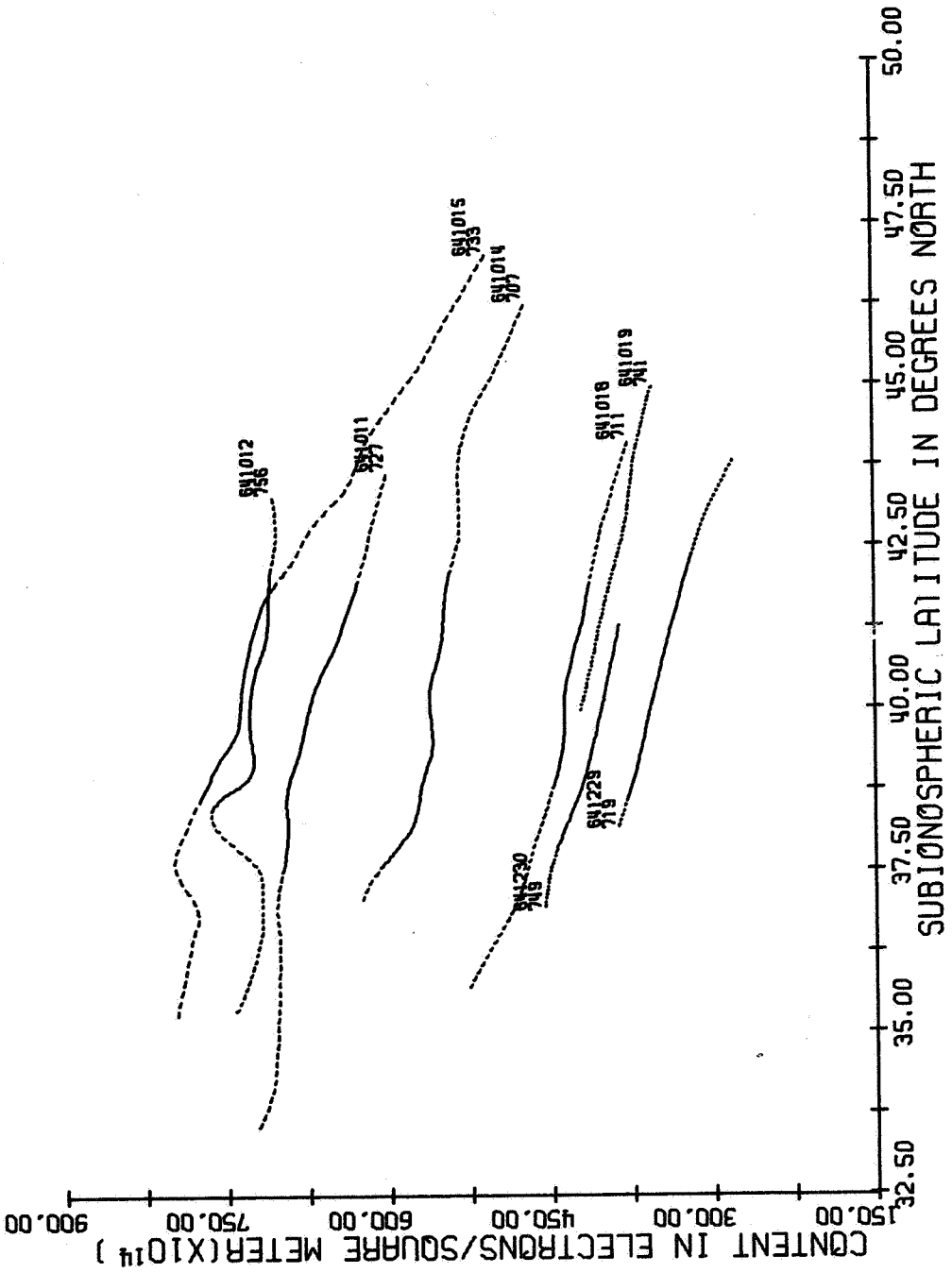
TIME INTERVAL FROM 700 TO 800 CST
SUBIONOSPHERIC LATITUDE IN DEGREES NORTH
32.50
35.00
37.50
40.00
42.50
45.00
47.50
50.00
CONTENT IN ELECTRONS/SQUARE METER(X10^14)
150.00
300.00
450.00
600.00
750.00
900.00
6W1012
6W1011
6W1015
6W1014
6W1018
6W1019
6W1229
6W1230

Figure 20.

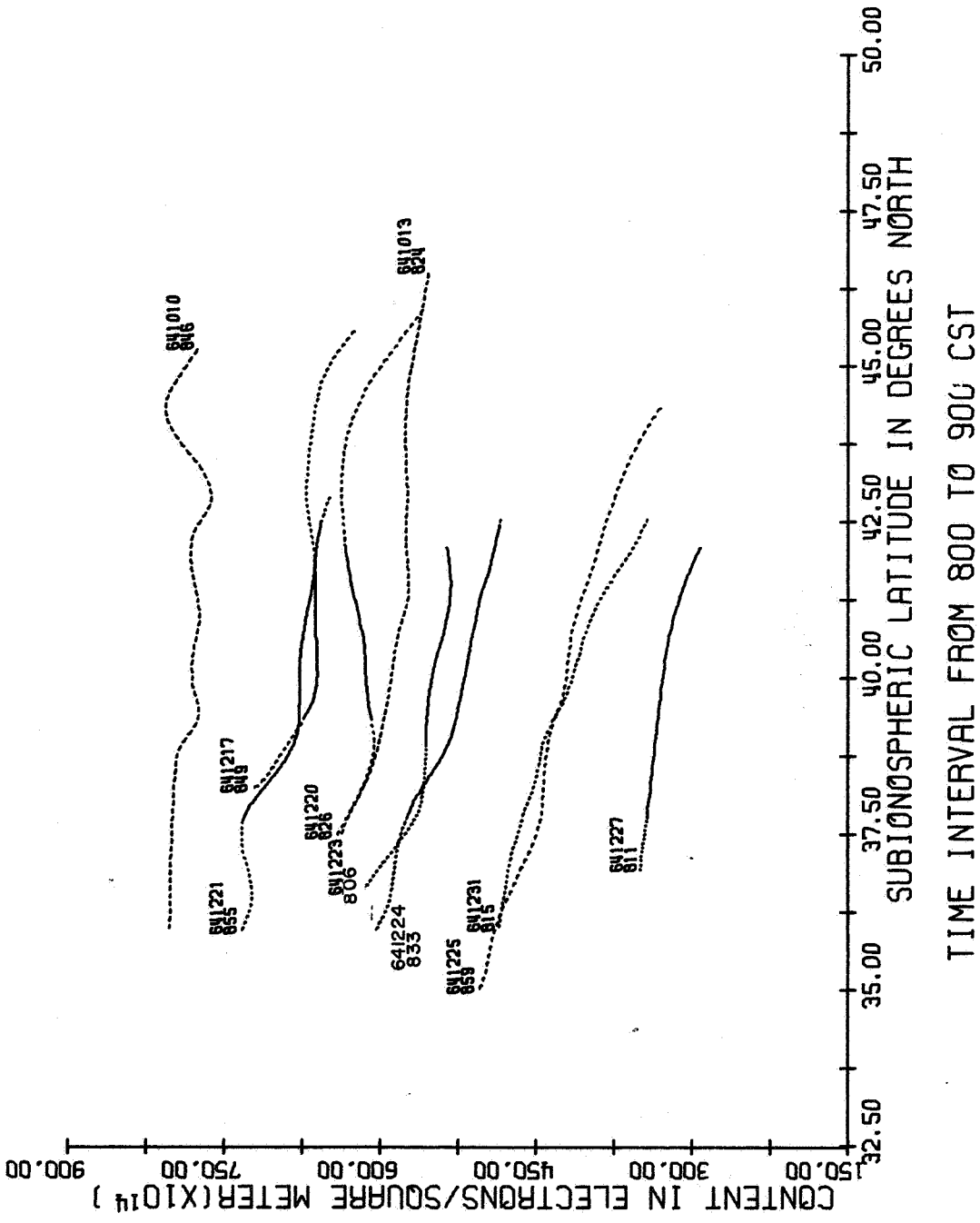
TIME INTERVAL FROM 800 TO 900 CST
SUBIONOSPHERIC LATITUDE IN DEGREES NORTH
32.50
35.00
37.50
40.00
42.50
45.00
47.50
50.00
CONTENT IN ELECTRONS/SQUARE METER(X10¹⁴)
150.00
300.00
450.00
600.00
750.00
900.00
6W1010
846
6W1013
824
6W1217
849
6W1220
826
6W1221
855
6W1223
806
6W1224
833
6W1225
859
6W1231
815
6W1227
811

Figure 21.

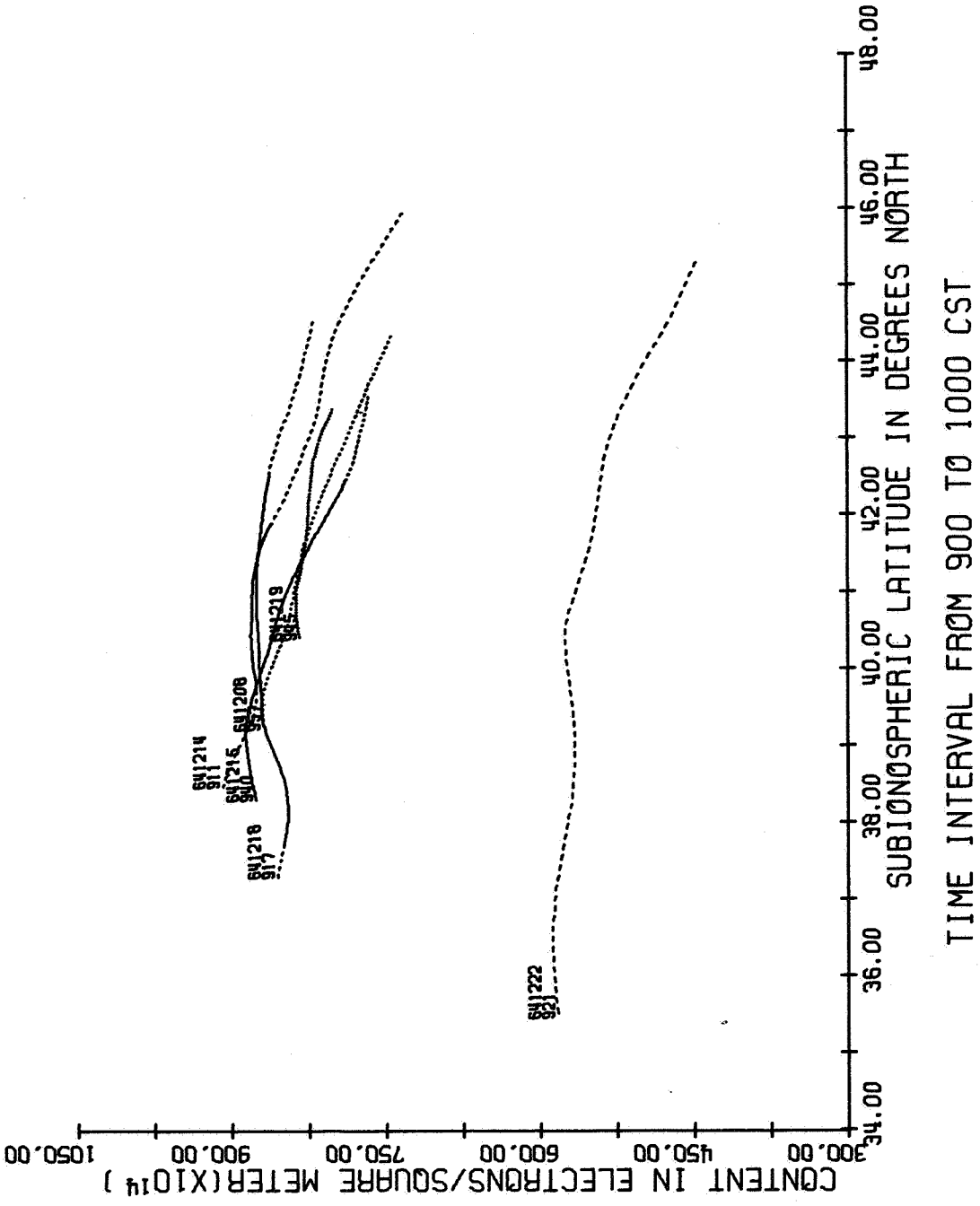
CONTENT IN ELECTRONS/SQUARE METER(X10¹⁴)
300.00
450.00
600.00
750.00
900.00
1050.00
34.00
36.00
38.00
40.00
42.00
44.00
46.00
48.00
SUBIONOSPHERIC LATITUDE IN DEGREES NORTH
TIME INTERVAL FROM 900 TO 1000 CST
6W1214
911
6W1215
910
6W1206
6W1218
917
6W1219
905
6W1222
923

Figure 22.

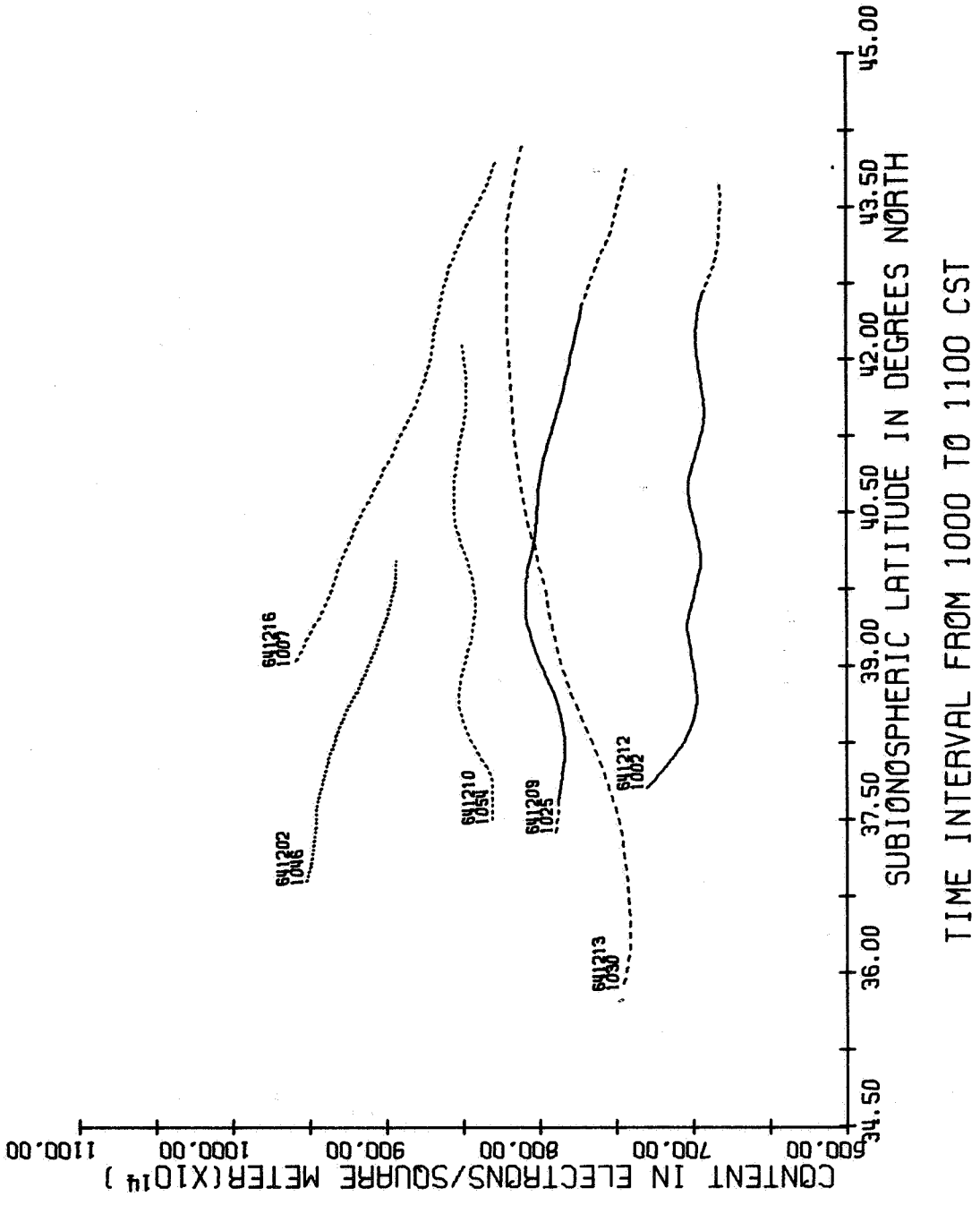
CONTENT IN ELECTRONS/SQUARE METER(X10¹⁴)
500.00
700.00
800.00
900.00
1000.00
1100.00
34.50
36.00
37.50
39.00
40.50
42.00
43.50
45.00
SUBIONOSPHERIC LATITUDE IN DEGREES NORTH
TIME INTERVAL FROM 1000 TO 1100 CST
64J216 1007
64J202 1006
64J210 1054
64J209 1025
64J212 1002
64J213 1030

Figure 23.

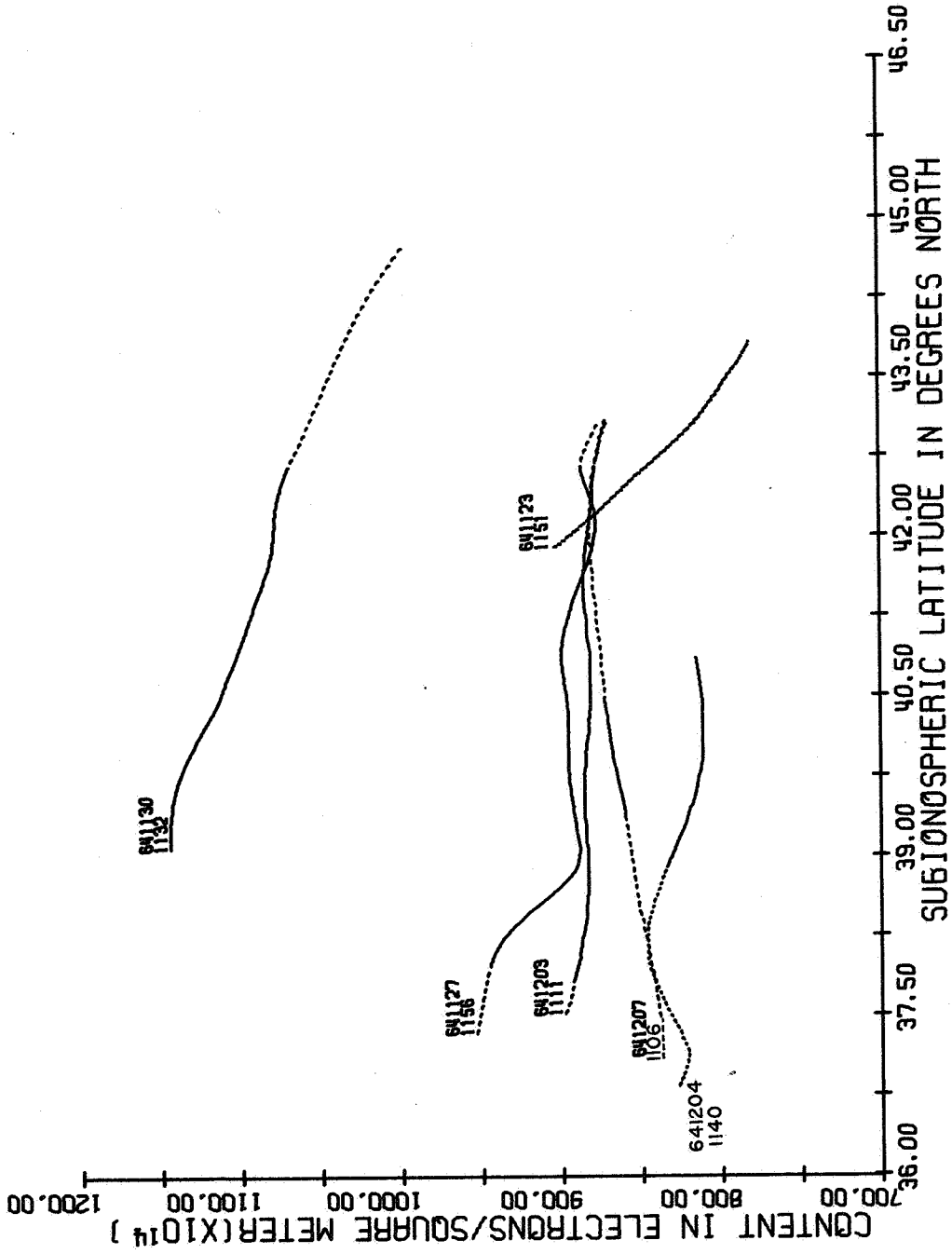
TIME INTERVAL FROM 1100 TO 1200 CST
SUBIONOSPHERIC LATITUDE IN DEGREES NORTH
36.00
37.50
39.00
40.50
42.00
43.50
45.00
46.50
CONTENT IN ELECTRONS/SQUARE METER(X10^14)
700.00
800.00
900.00
1000.00
1100.00
1200.00
6N1130
1158
6N1127
1156
6N1209
1111
6N1123
1151
6N1207
1106
641204
1140

Figure 24.

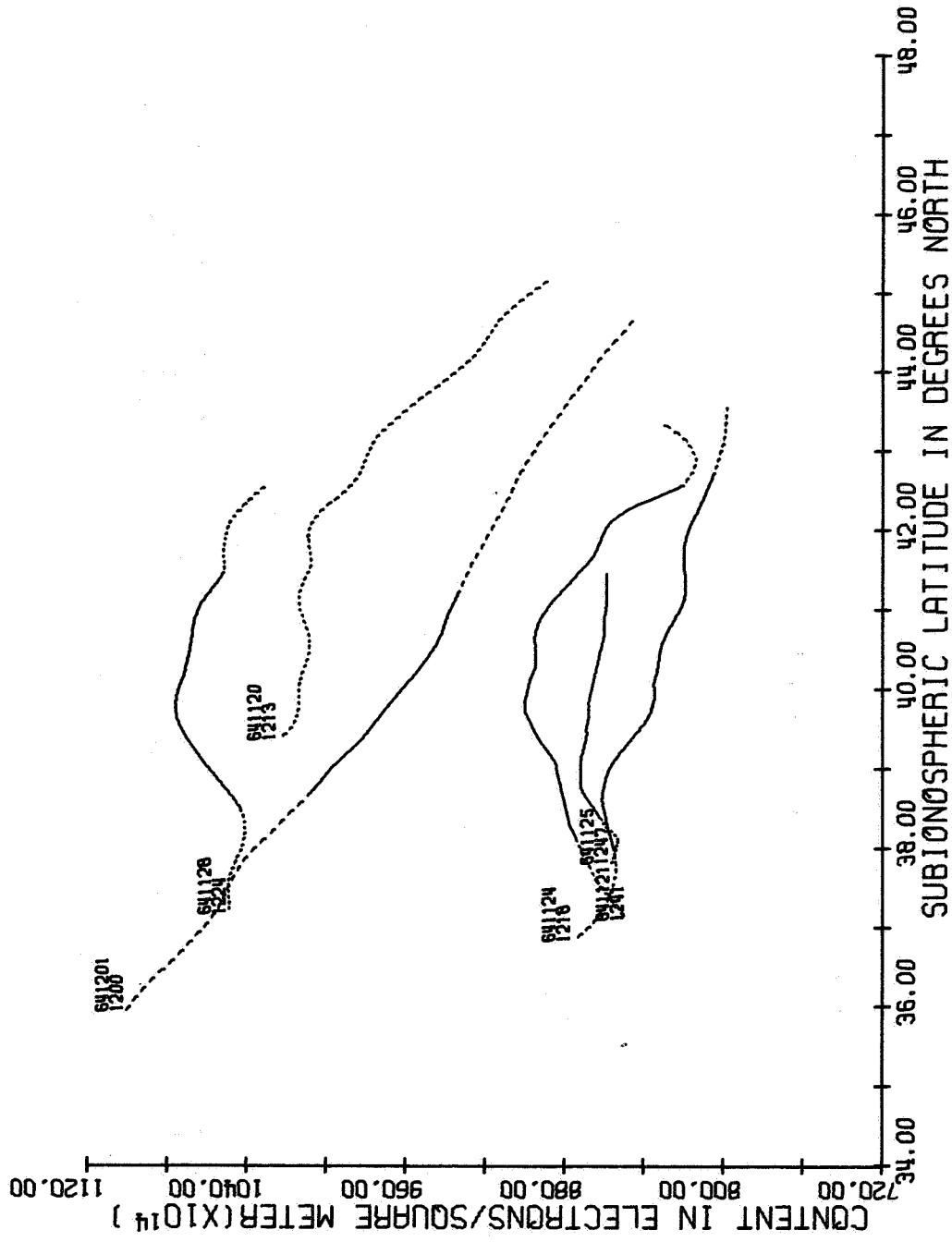
CONTENT IN ELECTRONS/SQUARE METER(X10¹⁴)
720.00
800.00
880.00
960.00
1040.00
1120.00
34.00
36.00
38.00
40.00
42.00
44.00
46.00
48.00
SUBIONOSPHERIC LATITUDE IN DEGREES NORTH
TIME INTERVAL FROM 1200 TO 1300 CST

Figure 25.

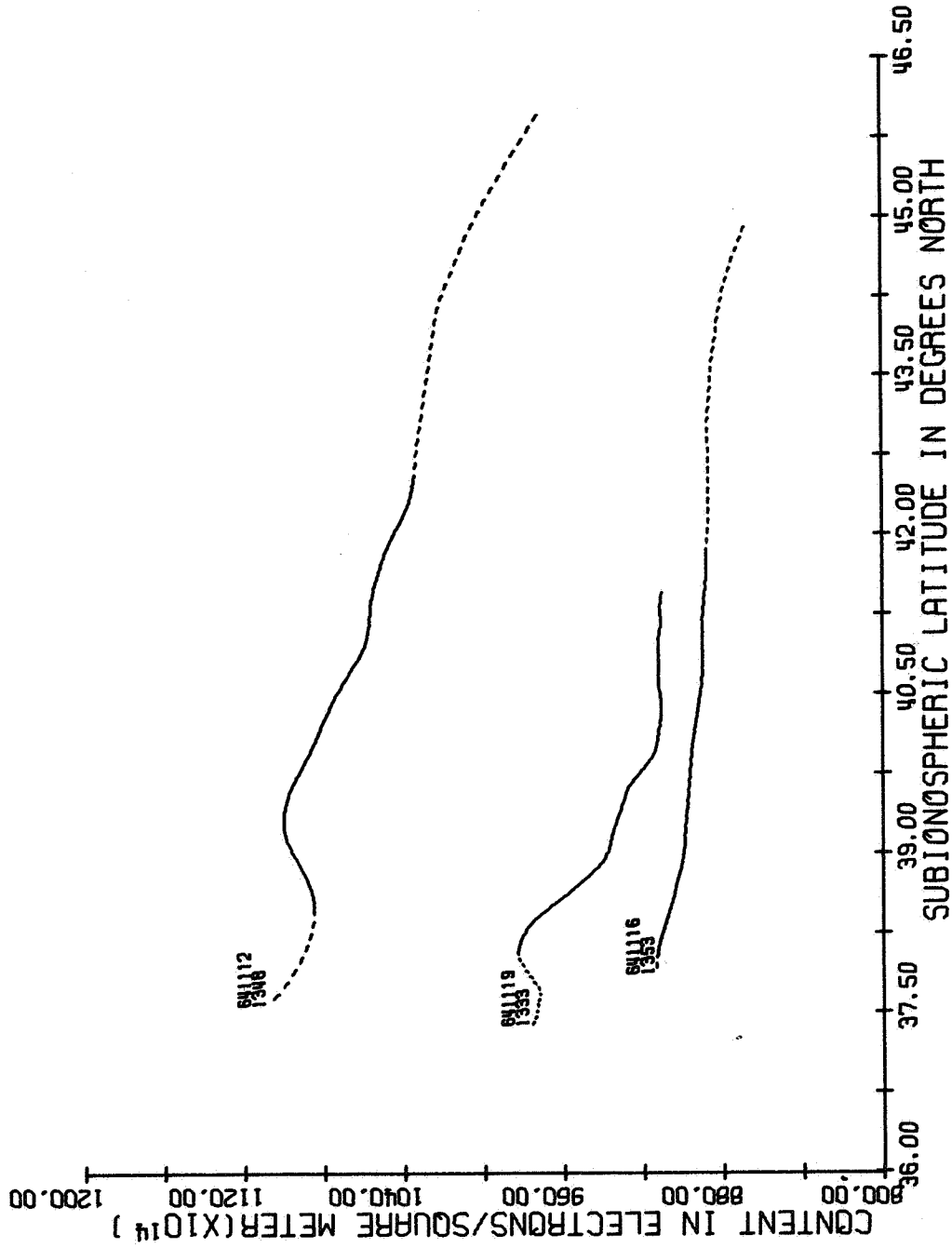
TIME INTERVAL FROM 1300 TO 1400 CST
SUBIONOSPHERIC LATITUDE IN DEGREES NORTH
36.00
37.50
39.00
40.50
42.00
43.50
45.00
46.50
CONTENT IN ELECTRONS/SQUARE METER(X10^14)
800.00
880.00
960.00
1040.00
1120.00
1200.00
6W1112
1348
6W1119
1355
6W1116
1353

Figure 26.

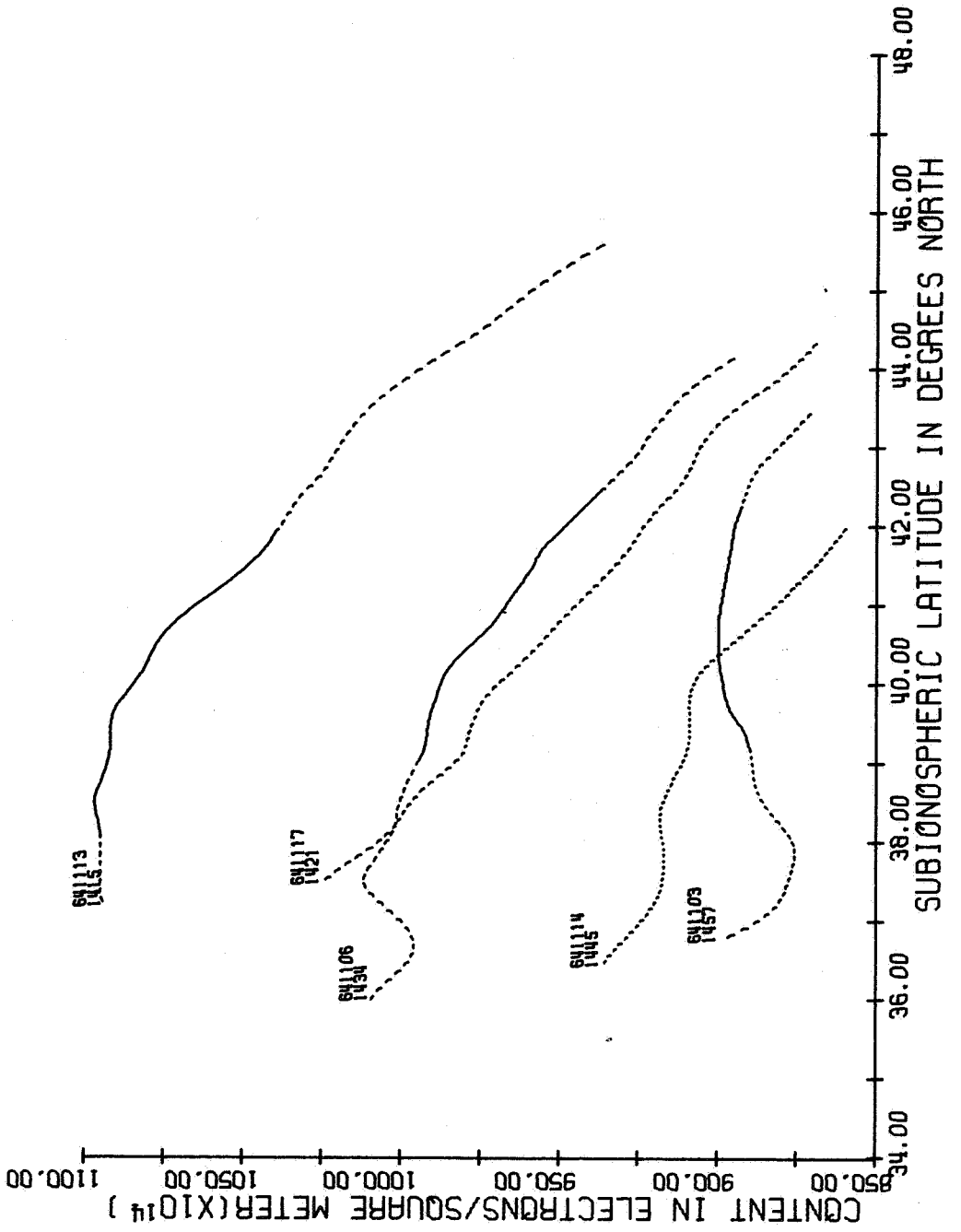
TIME INTERVAL FROM 1400 TO 1500 CST
SUBIONOSPHERIC LATITUDE IN DEGREES NORTH
34.00
36.00
38.00
40.00
42.00
44.00
46.00
48.00
CONTENT IN ELECTRONS/SQUARE METER(X10^14)
850.00
900.00
950.00
1000.00
1050.00
1100.00
6W1113
1413
6W1117
1421
6W1106
1430
6W1114
1445
6W1103
1457

Figure 27.

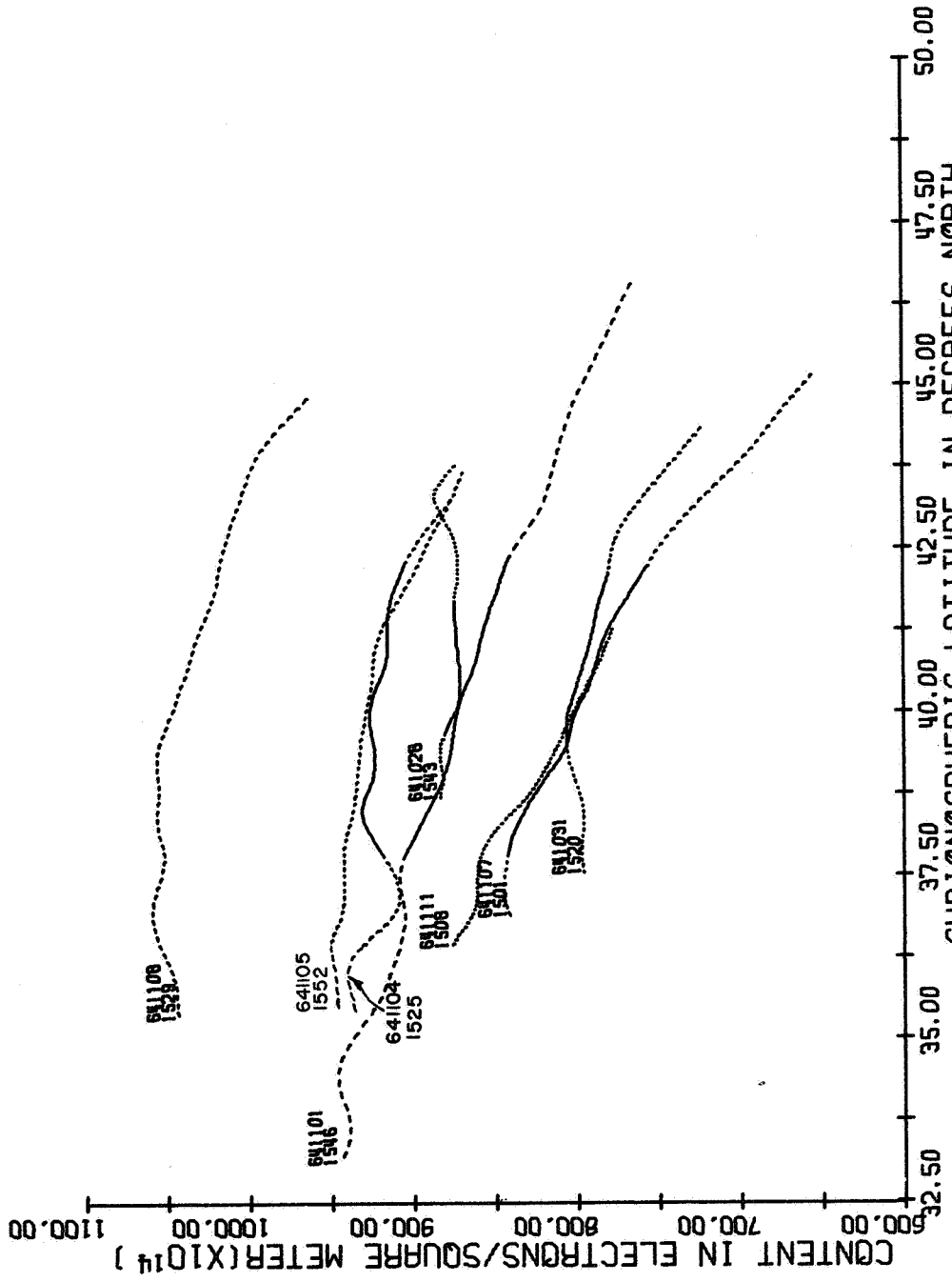
TIME INTERVAL FROM 1500 TO 1600 CST
SUBIONOSPHERIC LATITUDE IN DEGREES NORTH
32.50
35.00
37.50
40.00
42.50
45.00
47.50
50.00
CONTENT IN ELECTRONS/SQUARE METER(X10^14)
600.00
700.00
800.00
900.00
1000.00
1100.00
641101 1546
641105 1552
641104 1525
641111 1508
641107 1501
641031 1520
641026 1543
641108 1529

Figure 28.

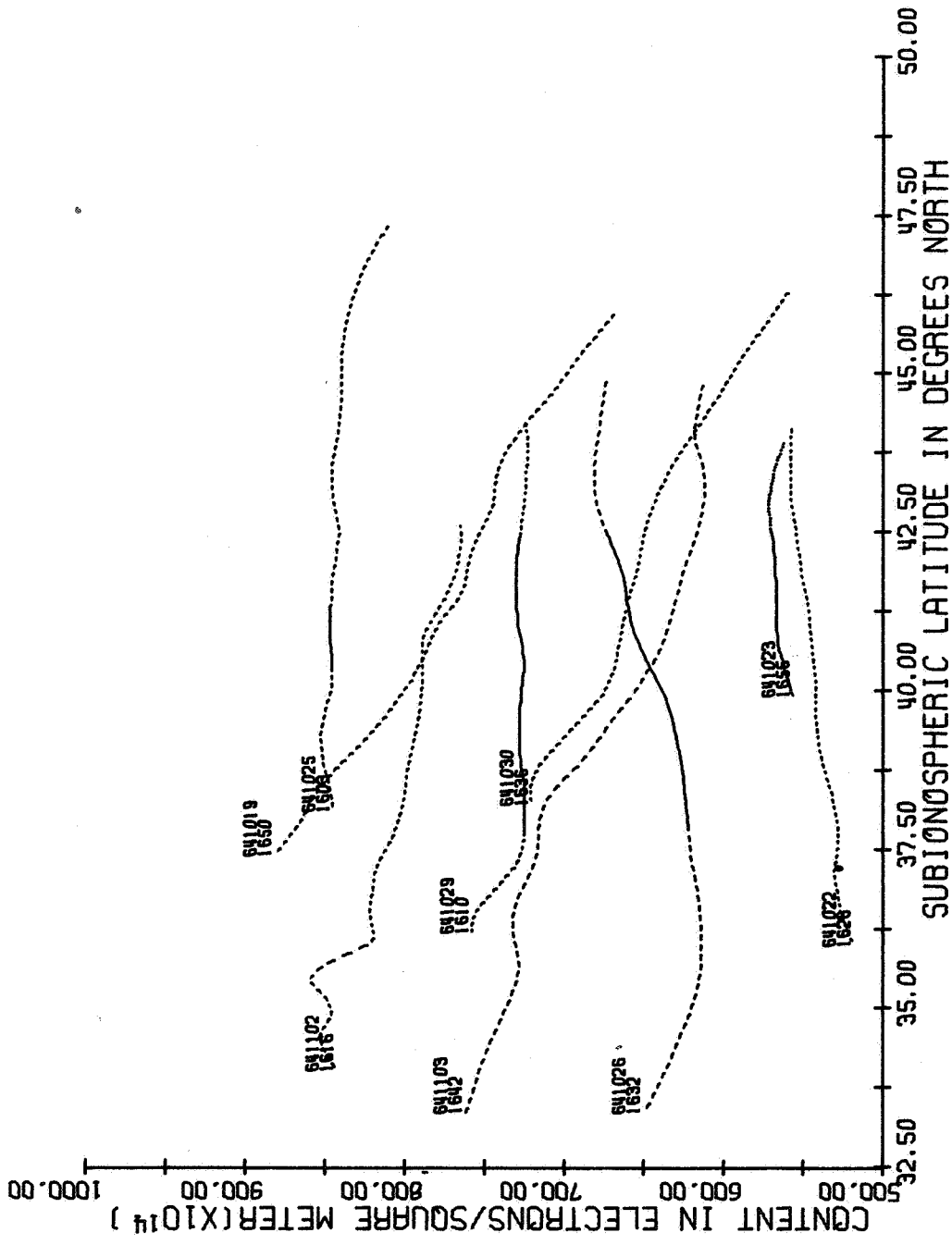
CONTENT IN ELECTRONS/SQUARE METER(X10¹⁴)
1000.00
900.00
800.00
700.00
600.00
500.00
32.50
35.00
37.50
40.00
42.50
45.00
47.50
50.00
SUBIONOSPHERIC LATITUDE IN DEGREES NORTH
TIME INTERVAL FROM 1600 TO 1700 CST
641019 1650
641025 1606
641030 1636
641029 1610
641023 1556
641022 1648
641102 1618
641103 1642
641026 1632

Figure 29.

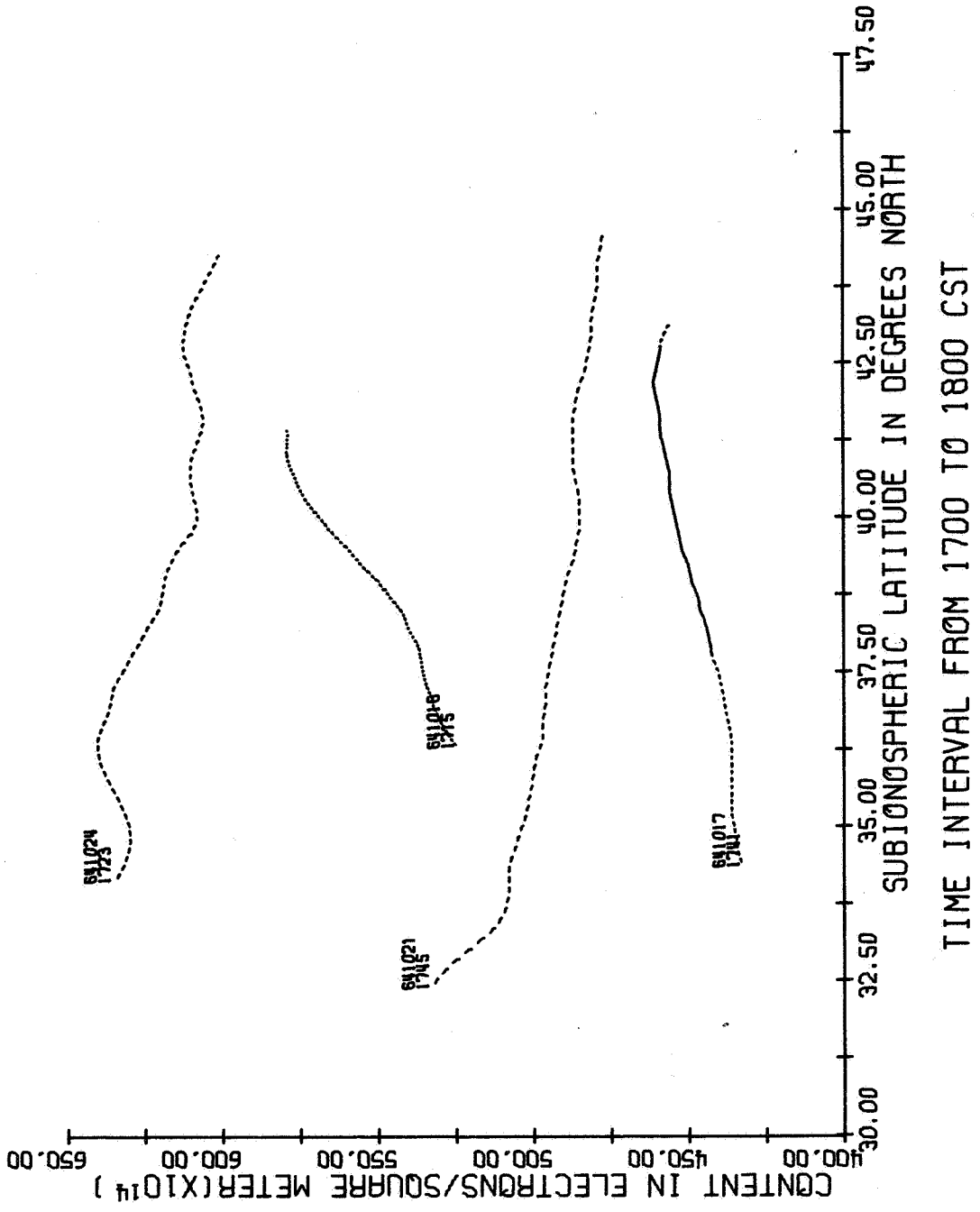
CONTENT IN ELECTRONS/SQUARE METER(X10¹⁴)
400.00
450.00
500.00
550.00
600.00
650.00
30.00
32.50
35.00
37.50
40.00
42.50
45.00
47.50
SUBIONOSPHERIC LATITUDE IN DEGREES NORTH
TIME INTERVAL FROM 1700 TO 1800 CST
6NOV24 1723
6NOV21 1745
6NOV18 1745
6NOV17 1700

Figure 30.

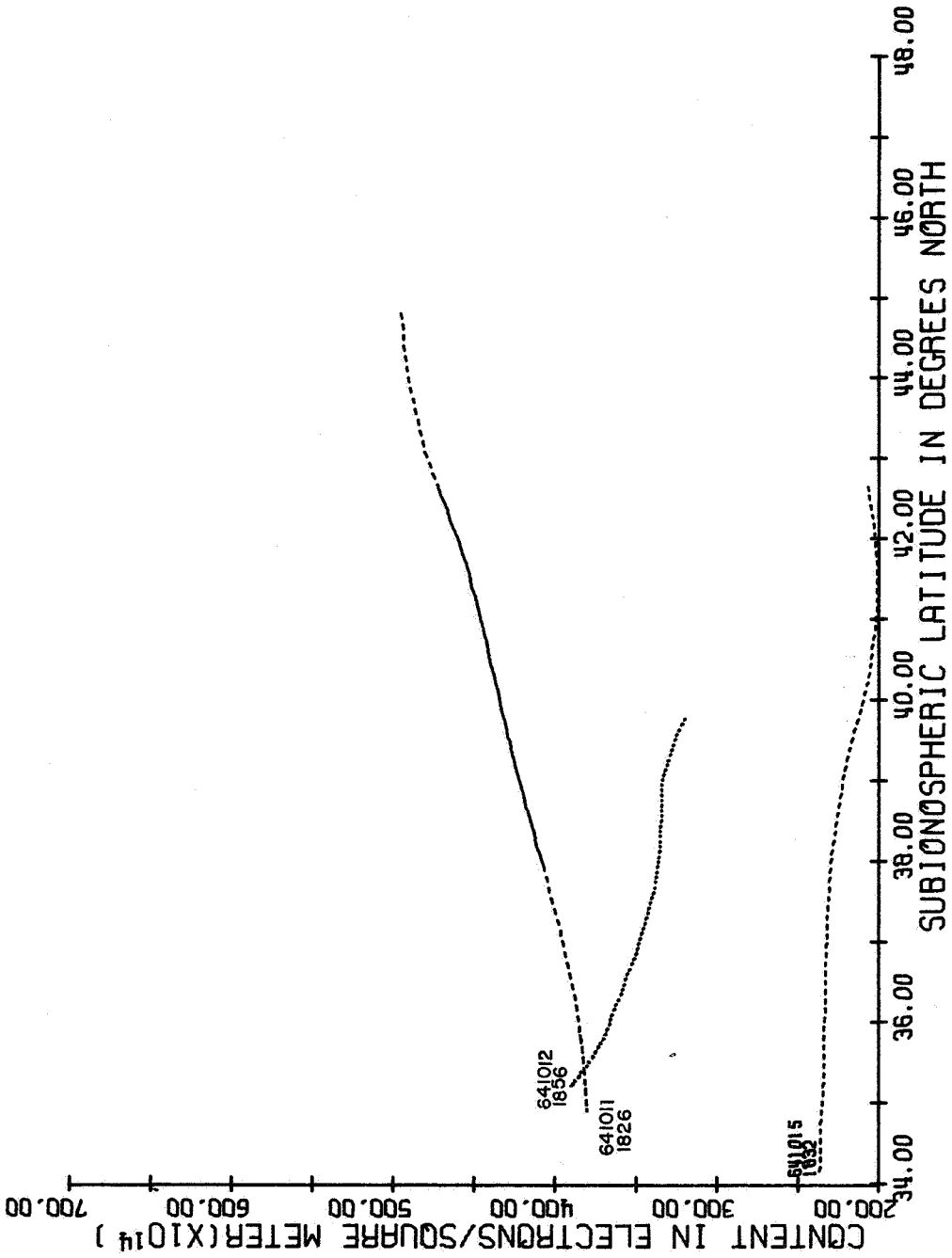
TIME INTERVAL FROM 1800 TO 1900 CST
SUBIONOSPHERIC LATITUDE IN DEGREES NORTH
CONTENT IN ELECTRONS/SQUARE METER(X10¹⁴)
34.00
36.00
38.00
40.00
42.00
44.00
46.00
48.00
200.00
300.00
400.00
500.00
600.00
700.00
641012
1856
641011
1826
641015
1832

Figure 31.

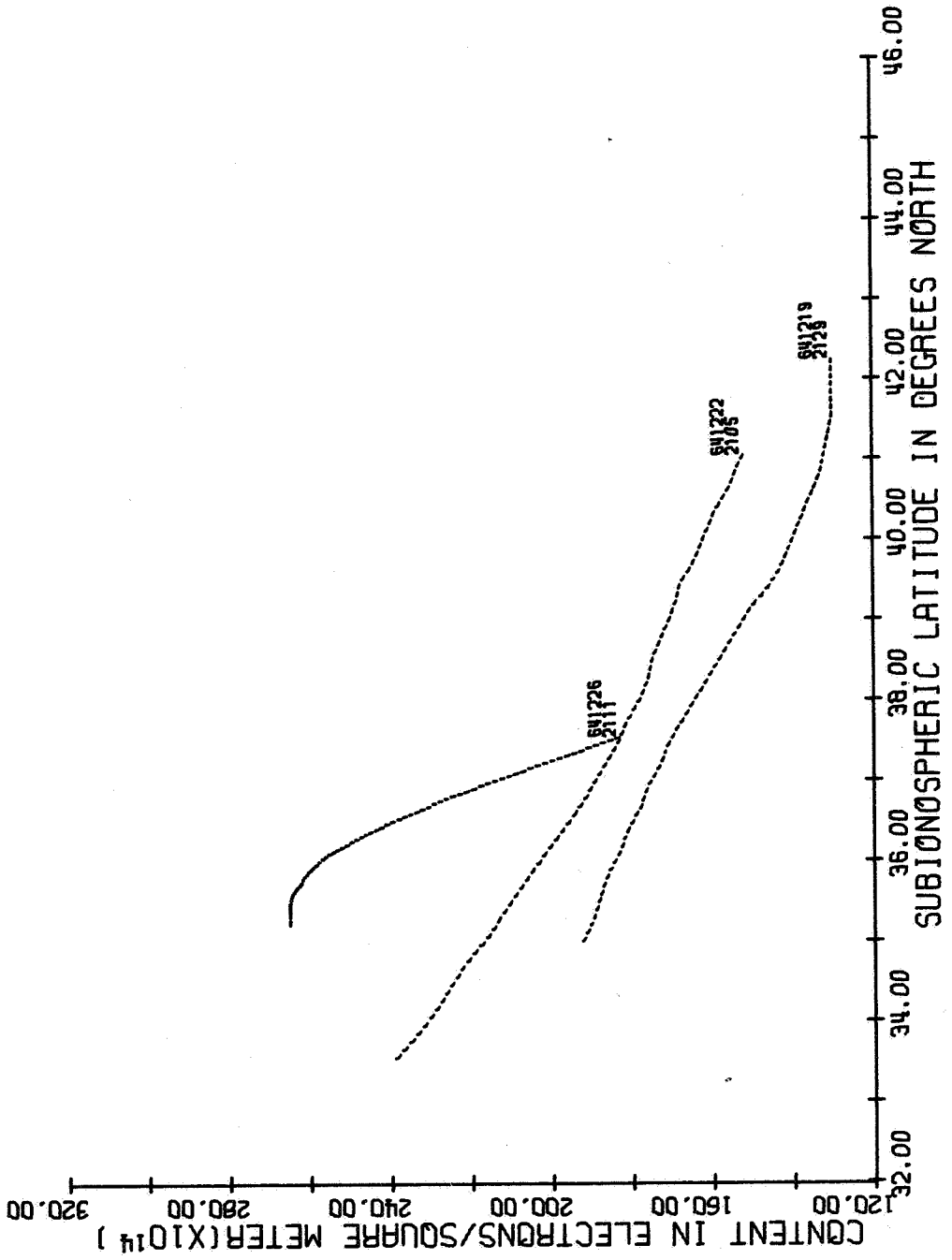
TIME INTERVAL FROM 2100 TO 2200 CST
SUBIONOSPHERIC LATITUDE IN DEGREES NORTH
CONTENT IN ELECTRONS/SQUARE METER(X10¹⁴)
32.00
34.00
36.00
38.00
40.00
42.00
44.00
46.00
120.00
160.00
200.00
240.00
280.00
320.00
6W1226 2111
6W1222 2105
6W1219 2129

Figure 32.

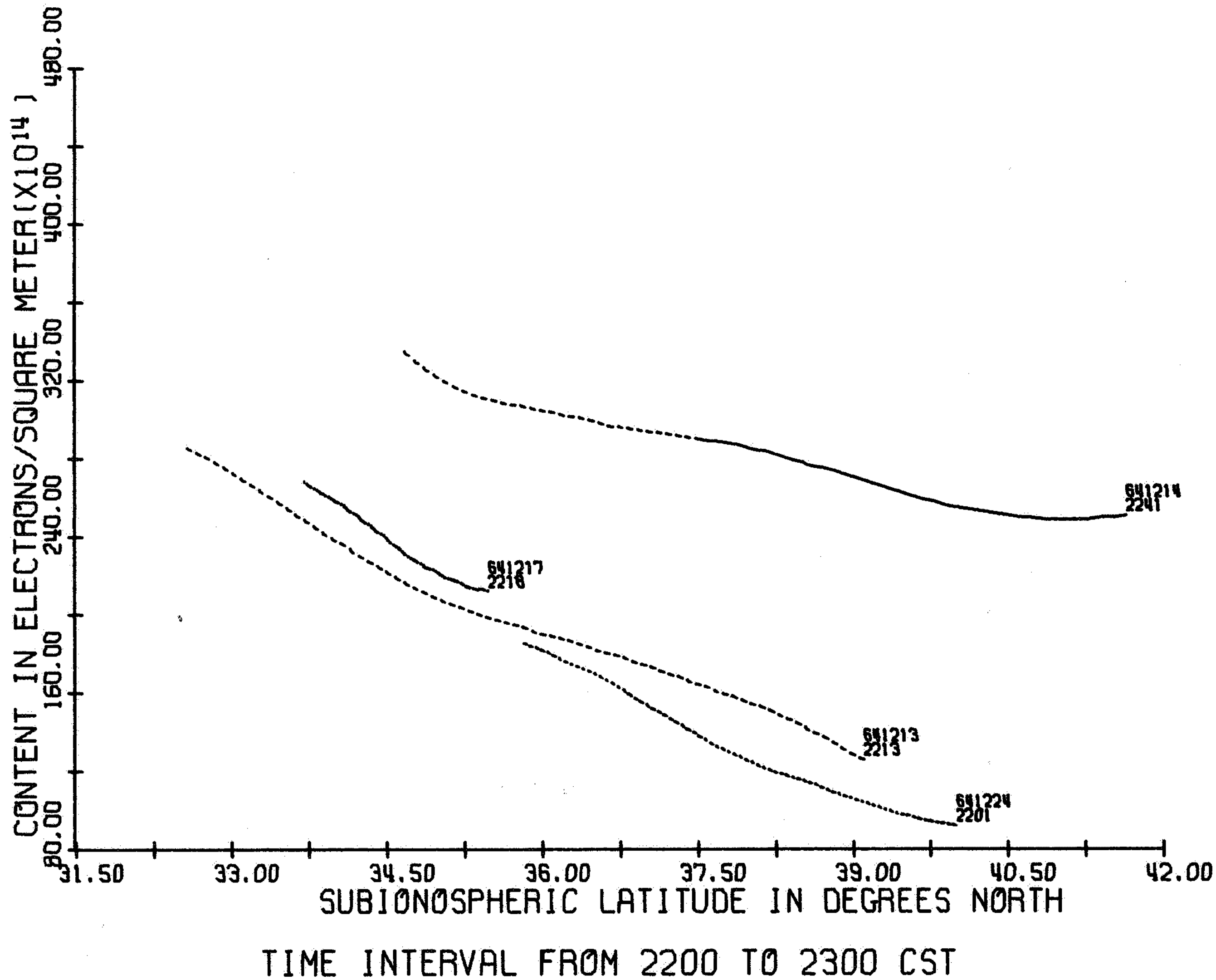
CONTENT IN ELECTRONS/SQUARE METER(X10^{14})
480.00
400.00
320.00
240.00
160.00
80.00
31.50
33.00
34.50
36.00
37.50
39.00
40.50
42.00
SUBIONOSPHERIC LATITUDE IN DEGREES NORTH
TIME INTERVAL FROM 2200 TO 2300 CST
641214
2241
641217
2216
641213
2213
641224
2201

Figure 33.

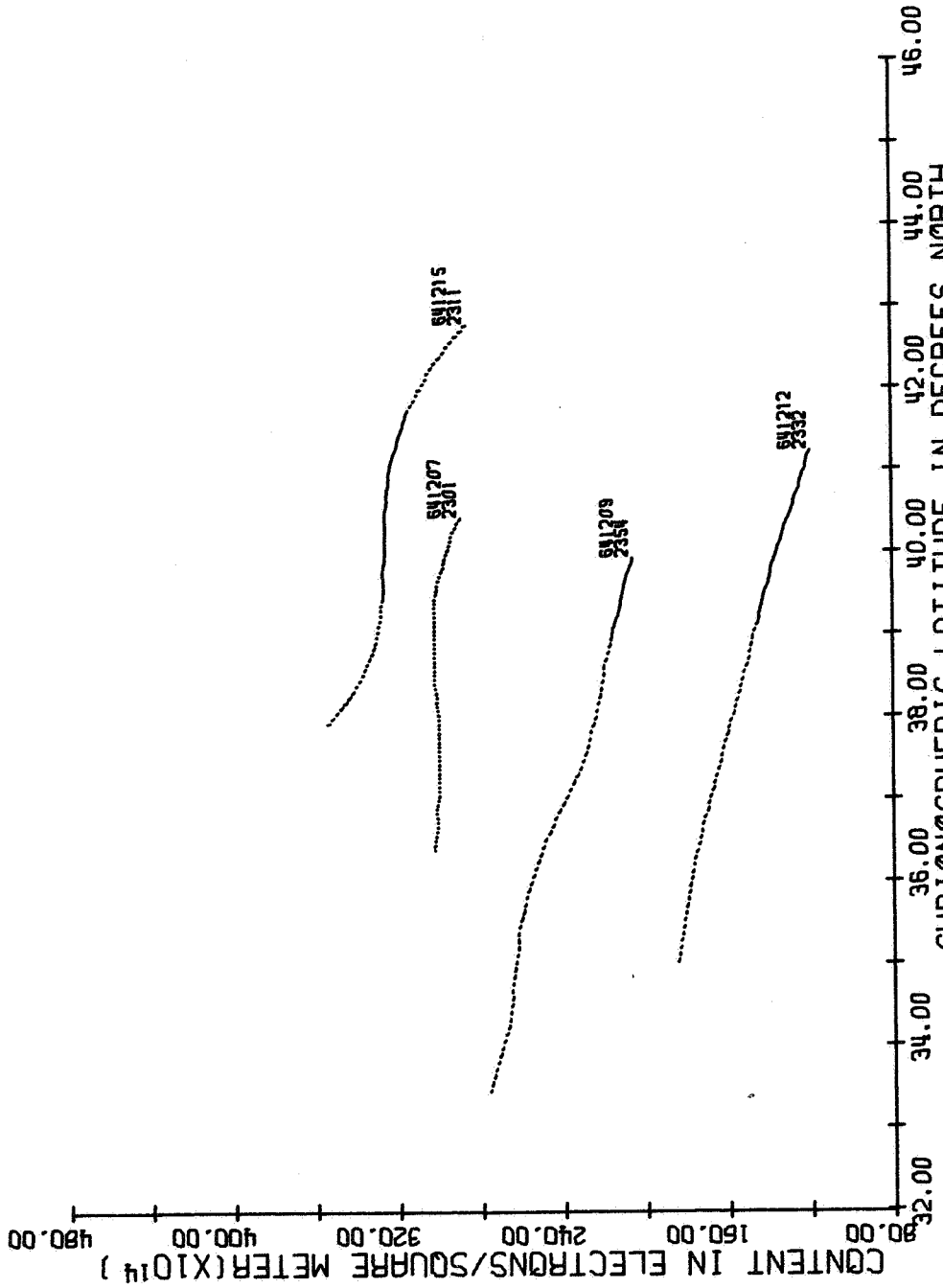
TIME INTERVAL FROM 2300 TO 2400 CST
SUBIONOSPHERIC LATITUDE IN DEGREES NORTH
32.00
34.00
36.00
38.00
40.00
42.00
44.00
46.00
CONTENT IN ELECTRONS/SQUARE METER(X10^14)
80.00
160.00
240.00
320.00
400.00
480.00
641215 2311
641207 2301
641209 2314
641212 2332

Figure 34.

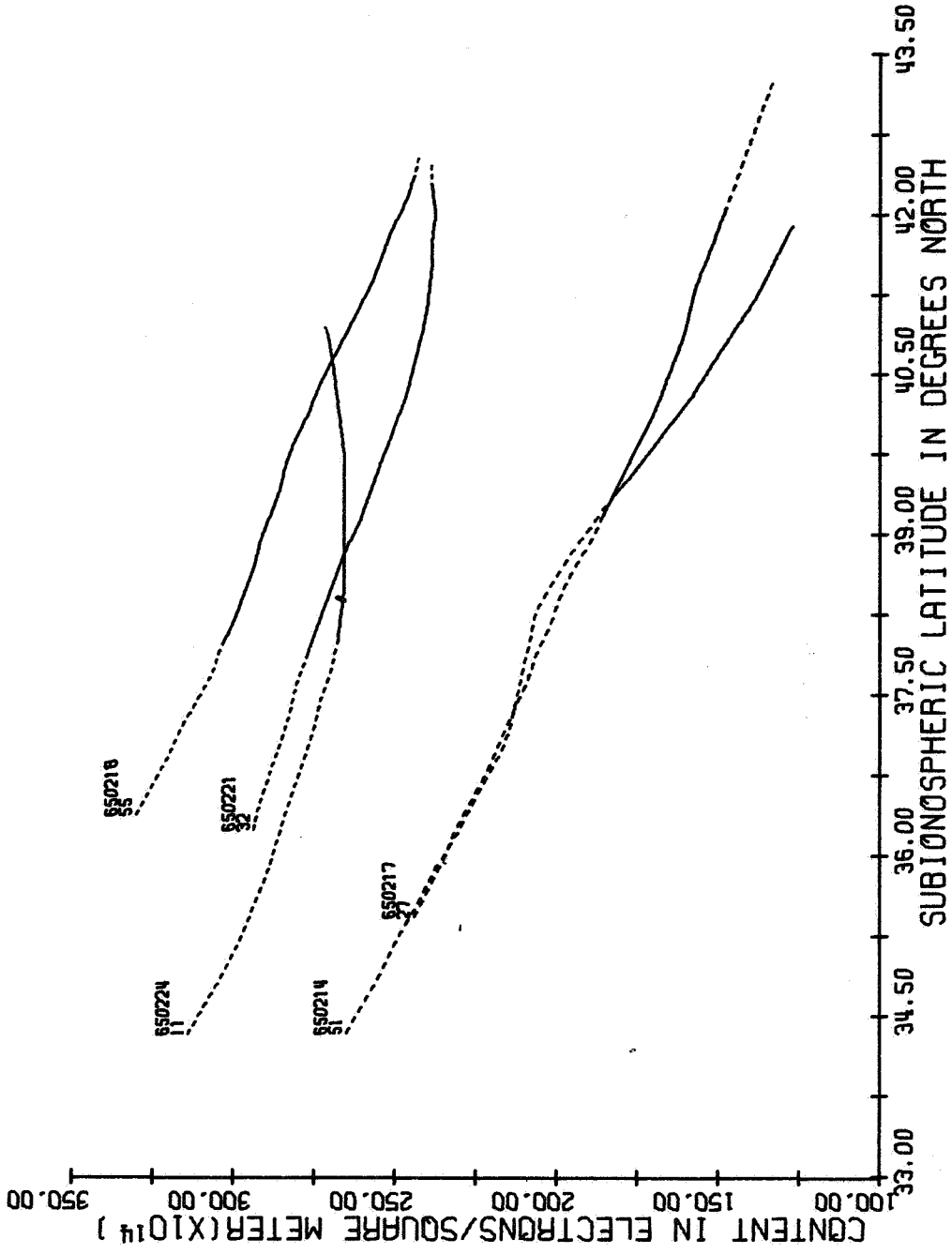
TIME INTERVAL FROM 0 TO 100 CST
SUBIONOSPHERIC LATITUDE IN DEGREES NORTH
33.00
34.50
36.00
37.50
39.00
40.50
42.00
43.50
CONTENT IN ELECTRONS/SQUARE METER(X10^14)
100.00
150.00
200.00
250.00
300.00
350.00
650218
55
650221
32
650224
11
650214
51
650217
21

Figure 35.

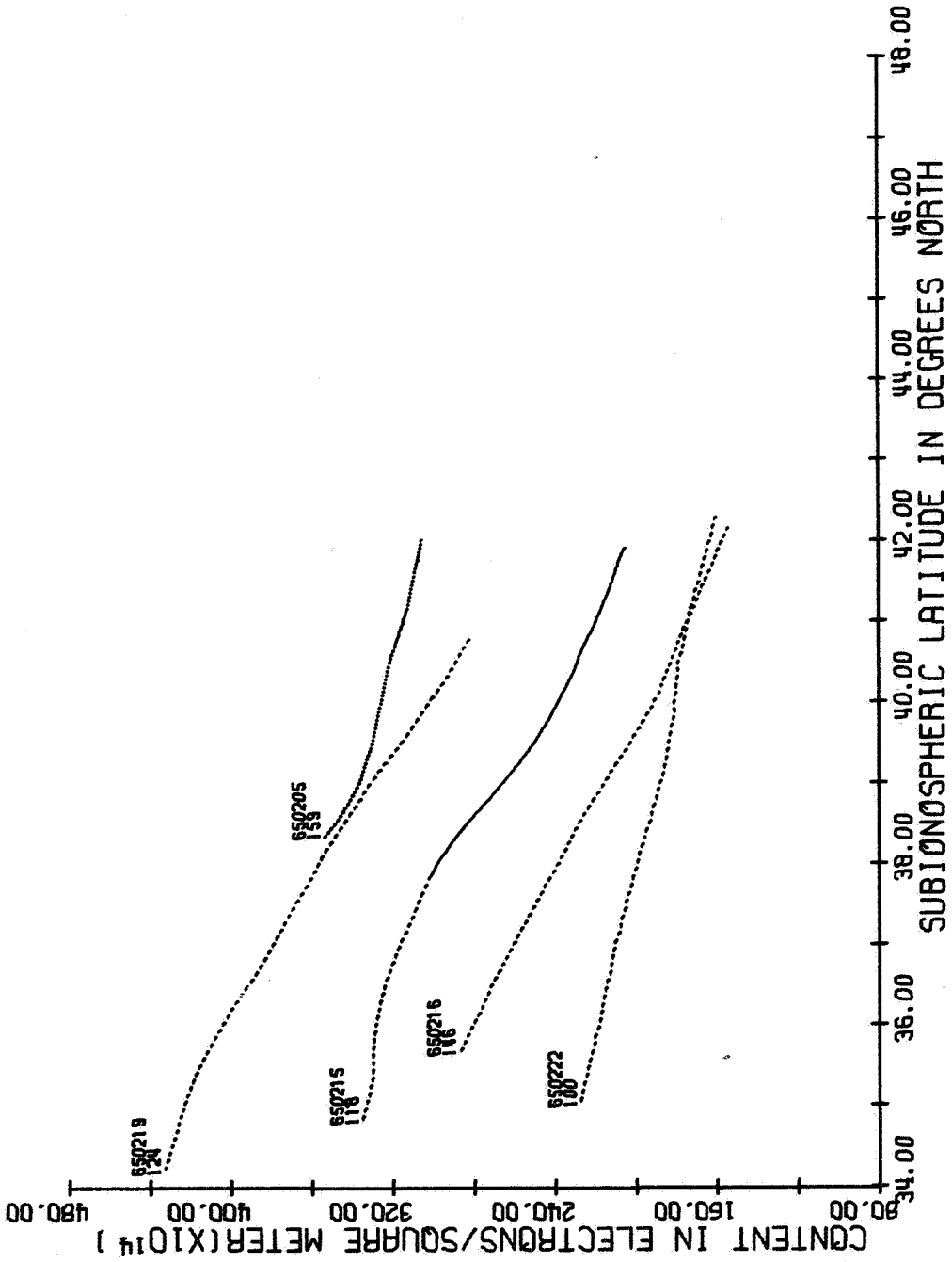
TIME INTERVAL FROM 100 TO 200 CST
SUBIONOSPHERIC LATITUDE IN DEGREES NORTH
34.00
36.00
38.00
40.00
42.00
44.00
46.00
48.00
CONTENT IN ELECTRONS/SQUARE METER(X10¹⁴)
80.00
160.00
240.00
320.00
400.00
480.00
650219
124
650205
139
650215
118
650216
116
650222
100

Figure 36.

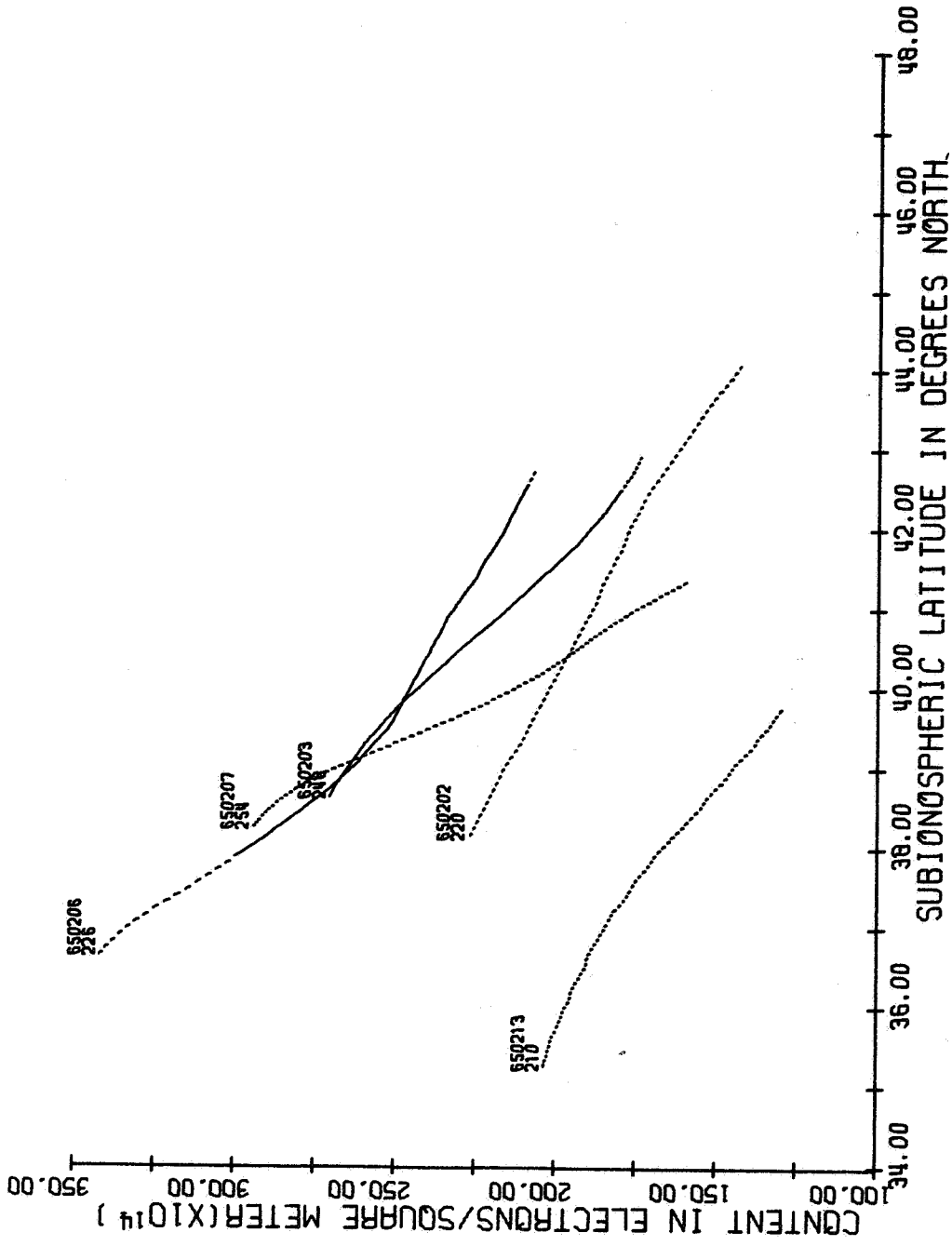
CONTENT IN ELECTRONS/SQUARE METER(X10¹⁴)
100.00
150.00
200.00
250.00
300.00
350.00
34.00
36.00
38.00
40.00
42.00
44.00
46.00
48.00
SUBIONOSPHERIC LATITUDE IN DEGREES NORTH
TIME INTERVAL FROM 200 TO 300 CST
650206
226
650207
234
650203
218
650202
220
650213
210

Figure 37.

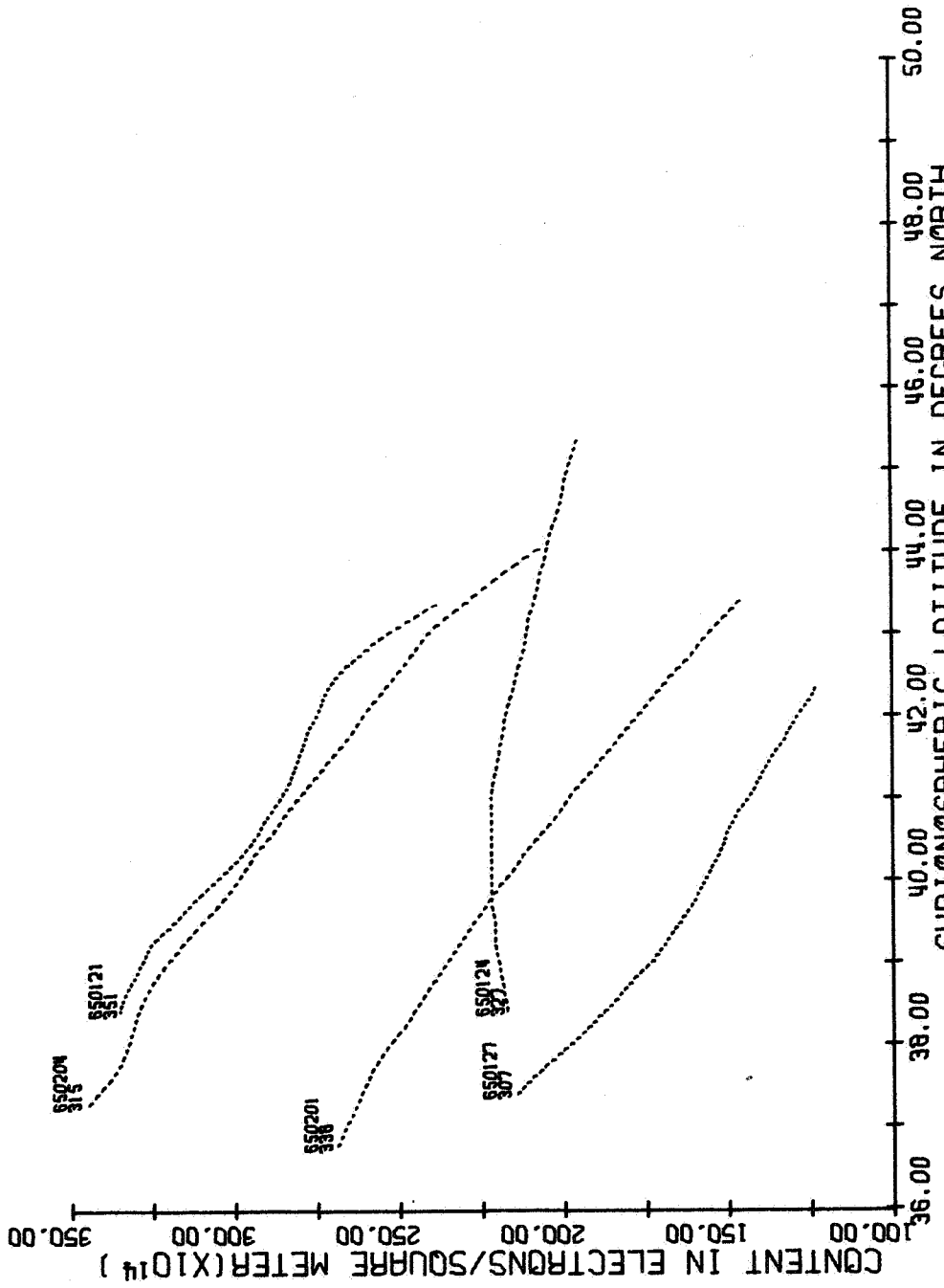
TIME INTERVAL FROM 300 TO 400 CST
SUBIONOSPHERIC LATITUDE IN DEGREES NORTH
36.00
38.00
40.00
42.00
44.00
46.00
48.00
50.00
CONTENT IN ELECTRONS/SQUARE METER(X10^14)
100.00
150.00
200.00
250.00
300.00
350.00
650204
315
650121
351
650201
338
650124
327
650127
307

Figure 38.

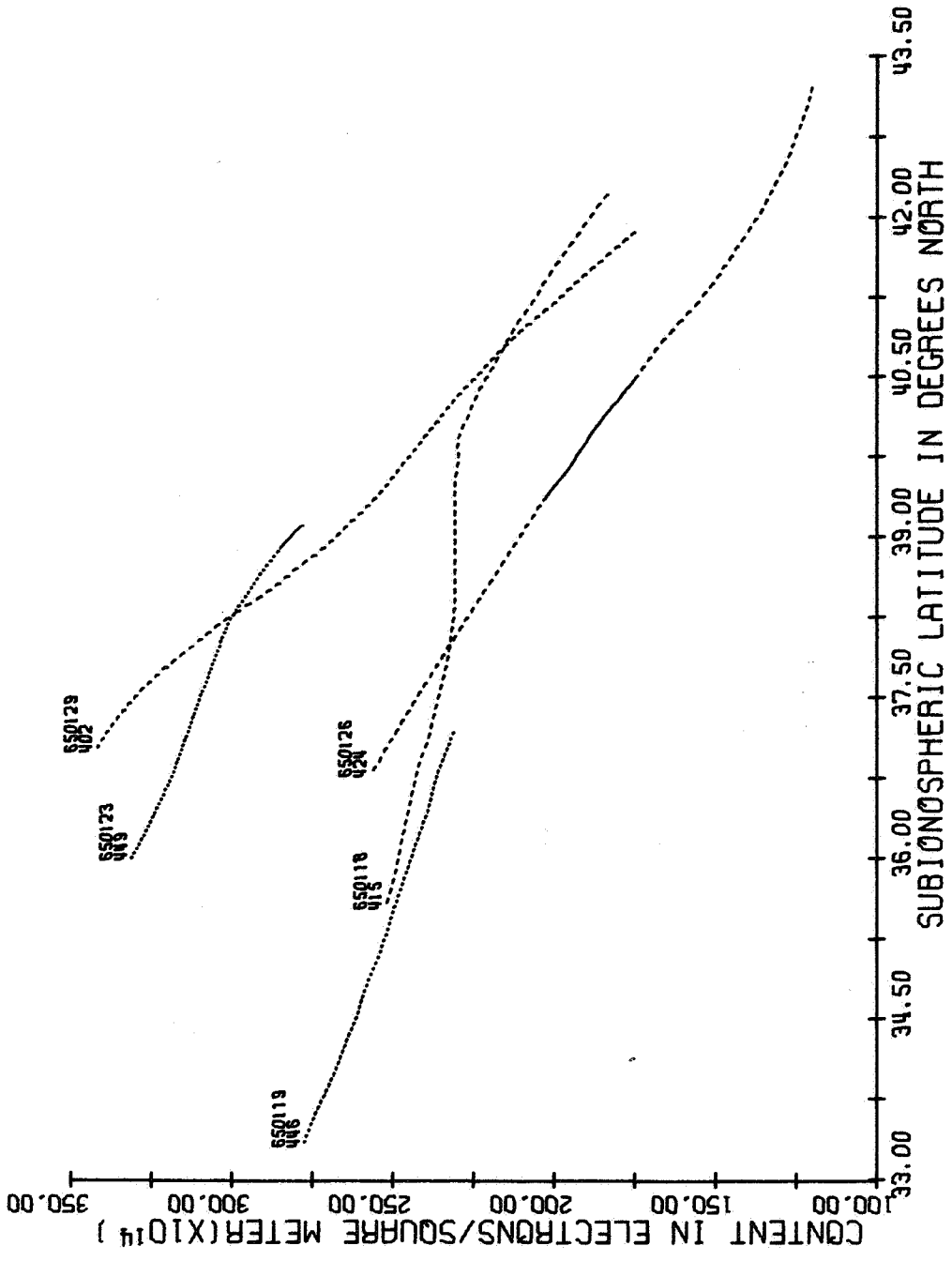
650129
650123
650126
650118
650119
CONTENT IN ELECTRONS/SQUARE METER(X10¹⁴)
100.00
150.00
200.00
250.00
300.00
350.00
SUBIONOSPHERIC LATITUDE IN DEGREES NORTH
33.00
34.50
36.00
37.50
39.00
40.50
42.00
43.50
TIME INTERVAL FROM 400 TO 500 CST

Figure 39.

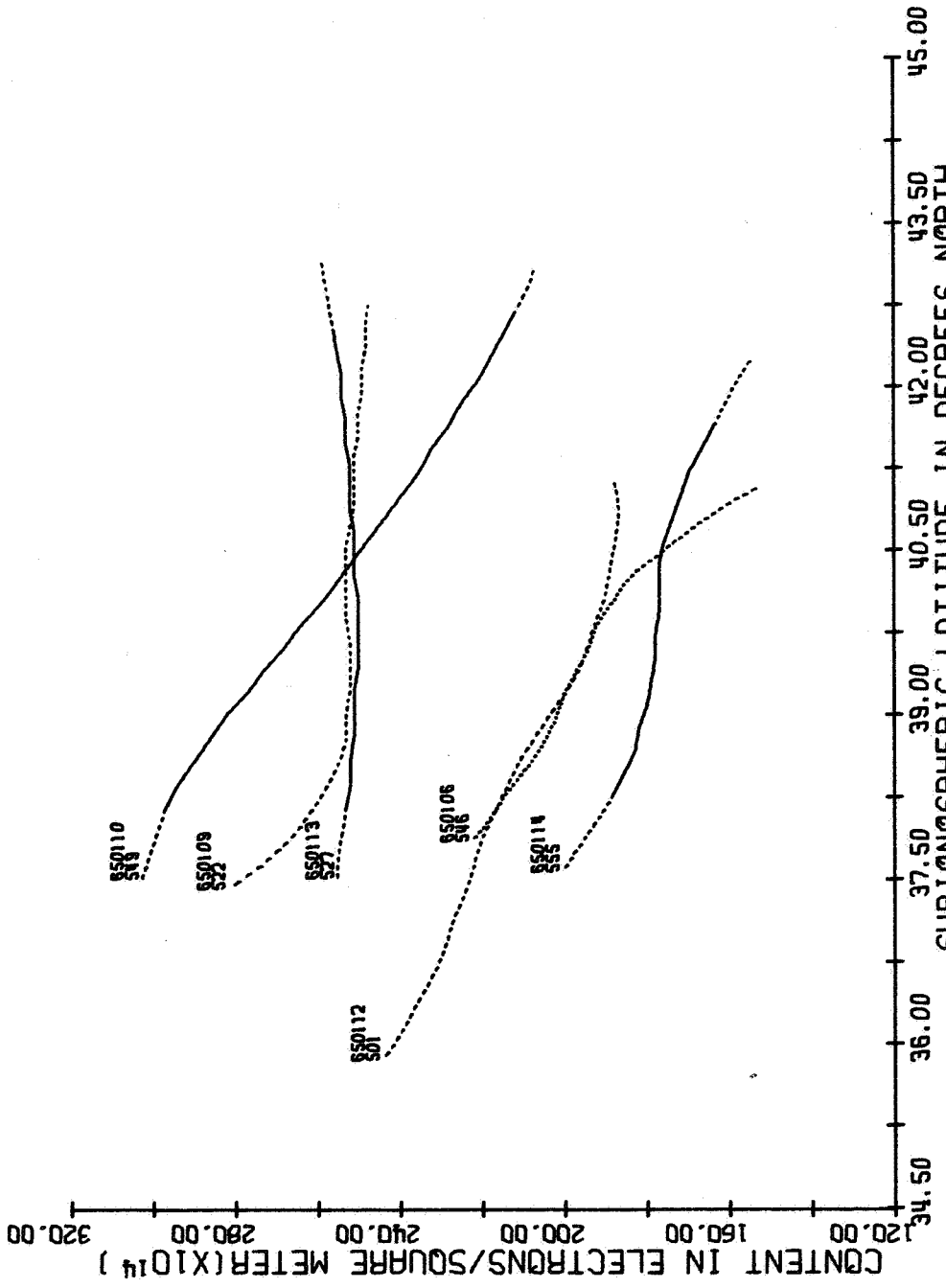
TIME INTERVAL FROM 500 TO 600 CST
SUBIONOSPHERIC LATITUDE IN DEGREES NORTH
34.50
36.00
37.50
39.00
40.50
42.00
43.50
45.00
CONTENT IN ELECTRONS/SQUARE METER(X10^14)
120.00
160.00
200.00
240.00
280.00
320.00
650110
S18
650109
S22
650113
S27
650112
S01
650106
S06
650114
S35

Figure 40.

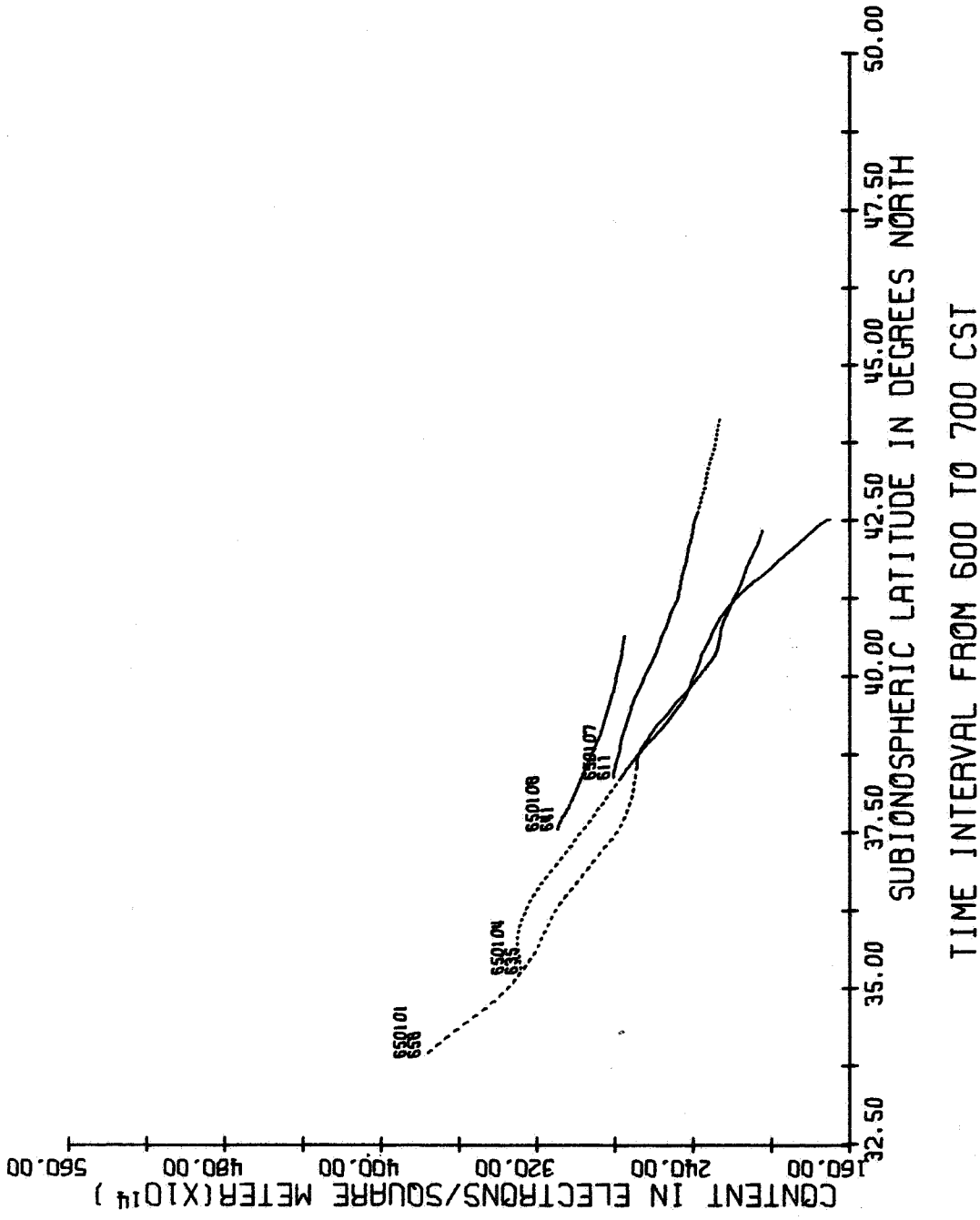
CONTENT IN ELECTRONS/SQUARE METER(X10¹⁴)
160.00
240.00
320.00
400.00
480.00
560.00
32.50
35.00
37.50
40.00
42.50
45.00
47.50
50.00
SUBIONOSPHERIC LATITUDE IN DEGREES NORTH
TIME INTERVAL FROM 600 TO 700 CST
650101
650104
650108
650107

Figure 41.

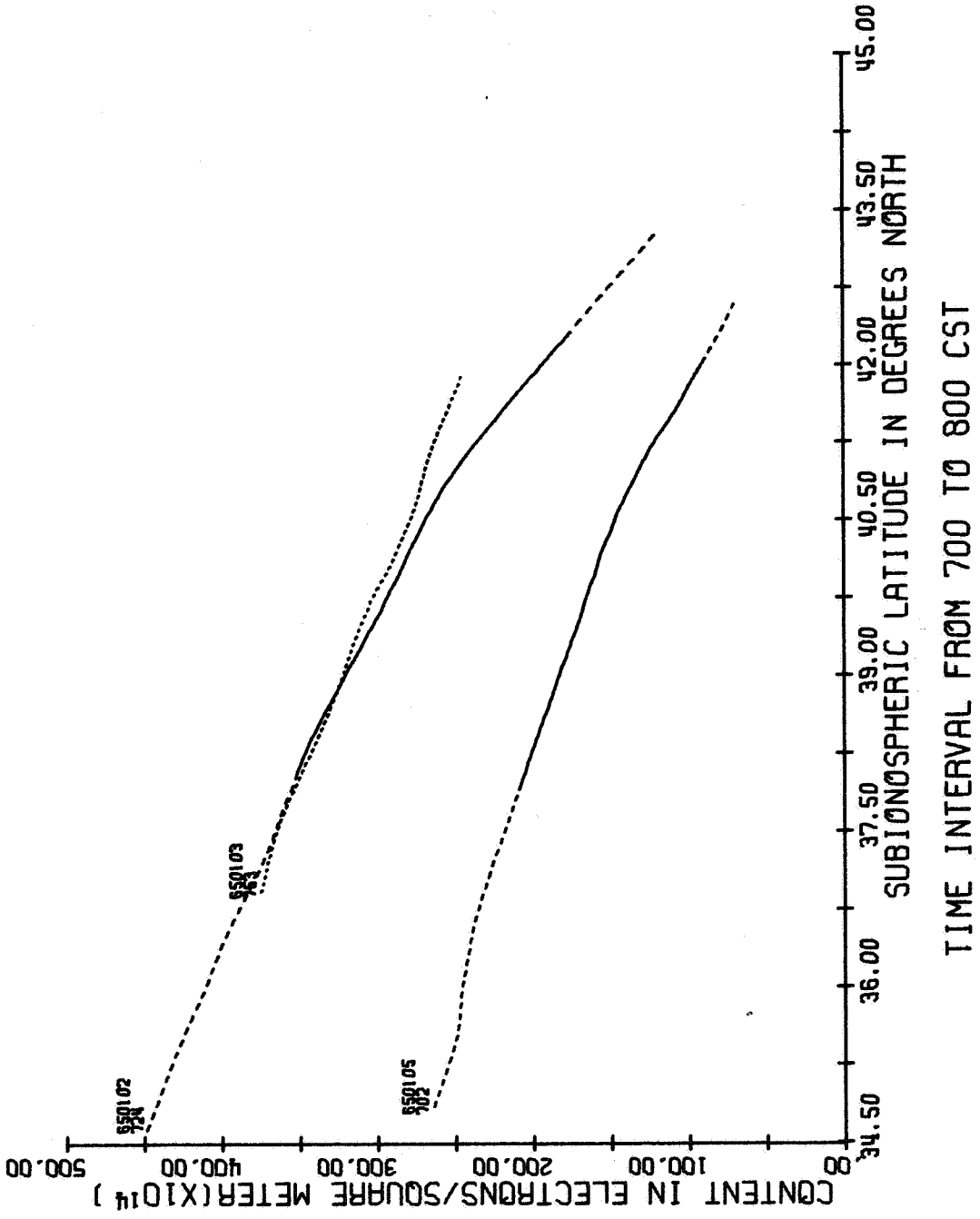
TIME INTERVAL FROM 700 TO 800 CST
SUBIONOSPHERIC LATITUDE IN DEGREES NORTH
34.50
36.00
37.50
39.00
40.50
42.00
43.50
45.00
CONTENT IN ELECTRONS/SQUARE METER(X10^14)
0.0
100.00
200.00
300.00
400.00
500.00
650102
650103
650105

Figure 42.

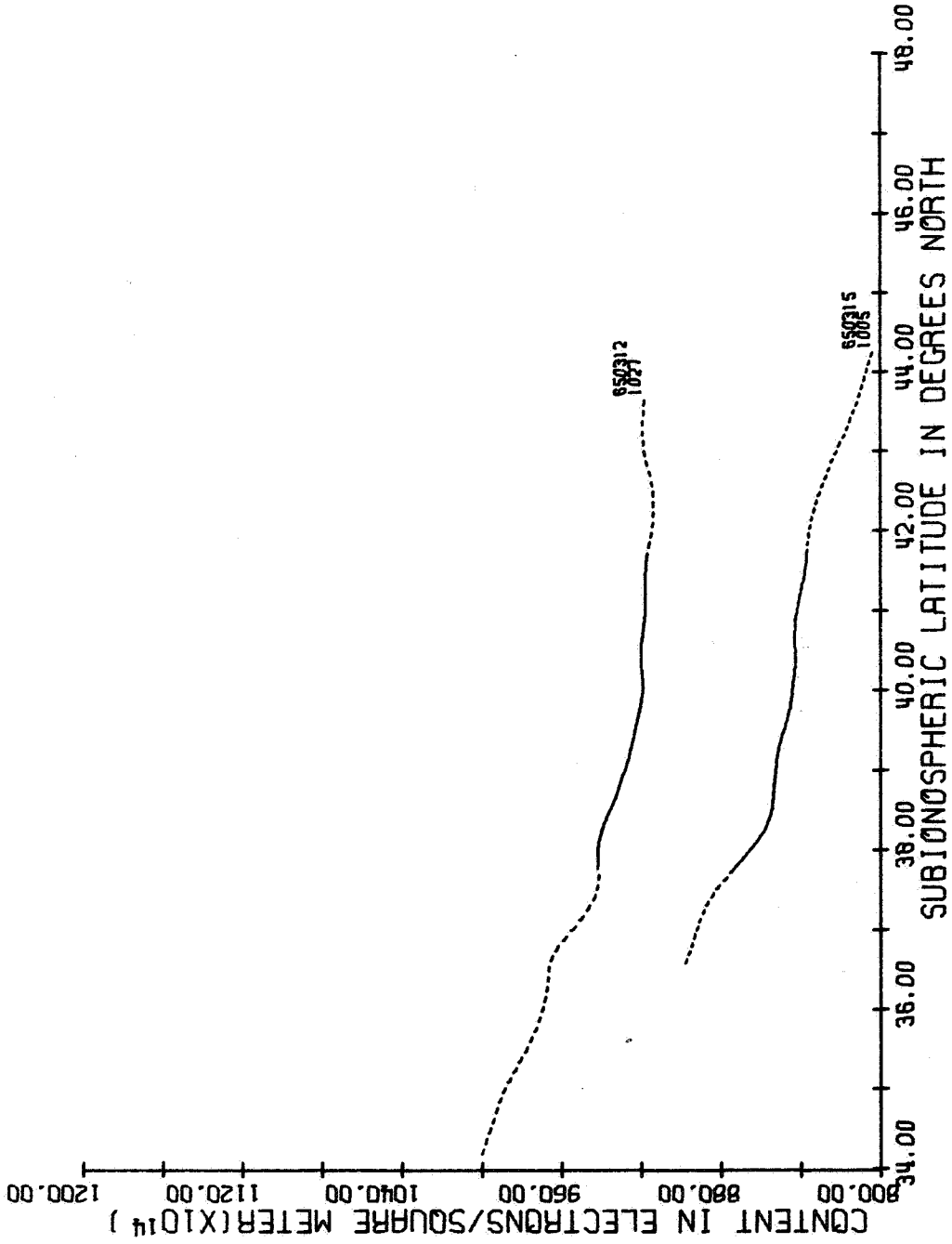
CONTENT IN ELECTRONS/SQUARE METER(X10¹⁴)
800.00
880.00
960.00
1040.00
1120.00
1200.00
34.00
36.00
38.00
40.00
42.00
44.00
46.00
48.00
SUBIONOSPHERIC LATITUDE IN DEGREES NORTH
TIME INTERVAL FROM 1000 TO 1100 CST
650312
1027
650315
1005

Figure 43.

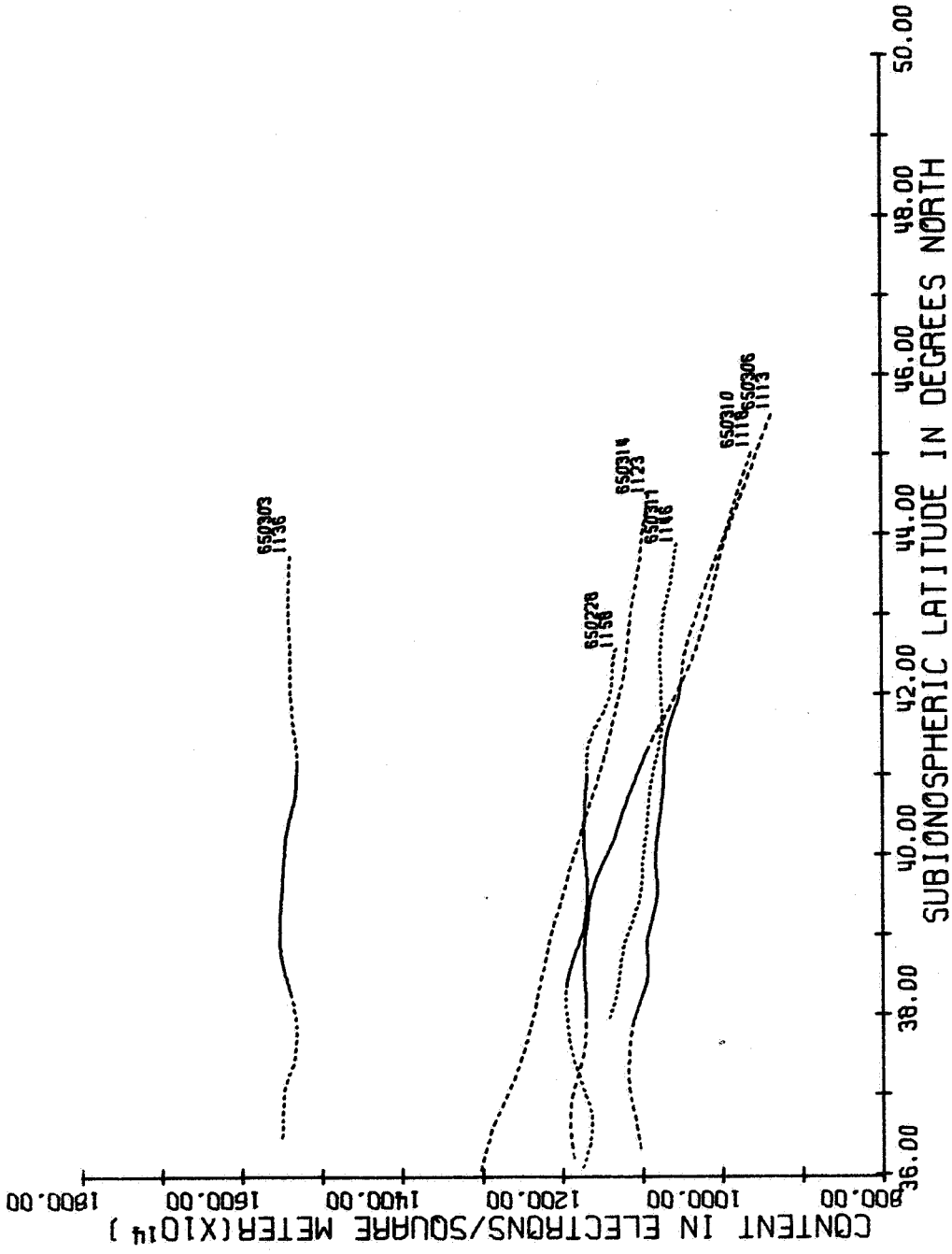
TIME INTERVAL FROM 1100 TO 1200 CST
SUBIONOSPHERIC LATITUDE IN DEGREES NORTH
36.00
38.00
40.00
42.00
44.00
46.00
48.00
50.00
CONTENT IN ELECTRONS/SQUARE METER(X10^14)
800.00
1000.00
1200.00
1400.00
1600.00
1800.00
650303 1136
650228 1158
650311 1108
650314 1123
650310 1116
650306 1113

Figure 44.

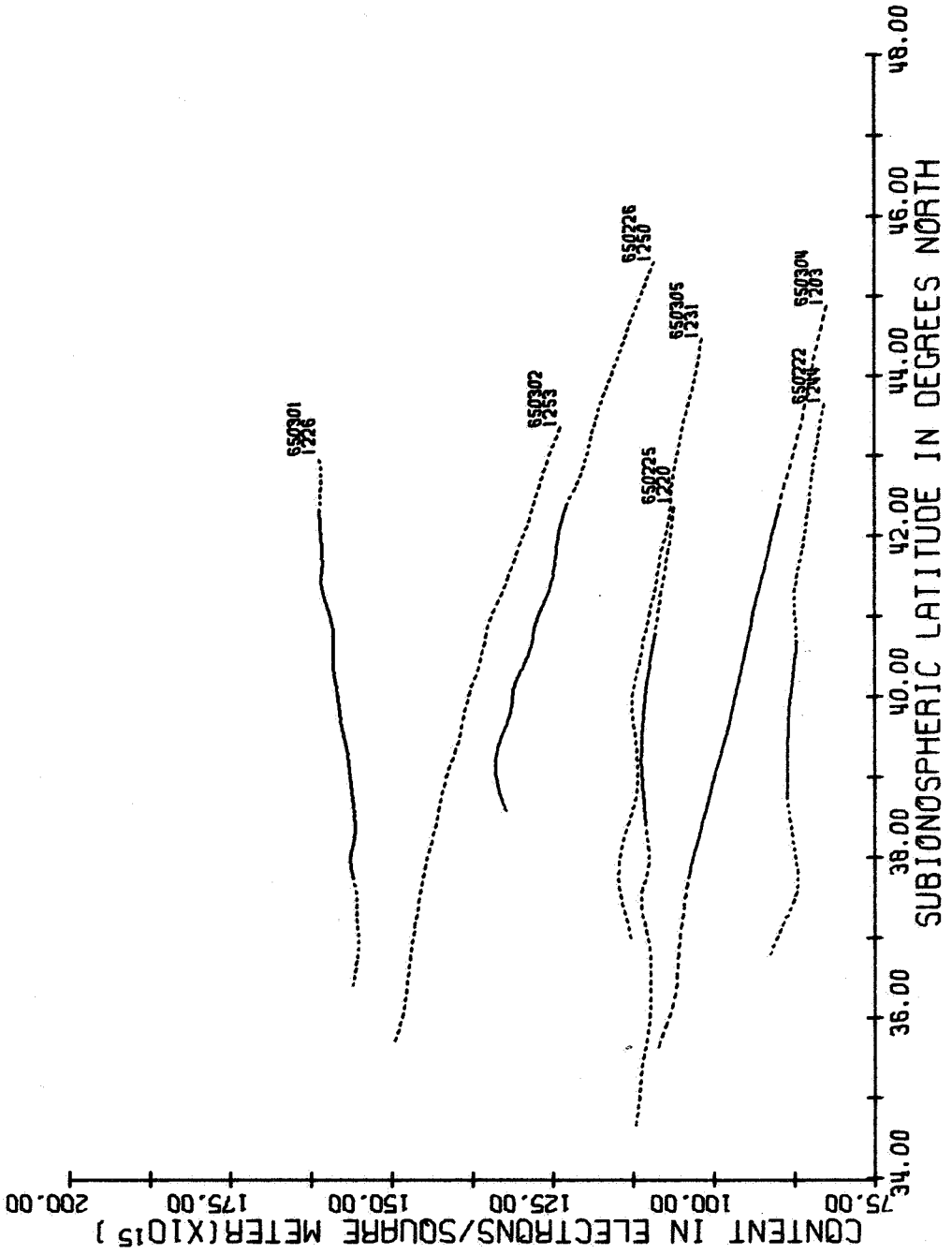
650301
1226
650302
1253
650725
1220
650726
1250
650305
1231
650722
1244
650304
1203
CONTENT IN ELECTRONS/SQUARE METER(X10^15)
75.00
100.00
125.00
150.00
175.00
200.00
SUBIONOSPHERIC LATITUDE IN DEGREES NORTH
34.00
36.00
38.00
40.00
42.00
44.00
46.00
48.00
TIME INTERVAL FROM 1200 TO 1300 CST

Figure 45.

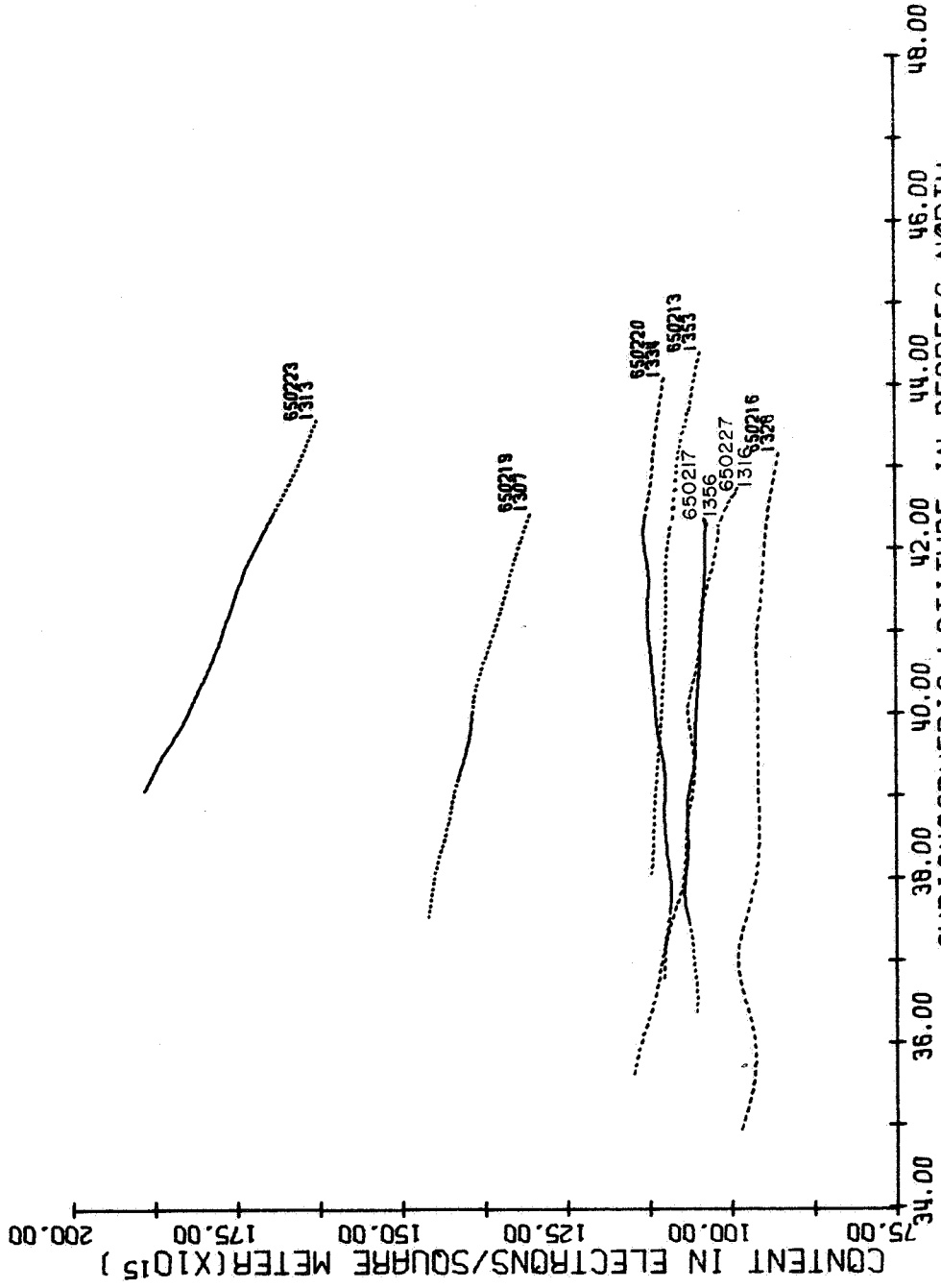
TIME INTERVAL FROM 1300 TO 1400 CST
SUBIONOSPHERIC LATITUDE IN DEGREES NORTH
34.00
36.00
38.00
40.00
42.00
44.00
46.00
48.00
CONTENT IN ELECTRONS/SQUARE METER(X10^15)
75.00
100.00
125.00
150.00
175.00
200.00
650223
1313
650219
1307
650220
1334
650213
1353
650217
1356
650227
1316
650216
1328

Figure 46.

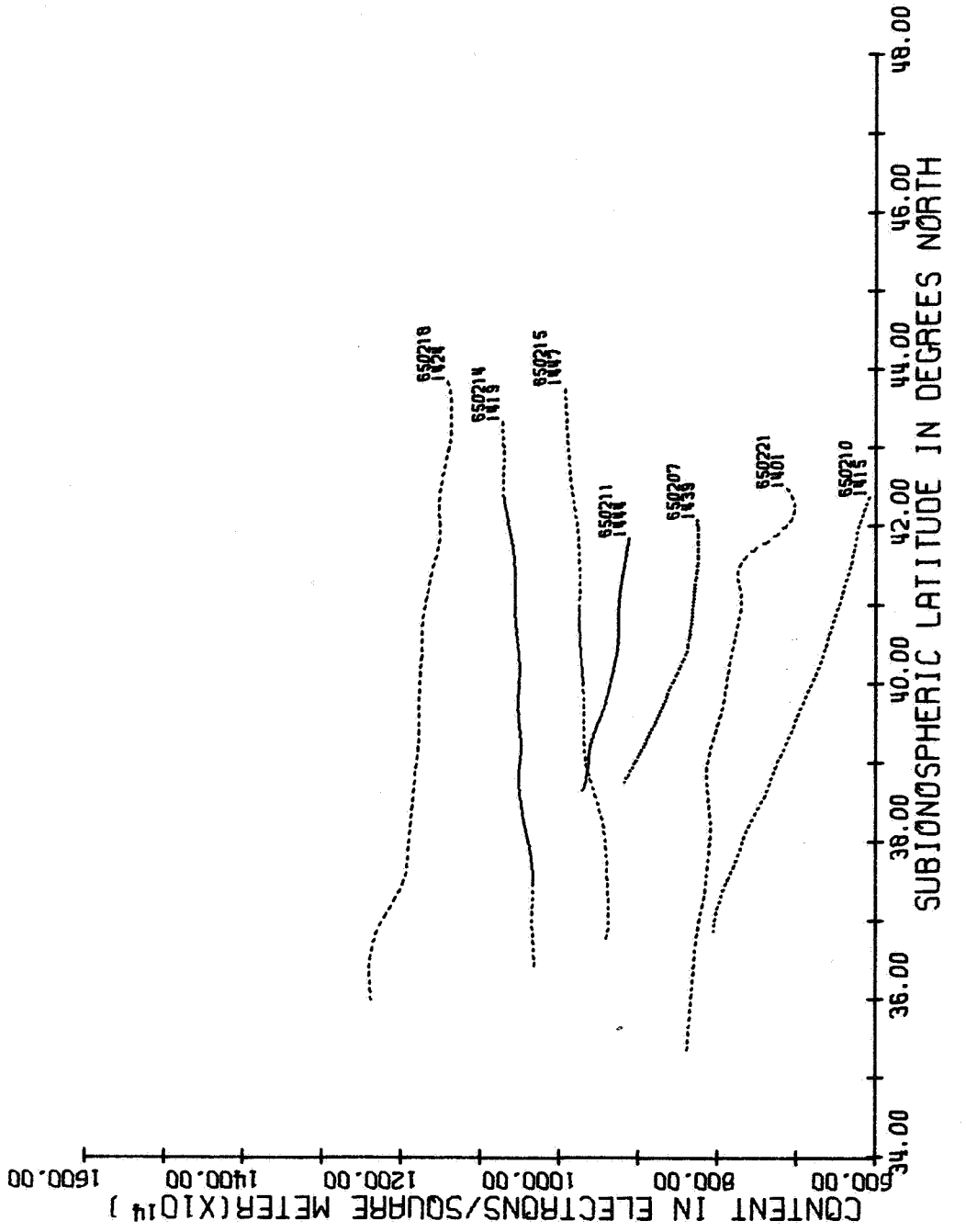
TIME INTERVAL FROM 1400 TO 1500 CST
SUBIONOSPHERIC LATITUDE IN DEGREES NORTH
34.00
36.00
38.00
40.00
42.00
44.00
46.00
48.00
CONTENT IN ELECTRONS/SQUARE METER(X10¹⁴)
600.00
800.00
1000.00
1200.00
1400.00
1600.00
650218
1424
650214
1413
650215
1409
650211
1408
650207
1439
650221
1401
650210
1415

Figure 47.

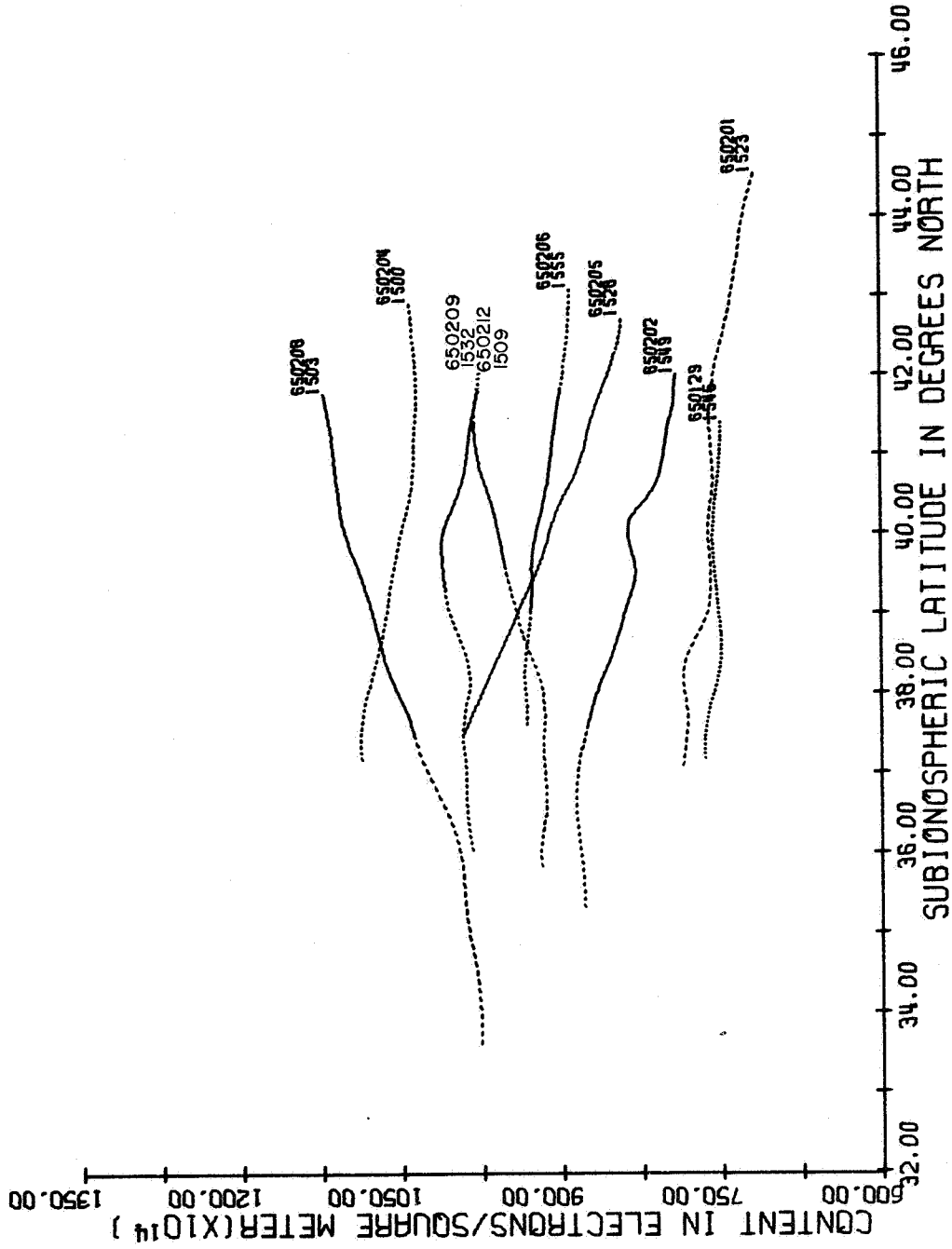
TIME INTERVAL FROM 1500 TO 1600 CST
SUBIONOSPHERIC LATITUDE IN DEGREES NORTH
32.00
34.00
36.00
38.00
40.00
42.00
44.00
46.00
CONTENT IN ELECTRONS/SQUARE METER(X10^14)
500.00
750.00
900.00
1050.00
1200.00
1350.00
650206 1503
650204 1500
650209 1532
650212 1509
650206 1555
650205 1528
650202 1518
650129 1516
650201 1523

Figure 48.

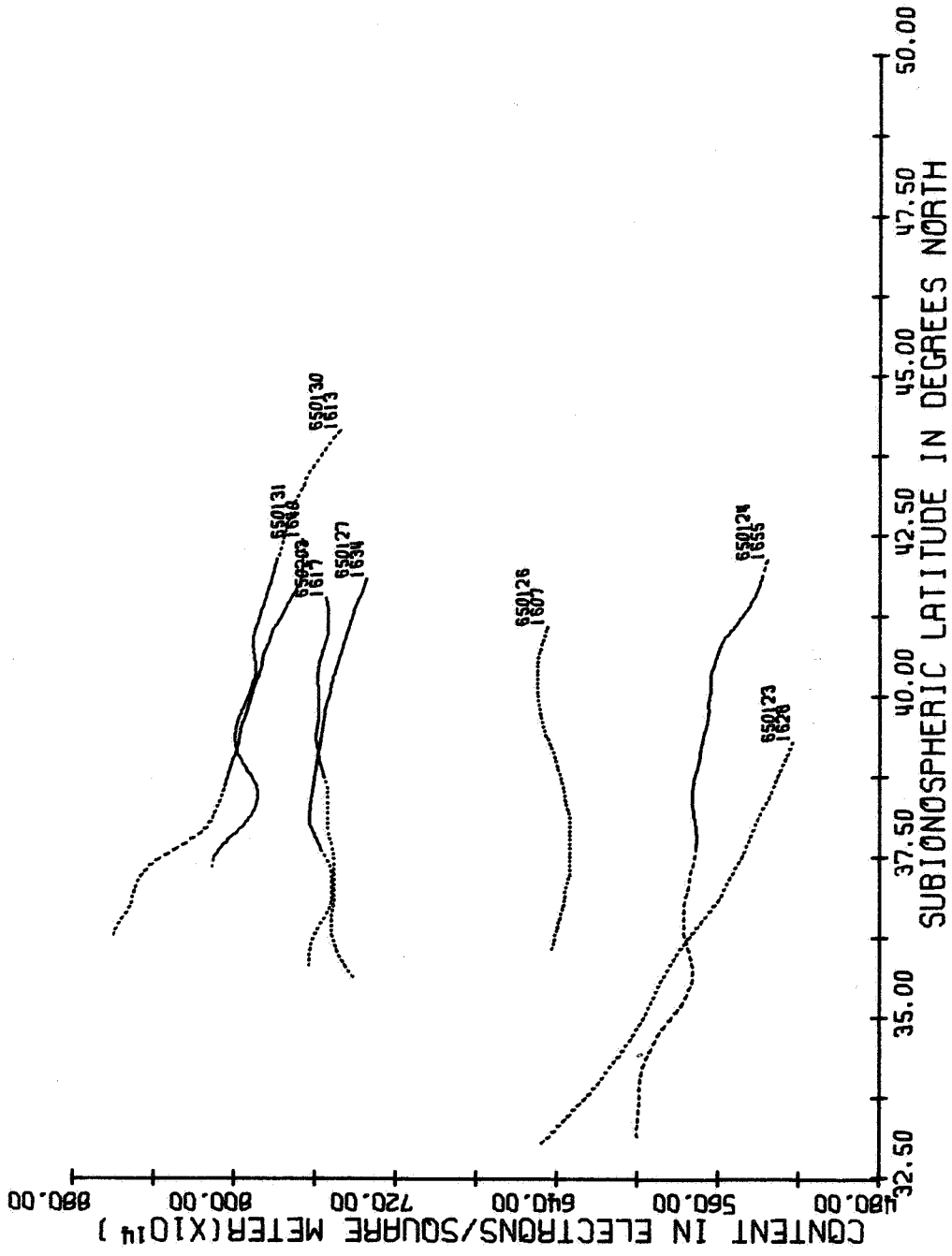
TIME INTERVAL FROM 1600 TO 1700 CST
SUBIONOSPHERIC LATITUDE IN DEGREES NORTH
32.50
35.00
37.50
40.00
42.50
45.00
47.50
50.00
CONTENT IN ELECTRONS/SQUARE METER(X10^14)
480.00
560.00
640.00
720.00
800.00
880.00
650130
1613
650131
1648
650127
1634
650126
1607
650124
1655
650123
1626

Figure 49.

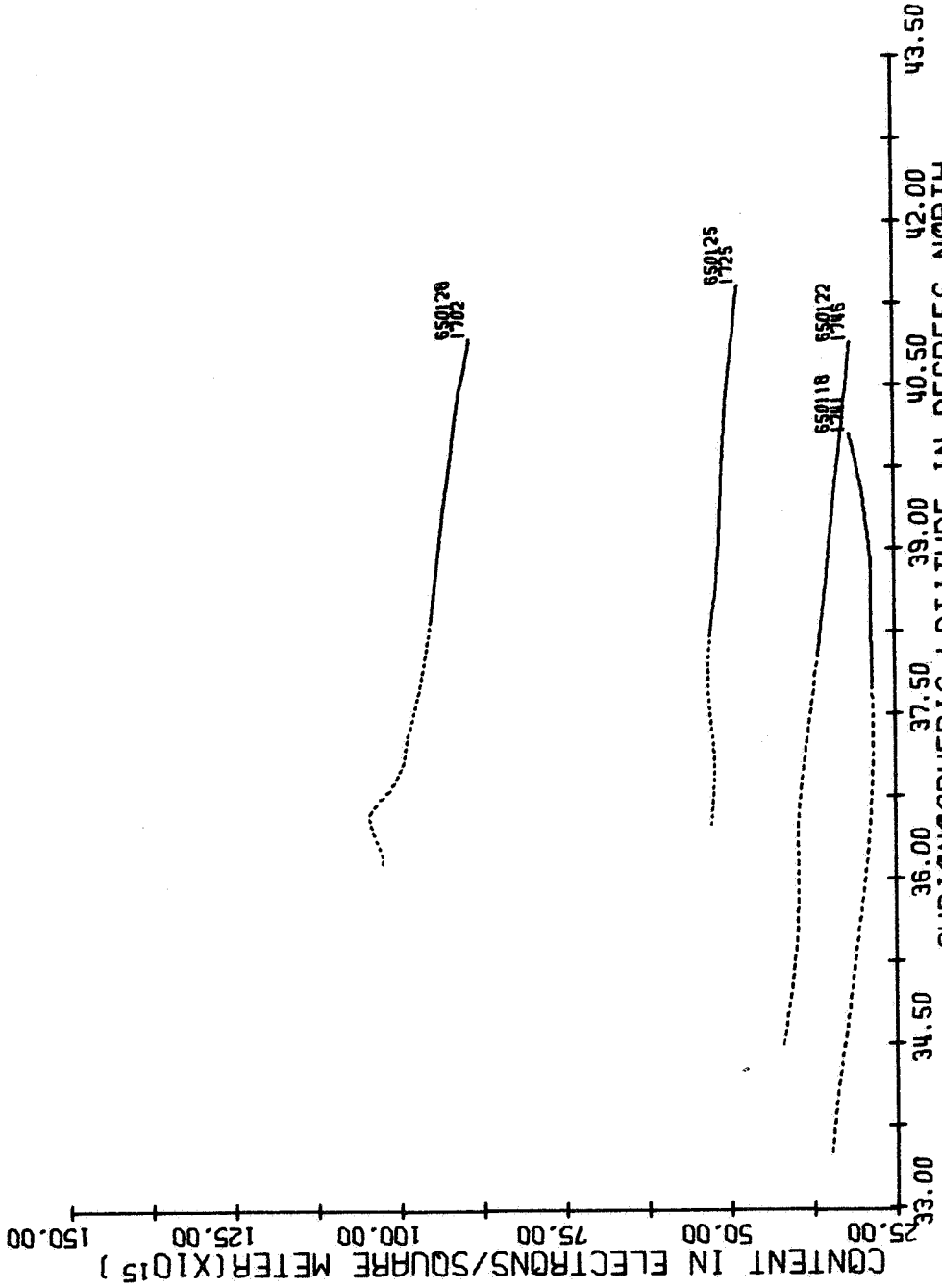
TIME INTERVAL FROM 1700 TO 1800 CST
SUBIONOSPHERIC LATITUDE IN DEGREES NORTH
33.00
34.50
36.00
37.50
39.00
40.50
42.00
43.50
CONTENT IN ELECTRONS/SQUARE METER(X10¹⁵)
25.00
50.00
75.00
100.00
125.00
150.00
650126 1702
650125 1725
650122 1745
650118 1801

Figure 50.

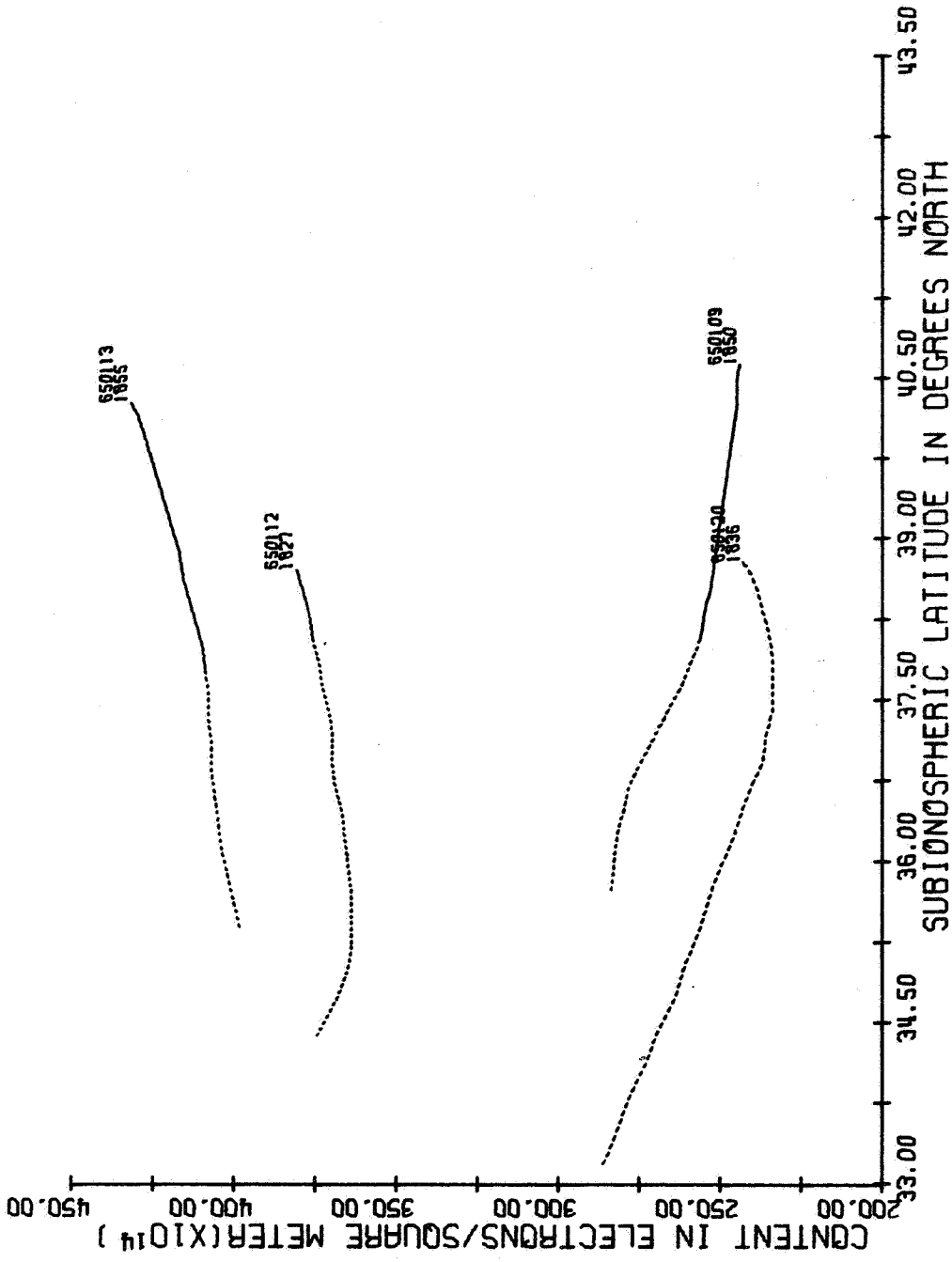
CONTENT IN ELECTRONS/SQUARE METER(X10¹⁴)
200.00
250.00
300.00
350.00
400.00
450.00
33.00
34.50
36.00
37.50
39.00
40.50
42.00
43.50
SUBIONOSPHERIC LATITUDE IN DEGREES NORTH
TIME INTERVAL FROM 1800 TO 1900 CST
650113 1855
650112 1821
650109 1850
650130 1836

Figure 51.

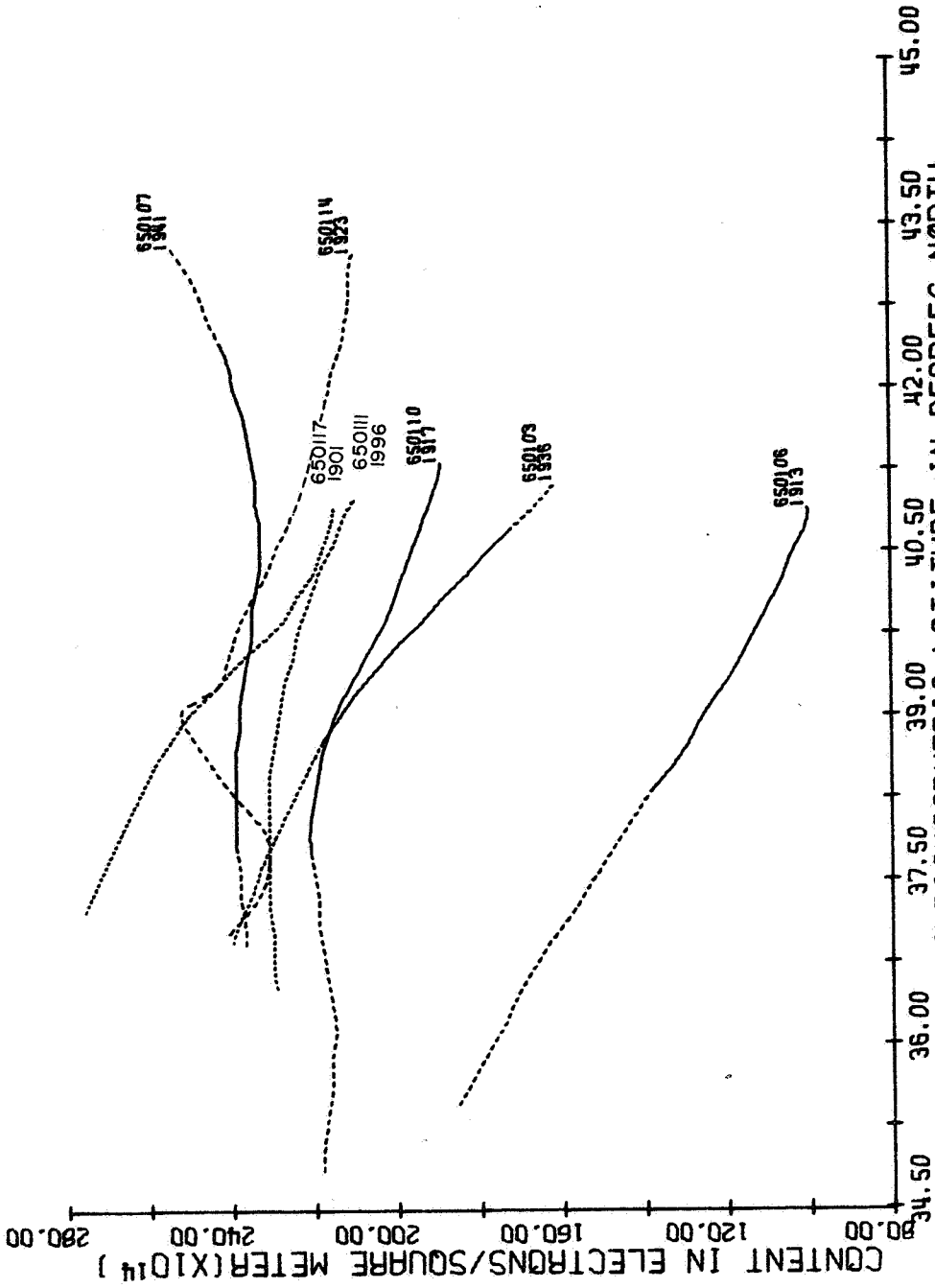
650107
1961
650114
1923
650117
1901
650111
1996
650110
1917
650103
1936
650106
1913
CONTENT IN ELECTRONS/SQUARE METER(X10¹⁴)
80.00
120.00
160.00
200.00
240.00
280.00
34.50
36.00
37.50
39.00
40.50
42.00
43.50
45.00
SUBIONOSPHERIC LATITUDE IN DEGREES NORTH
TIME INTERVAL FROM 1900 TO 2000 CST

Figure 52.

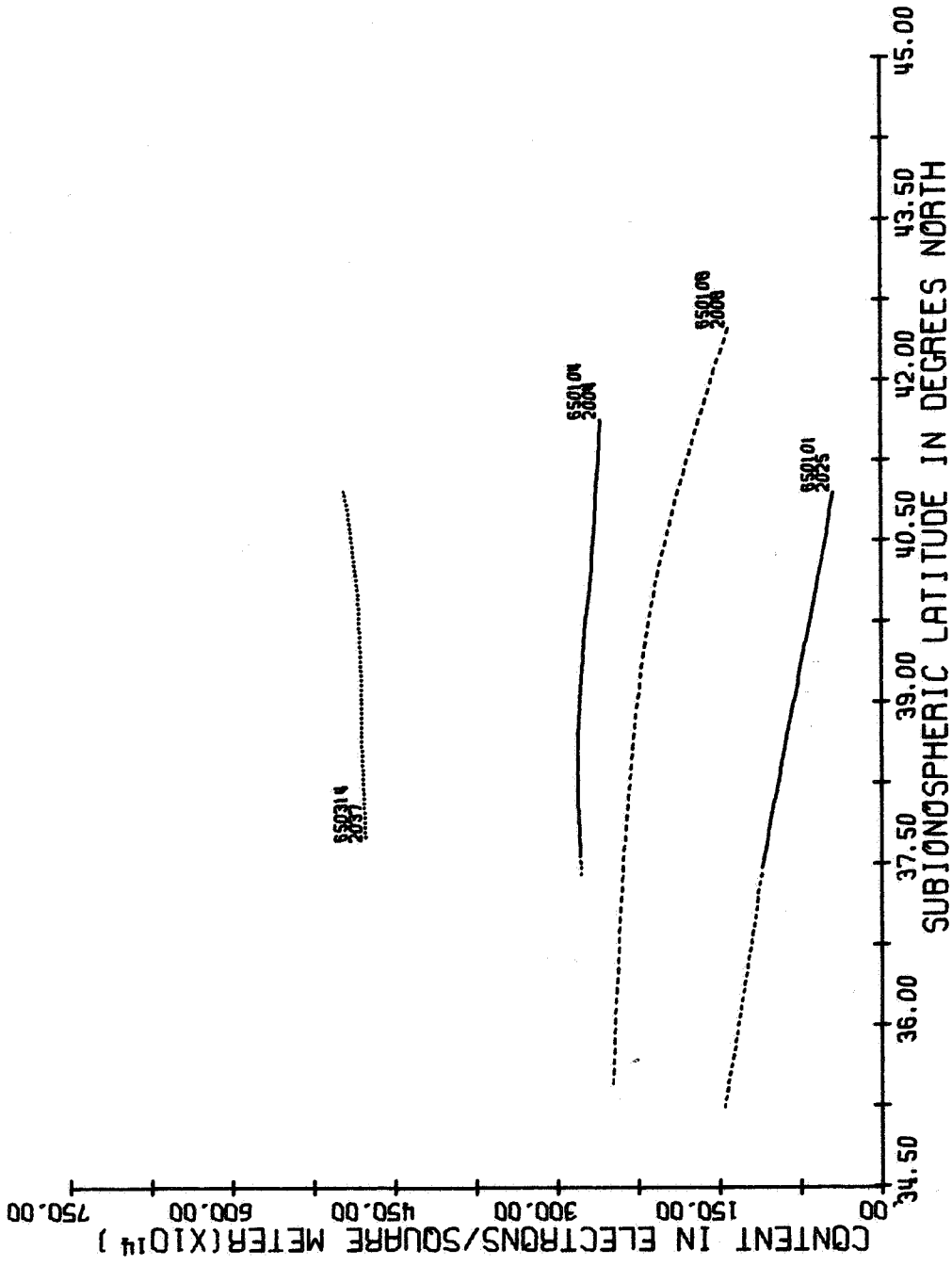
TIME INTERVAL FROM 2000 TO 2100 CST
SUBIONOSPHERIC LATITUDE IN DEGREES NORTH
34.50
36.00
37.50
39.00
40.50
42.00
43.50
45.00
CONTENT IN ELECTRONS/SQUARE METER(X10^14)
0.00
150.00
300.00
450.00
600.00
750.00

Figure 53.

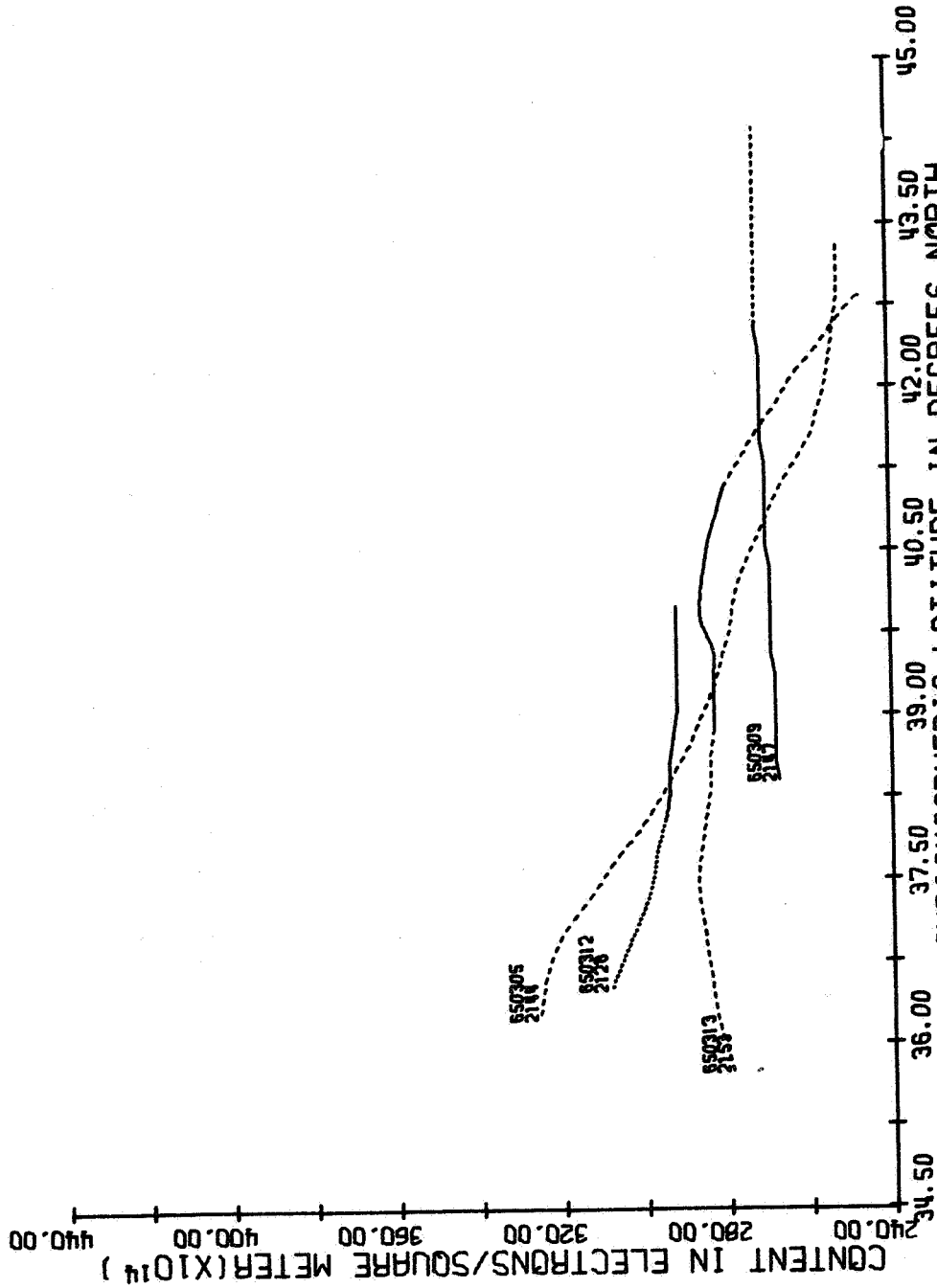
TIME INTERVAL FROM 2100 TO 2200 CST
SUBIONOSPHERIC LATITUDE IN DEGREES NORTH
34.50
36.00
37.50
39.00
40.50
42.00
43.50
45.00
CONTENT IN ELECTRONS/SQUARE METER(X10¹⁴)
240.00
280.00
320.00
360.00
400.00
440.00

Figure 54.

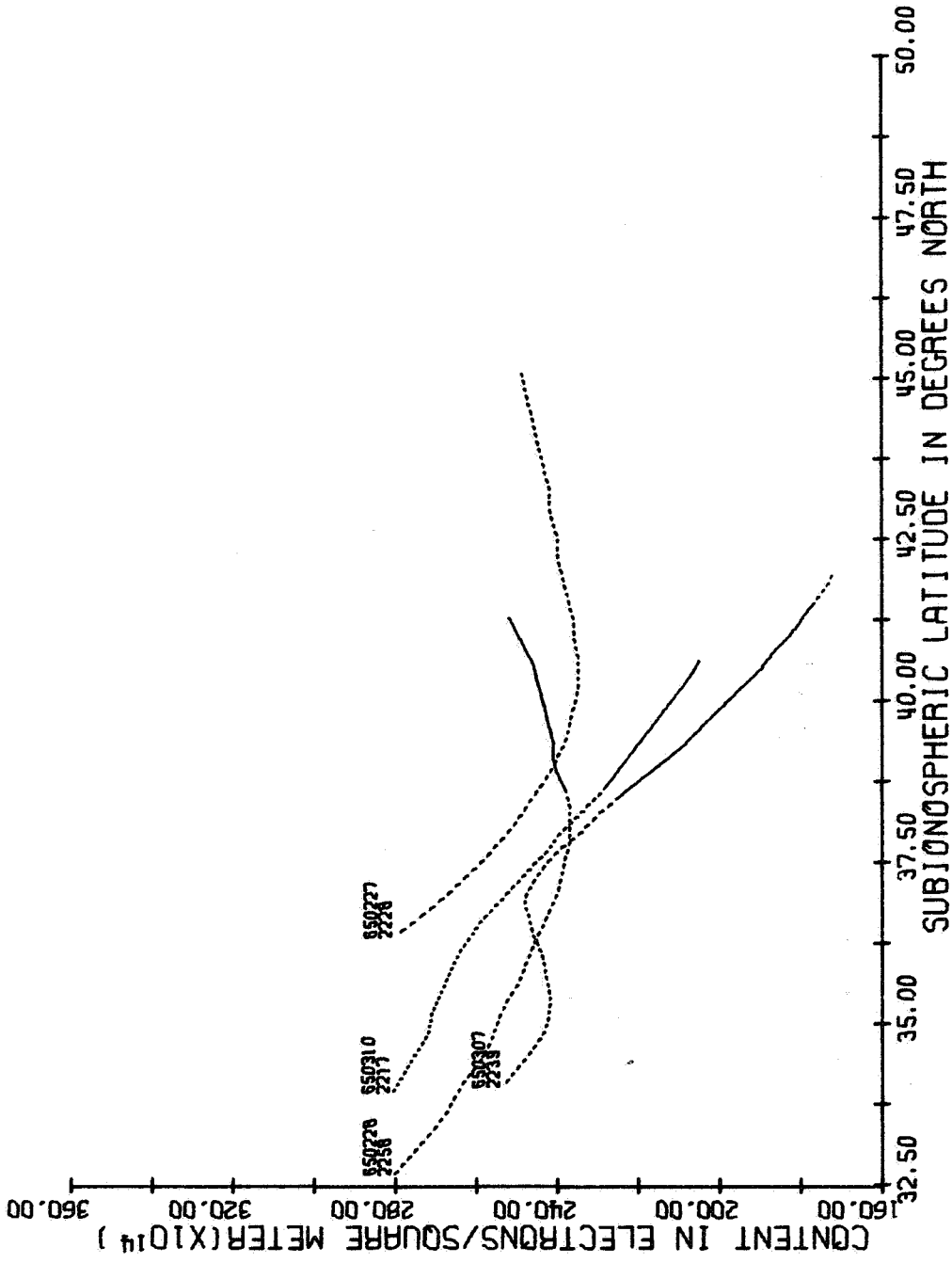
TIME INTERVAL FROM 2200 TO 2300 CST
SUBIONOSPHERIC LATITUDE IN DEGREES NORTH
32.50
35.00
37.50
40.00
42.50
45.00
47.50
50.00
CONTENT IN ELECTRONS/SQUARE METER(X10¹⁴)
160.00
200.00
240.00
280.00
320.00
360.00
650227
2228
650310
2217
650307
2233
650226
2258

Figure 55.

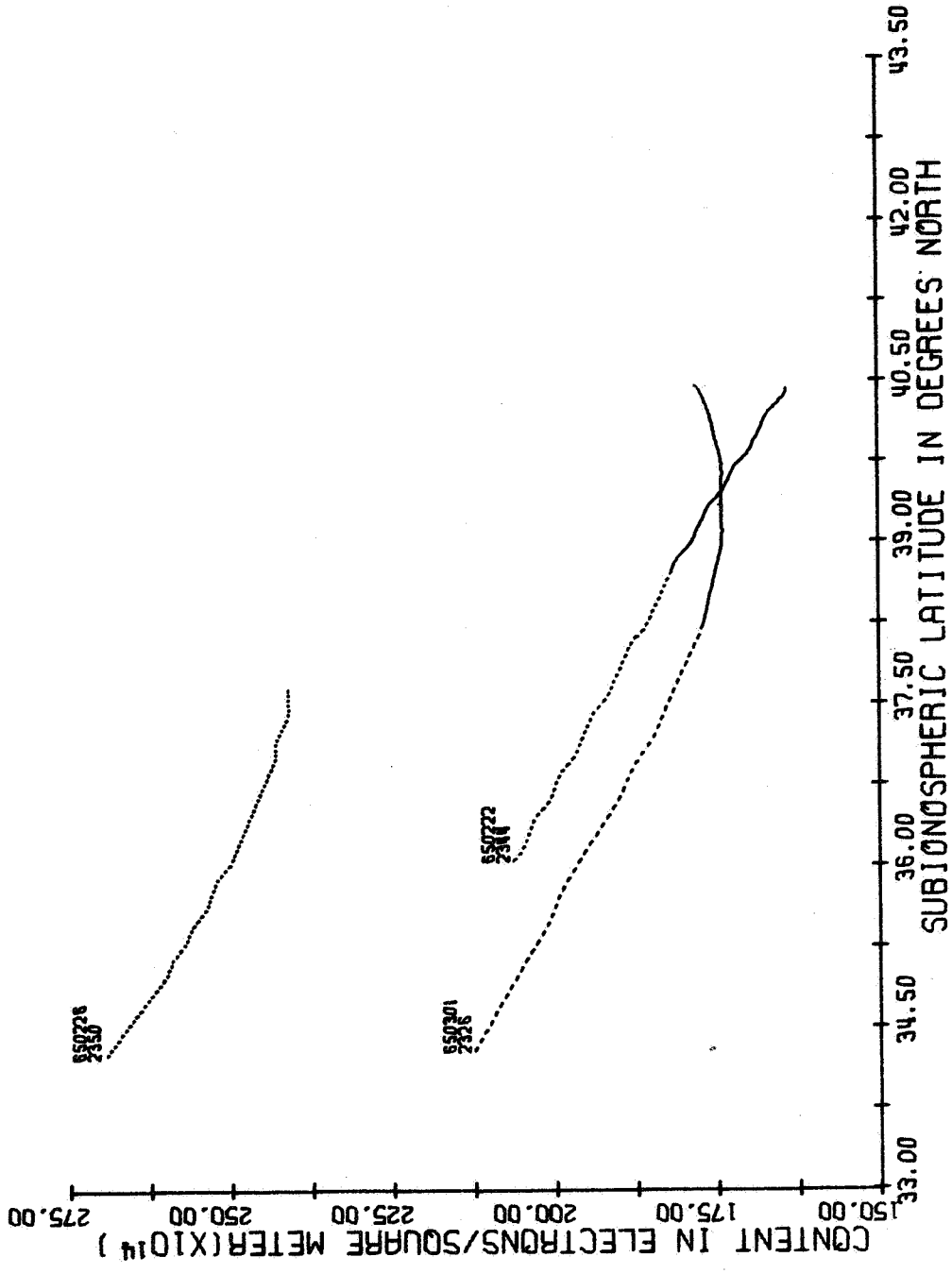
CONTENT IN ELECTRONS/SQUARE METER(X10¹⁴)
150.00
175.00
200.00
225.00
250.00
275.00
SUBIONOSPHERIC LATITUDE IN DEGREES NORTH
33.00
34.50
36.00
37.50
39.00
40.50
42.00
43.50
TIME INTERVAL FROM 2300 TO 2400 CST

Figure 56.